

Unlocking Andean sigmodontine diversity: Five new species of *Chilomys* (Rodentia: Cricetidae) from the montane forests of Ecuador (#68489)

1

First submission

Guidance from your Editor

Please submit by **29 Dec 2021** for the benefit of the authors (and your \$200 publishing discount) .



Structure and Criteria

Please read the 'Structure and Criteria' page for general guidance.



Custom checks

Make sure you include the custom checks shown below, in your review.



Author notes

Have you read the author notes on the [guidance page](#)?



Raw data check

Review the raw data.



Image check

Check that figures and images have not been inappropriately manipulated.

Privacy reminder: If uploading an annotated PDF, remove identifiable information to remain anonymous.

Files

Download and review all files from the [materials page](#).

21 Figure file(s)

6 Table file(s)

4 Other file(s)

! Custom checks

DNA data checks

- ! Have you checked the authors [data deposition statement](#)?
- ! Can you access the deposited data?
- ! Has the data been deposited correctly?
- ! Is the deposition information noted in the manuscript?

Vertebrate animal usage checks

- ! Have you checked the authors [ethical approval statement](#)?
- ! Were the experiments necessary and ethical?
- ! Have you checked our [animal research policies](#)?

Field study

- ! Have you checked the authors [field study permits](#)?
- ! Are the field study permits appropriate?

New species checks

- ! Have you checked our [new species policies](#)?
- ! Do you agree that it is a new species?
- ! Is it correctly described e.g. meets ICZN standard?


For assistance email peer.review@peerj.com



Structure your review

The review form is divided into 5 sections. Please consider these when composing your review:

1. **BASIC REPORTING**
2. **EXPERIMENTAL DESIGN**
3. **VALIDITY OF THE FINDINGS**
4. General comments
5. Confidential notes to the editor






 You can also annotate this PDF and upload it as part of your review

When ready [submit online](#).





Editorial Criteria

Use these criteria points to structure your review. The full detailed editorial criteria is on your [guidance page](#).




BASIC REPORTING

-  Clear, unambiguous, professional English language used throughout.
-  Intro & background to show context. Literature well referenced & relevant.
-  Structure conforms to [PeerJ standards](#), discipline norm, or improved for clarity.
-  Figures are relevant, high quality, well labelled & described.
-  Raw data supplied (see [PeerJ policy](#)).

EXPERIMENTAL DESIGN

-  Original primary research within [Scope of the journal](#).
-  Research question well defined, relevant & meaningful. It is stated how the research fills an identified knowledge gap.
-  Rigorous investigation performed to a high technical & ethical standard.
-  Methods described with sufficient detail & information to replicate.

VALIDITY OF THE FINDINGS

-  Impact and novelty not assessed. *Meaningful* replication encouraged where rationale & benefit to literature is clearly stated.
-  All underlying data have been provided; they are robust, statistically sound, & controlled.
-  Conclusions are well stated, linked to original research question & limited to supporting results.



The best reviewers use these techniques

Tip

Example

Support criticisms with evidence from the text or from other sources

Smith et al (J of Methodology, 2005, V3, pp 123) have shown that the analysis you use in Lines 241-250 is not the most appropriate for this situation. Please explain why you used this method.

Give specific suggestions on how to improve the manuscript

Your introduction needs more detail. I suggest that you improve the description at lines 57- 86 to provide more justification for your study (specifically, you should expand upon the knowledge gap being filled).

Comment on language and grammar issues

The English language should be improved to ensure that an international audience can clearly understand your text. Some examples where the language could be improved include lines 23, 77, 121, 128 – the current phrasing makes comprehension difficult. I suggest you have a colleague who is proficient in English and familiar with the subject matter review your manuscript, or contact a professional editing service.

Organize by importance of the issues, and number your points

1. Your most important issue
2. The next most important item
3. ...
4. The least important points

Please provide constructive criticism, and avoid personal opinions

I thank you for providing the raw data, however your supplemental files need more descriptive metadata identifiers to be useful to future readers. Although your results are compelling, the data analysis should be improved in the following ways: AA, BB, CC

Comment on strengths (as well as weaknesses) of the manuscript

I commend the authors for their extensive data set, compiled over many years of detailed fieldwork. In addition, the manuscript is clearly written in professional, unambiguous language. If there is a weakness, it is in the statistical analysis (as I have noted above) which should be improved upon before Acceptance.

Unlocking Andean sigmodontine diversity: Five new species of *Chilomys* (Rodentia: Cricetidae) from the montane forests of Ecuador

Jorge Brito^{Corresp., Equal first author, 1}, Nicolás Tinoco², C. Miguel Pinto³, Rubí García¹, Claudia Koch⁴, Vincent Fernandez⁵, Santiago Burneo², Ulyses F. J. Pardiñas^{Equal first author, 6, 7}

¹ Sección de Mastozoología, Instituto Nacional de Biodiversidad (INABIO), Quito, Pichincha, Ecuador

² Sección de Mastozoología, Museo de Zoología, Facultad de Ciencias Exactas y Naturales, Pontificia Universidad Católica del Ecuador, Quito, Pichincha, Ecuador

³ Observatorio de Biodiversidad Ambiente y Salud (OBBAS), Quito, Pichincha, Ecuador

⁴ Zoologisches Forschungsmuseum Alexander Koenig (ZFMK), Bonn, Germany

⁵ Imaging and Analysis Centre, Natural History Museum (NHM), London, United Kingdom

⁶ Instituto de Diversidad y Evolución Austral (IDEAus - CONICET), Puerto Madryn, Chubut, Argentina

⁷ Instituto Nacional de Biodiversidad (INABIO), Quito, Ecuador

Corresponding Author: Jorge Brito

Email address: jorgeyakuma@yahoo.es

The Andean cloud forests of Ecuador are home to several endemic mammals. Members of the Thomasomyini rodents are well represented in the Andes, with *Thomasomys* being the largest genus (47 species) of the subfamily Sigmodontinae. Within this tribe, however, there are genera that have escaped a taxonomic revision, and *Chilomys* Thomas, 1897, constitutes a paradigmatic example of these “forgotten” Andean cricetids. Described more than a century ago, current knowledge of this externally unmistakable montane rodent is very limited, and doubts persist as to whether or not it is monotypic. After several years of field efforts in Ecuador, a considerable quantity of specimens of *Chilomys* were collected from various localities representing both Andean chains. Based on an extensive genetic survey of the obtained material, we can demonstrate that what is currently treated as *C. instans* in Ecuador is a complex comprising at least five new species which are described in this paper. In addition, based on these noteworthy new evidence, we amended the generic diagnosis discussed in detail and several key craniodental traits, such as incisor procumbence and microdonta. These results indicate that *Chilomys* probably has a hidden additional diversity in large parts of the Colombian and Peruvian territories, inviting a necessary revision of the entire genus.

Unlocking Andean sigmodontine diversity: Five new species of *Chilomys* (Rodentia: Cricetidae) from the montane forests of Ecuador

Jorge Brito¹, Nicolás Tinoco², C. Miguel Pinto³, Rubí García¹, Claudia Koch⁴, Vincent Fernandez⁵, Santiago Burneo² and Ulyses F. J. Pardiñas^{6, 1}

¹ Instituto Nacional de Biodiversidad (INABIO), Quito, Ecuador

² Sección de Mastozoología, Museo de Zoología, Facultad de Ciencias Exactas y Naturales, Pontificia Universidad Católica del Ecuador, Quito, Ecuador

³ Observatorio de Biodiversidad Ambiente y Salud (OBBAS), Quito, Ecuador

⁴ Zoologisches Forschungsmuseum Alexander Koenig (ZFMK), Bonn, Germany

⁵ Imaging and Analysis Centre, Natural History Museum (NHM), London, United Kingdom

⁶ Instituto de Diversidad y Evolución Austral (IDEAus – CONICET), Puerto Madryn, Chubut, Argentina

Corresponding Author:

Jorge Brito

19 Instituto Nacional de Biodiversidad (INABIO), Quito, Pichincha, Zip code 17-07-8976, Ecuador

20 Email address: jorgeyakuma@yahoo.es

21

22 **ABSTRACT**

23 The Andean cloud forests of Ecuador are home to several endemic mammals. Members of the
 24 Thomasomyini rodents are well represented in the Andes, with *Thomasomys* being the largest
 25 genus (47 species) of the subfamily Sigmodontinae. Within this tribe, however, there are genera
 26 that have escaped a taxonomic revision, and *Chilomys* Thomas, 1897, constitutes a paradigmatic
 27 example of these “forgotten” Andean cricetids. Described more than a century ago, current
 28 knowledge of this externally unmistakable montane rodent is very limited, and doubts persist as
 29 to whether or not it is monotypic. After several years of field efforts in Ecuador, a considerable
 30 quantity of specimens of *Chilomys* were collected from various localities representing both
 31 Andean chains. Based on an extensive genetic survey of the obtained material, we can
 32 demonstrate that what is currently treated as *C. instans* in Ecuador is a complex comprising at
 33 least five new species which are described in this paper. In addition, based on these noteworthy
 34 new evidence, we **amend** the generic diagnosis **in detail and add** several key craniodental
 35 traits, such as incisor **procumbency** and microdonty. These results indicate that *Chilomys*
 36 probably has a hidden additional diversity in large parts of the Colombian and Peruvian
 37 territories, inviting a necessary revision of the entire genus.

38

39 **Subjects** Biodiversity, Phylogenetics, Taxonomy, Zoology

40 **Keywords** Andes, CT, proodonty, microdonty, Thomasomyini, Sigmodontinae

41

42 INTRODUCTION

43 Our current understanding of Andean sigmodontine rodents is mostly driven by the noticeable
 44 diversity of the genera *Calomys*, *Phyllotis* and *Thomasomys*. Clearly, they are emblematic
 45 widespread and speciose taxa. *Thomasomys* is the largest genus of the subfamily with 47 species
 46 (see Brito *et al.*, 2021; Ruelas & Pacheco, 2021), and received extensive attention covering
 47 aspects from alpha taxonomy (e.g., Pearson, 1957; Hershkovitz, 1962; Zeballos *et al.*, 2014;
 48 Salazar-Bravo, 2015; Stepan & Ramirez, 2015; Pacheco, 2015a; Martínez, Sandoval &
 49 Carrizo, 2016) to physiology, reproduction, etc. (e.g., Arana *et al.*, 2002; Tirado, Cortés &
 50 Bozinovic, 2008; Brito & Batallas, 2014; Sahley *et al.*, 2015, 2016). In the Andes, however,
 51 several other sigmodontine genera exist that are much less studied and are considered
 52 paucispecific, such as *Aepeomys*, *Chilomys*, *Galenomys*, or *Neomicroxus*. These taxa,
 53 characterized by being poorly represented in biological collections (e.g., *Galenomys*; Pearson,
 54 1957) and sometime considered rare (e.g., *Aepeomys*; Handley, 1976), have traditionally escaped
 55 systematic revisions. Nevertheless, they constitute a substantial expression of Andean
 56 sigmodontine diversity, particularly in northern South America, and have the potential to expand
 57 our current comprehension of cricetid evolution in this complex part of the continent (e.g.,
 58 Soriano *et al.*, 1993; Voss, 2003; Anderson *et al.*, 2012; Cañón *et al.*, 2020).

59 *Chilomys* Thomas, 1897, constitutes a paradigmatic example of these ‘forgotten’ Andean
 60 cricetids. Described more than a century ago, our current knowledge of this externally
 61 unmistakable montane rodent is very scarce (Thomas, 1895; Osgood, 1912, Pacheco, 2015b;
 62 Brito & Pardiñas, 2017). Although this genus was considered monotypic for most of its history,

it now consists of two speciesm *C. fumeus* Osgood, 1912, restricted to the northernmost Andes in Colombia and Venezuela, and the widespread *C. instans* (Thomas, 1895), the type species of the genus, which occurs from central Colombia to northern Perú (Medina *et al.*, 2017). Both forms are considered very similar (in fact, they have been largely considered synonyms, see Musser & Carleton, 2005) and were distinguished by subtle metric characters (Pacheco, 2015b: 578). But the existence of possible undescribed species has also been suggested for Colombian (Pacheco, 2015b: 580), Ecuadorian (Pinto *et al.*, 2018: 18) and Peruvian populations (Medina *et al.*, 2016: 317).

After several years of field efforts in Ecuador, researchers have collected a considerable quantity of specimens of *Chilomys* from various localities representing both Andean chains. These populational samples allowed surpassing a traditional impediment in the systematic revision of this genus: the scarcity of available material to assess variability (Voss, 2003). Based on an extensive genetical survey of the obtained material, we can demonstrate that what is currently understood as *C. instans* in Ecuador is a complex comprising at least five new species. The purpose of the present contribution is to document these findings to initiate a much-needed revision of the entire genus.

MATERIALS AND METHODS

Studied specimens

This study implies a qualitative and metrical revision based on 97 specimens belonging to the genus *Chilomys* from populations in Ecuador and, subsidiarily, Colombia (Supplementary S1). Most of the Ecuadorian specimens studied were collected by the senior author and collaborators

during recent field trips conducted in the Cordillera de Kutukú, Reserva Dracula, Parque Nacional Sangay, the Cordillera de Chilla, Reserva Geobotánica Pululahua and Reserva Naturetrek Vizcaya. These surveys involved a cumulative trap effort of 12,800 trap/nights. Capture, handling and preservation of specimens secured in the field followed established guidelines of the American Society of Mammalogists (*Sikes et al., 2016*). For the use and care of animals, we follow the guidelines of the Ministry of the Environment of Ecuador (scientific research authorization No 006-2015-IC-FLO-FAU-DPAC/MAE, 003-2019-ICFLO-FAU-DPAC/MAE, MAE-DNB-CM-2019-0126, and MAAE-ARSFC-2020-0642). The collected material was compared with specimens housed in the mammal collections of the following institutions: Centro Nacional Patagónico, Puerto Madryn, Chubut, Argentina (CNP); Instituto Nacional de Biodiversidad, Quito, Ecuador (MECN; formerly known as Museo Ecuatoriano de Ciencias Naturales); Museo de la Escuela Politécnica Nacional, Quito, Ecuador (MEPN); Museo de Zoología de la Pontificia Universidad Católica del Ecuador, Quito, Ecuador (QCAZ); Field Museum of Natural History, Chicago, USA (FMNH); and the Natural History Museum, London, United Kingdom (NHMUK).

Anatomy, age criteria and measurements

Terms used to describe cranial anatomy follow *Carleton & Musser (1989)*, *Musser et al. (1998)*, *Pacheco (2003)*, and *Voss (1993)*; occlusal molar morphology are based on *Reig (1977)* with upper and lower molars identified as M/m, respectively. The description of the coloration is made based on *Köhler (2012)*. Soft anatomy is assessed according to the concepts discussed by *Carleton (1973)* and *Vorontsov (1982)* on stomach and caecum, by *Vorontsov (1982)* and *Voss (1988)* on tongue, by *Quay (1954)* on soft palate, by *Ade (1999)* and *Haidarliu et al. (2013)* on

rhinarium, and by *Pacheco (2003)* on anus. Terminology and definitions follow *Tribe (1996)* and *Costa et al. (2011)* for age classes, and the term “adults” is restricted to individuals categorized as age 3 and 4. External measurements (always provided in millimetres, mm), were mostly recorded in the field and derive from specimens tags; these descriptors are: head and body length (HB), tail length (TL), hind foot length (HF, including claw), ear length (E), and body mass (W, in grams). Cranial measurements were obtained with a digital calliper to the nearest 0.01 mm, and include the following dimensions (see *Tribe, 1996; Voss, 2003; and Musser et al., 1998*, for definitions and illustrations): condylo-incisive length (CIL), condylo-basal length (CBL), zygomatic breadth (ZB), least interorbital breadth (LIB), length of rostrum (LR), breadth of rostrum (BR), length of nasals (LN), length of upper diastema (LD), crown length of maxillary toothrow (LM), length of incisive foramina (LIF), breadth of incisive foramina (BIF), breadth of bony palate (BBP), depth of upper incisor (DI), breadth of zygomatic plate (BZP), braincase breadth (BCB), length of mandible (LMN), crown length of mandibular toothrow (LLM), and depth of mandibular ramus (DR).

X-ray Micro CT

For more detailed analysis and representation of the morphological characteristics of the skulls, several specimens selected as holotypes (MECN 3723, MECN 5854, MECN 6024) of the new species described herein were scanned using a high-resolution X-ray micro-computed tomography desktop device (micro-CT; Bruker SkyScan 1173, Kontich, Belgium) at the Zoologisches Forschungsmuseum Alexander Koenig (ZFMK, Bonn, Germany). To avoid movements during scanning, the skulls were embedded in cotton wool and placed in a small plastic container. Acquisition parameters comprised: An X-ray beam (source voltage 30 kV and current 170 μ A) without the use of a filter; 800 (MECN 3723, MECN 6024) to 1200 (MECN

5854) projections of 900 ms exposure time each with a frame averaging of 6 (MECN 3723, MECN 6024) to 7 (MECN 5854); rotation steps of 0.2° (MECN 5854) to 0.3° (MECN 3723, MECN 6024) recorded over a 180° continuous rotation, resulting in a scan duration of 1 h 36 min (MECN 3723, MECN 6024) to 2 h 43 min (MECN 5854); and a magnification setup generating data with an isotropic voxel size of 14.55 µm (MECN 3723), 13.48 µm (MECN 5854) and 13.84 µm (MECN 6024), respectively. The CT-datasets were reconstructed with N-Recon software version 1.7.1.6 (Bruker MicroCT, Kontich, Belgium) and rendered in three dimensions using CTVox for Windows 64 bits version 3.0.0 r1114 (Bruker MicroCT, Kontich, Belgium). For comparison, the holotype of *Chilomys instans* (NHMUK 1985.10.14.1) was scanned at the Imaging Analysis Centre of the NHMUK using a Nikon Metrology XTH 225 ST (Nikon Metrology, Leuven, Belgium). Acquisition parameters comprised: an X-ray beam (source voltage 85 kV and current 118 µA) filtered with 0.1 mm of aluminium; 4476 projections of 250 ms exposure time each with a frame averaging of 2 recorded over a 360° continuous rotation; a magnification setup generating data with an isotropic voxel size of 11.57 µm. A filtered back projection algorithm was used for the tomographic reconstruction, using the CT-agent and CT-pro 3D software (Version 6, Nikon Metrology), producing an 8-bit uncompressed raw volume. Finally, this dataset was rendered in three dimensions with Amira software (Thermo Fisher Scientific, Hillsboro, USA).

Morphometric Analyses

The analyzed dataset of craniodental measurements comprised 21 variables, from 58 specimens belonging to six taxa, including typical *Chilomys instans* and the five new species described here. We performed all subsequent analyses in R version 3.6.2 (*R Core Team, 2019*), unless otherwise noted. We tested each measurement for normality using the Shapiro-Wilk test using

the R function *shapiro.test*. Four of these measurements were not normally distributed; thus we ~~long~~ transformed the whole dataset, using the R function *log*, to improve its statistical properties. The dataset ~~had 1% missing data so~~, to avoid eliminating individuals or measurements from the analyses, we performed imputation of missing data in the R implementation of the program *Amelia II* (Honaker, King & Blackwell, 2011) with the expectation-maximization (EM) method because of its higher accuracy (Strauss, Atanasov & de Oliveira, 2003; Clavel, Merceron & Escargue, 2014). We generated 100 imputed datasets ($m = 100$), which we averaged to obtain a single imputed dataset using the Python script *avg.py* (Mark, 2017). Prior to these analyses we checked for unusually high pair-wise correlations among measurements using the R function *cor*. The variables CIL, CBL and LD were highly correlated ($r > 0.95$), so we removed the variables CBL and LD from the multivariate analyses restricting the final dataset to 19 variables. We conducted 2 multivariate analyses: a principal component analysis (PCA) with the covariance matrix using the R function *princomp*, and a discriminant function analysis (DFA) using the R script *MorphoTools* version 1.1 (Koutecký, 2015). We drew the scatter plots of the PCA and DFA with the R function *plot*.

DNA amplification and sequencing

We used samples of liver and muscle tissues (preserved in 95% ethanol) and in some cases fragments of dry skin. We extracted DNA using the salt protocol (Bilton & Jaarola, 1996), and amplified by PCR two mitochondrial genes (Cytochrome b [Cytb] and Cytochrome Oxidase I [COI]). For Cytb we used the primers MVZ05, MVZ16H and MVZ14 (Smith & Patton, 1993) and thermal protocols reported by Bonvicino & Moreira (2001) and Smith & Patton (1999). We PCR amplified the COI gene using the cocktail of primers for mammals and the thermal protocol reported by Ivanova *et al.* (2007). We visually evaluated the quality of the PCR amplicons with

gel electrophoresis and subsequently we purified the amplicons with Exosap-IT (GE Healthcare, Chalfont St. Giles, UK). Macrogen Inc. (Seoul, South Korea) sequenced the PCR amplicons with Sanger technology.

Phylogenetic analysis

In Geneious R11 (<https://www.geneious.com>) we assembled and edited the sequences and aligned them using the ClustalW tool. We obtained the best partition schemes and respective models of evolution with PartitionFinder V.1 (*Lanfear et al., 2012*): for the Cytb gene: 1pos GTR + I + G, 2pos HKY + G, 3pos + I + G; and for COI gene the first, second and third positions used the model GTR + I + G. We ran the Bayesian Inference (BI) analysis with MrBayes 3.2 (*Ronquist et al., 2012*) with the following settings: four chains ran for 10,000,000 generations, with sampling every 1,000 generations and a burn-in of 0.25. We evaluated convergence by the effective sample size (EES) and the potential scale reduction factor (PSRF). For most of the parameters the EES should be ≥ 200 and for the PSRF most of the values of the parameters should be between 1.0 and 1.2. We conducted the Maximum Likelihood (ML) analysis with RAxML 8.2.10 (*Stamatakis, 2014*), using the GTRGAMMA model for all gene matrices, with 10 alternative runs on randomized maximum parsimony starting trees. We obtained nodal supports with the rapid bootstrapping algorithm under the MRE-based Bootstrapping criterion (1,000 replicates). We deposited the new sequences in GenBank, and all sequences used in the analyses are listed in Supplementary S2. We calculated the uncorrected genetic p distances (intraspecific and interspecific) with the software Mega X (*Kumar et al., 2018*).

Species delimitation

Due to the number of samples obtained from different parts of Ecuador, we decided to use two single-locus methods of species delimitation: the Poisson Tree Processes (PTP; *Zhang et al., 2013*) and the Automatic Discovery of Bar Code Gaps (ABGD; *Pullianandre et al., 2011*). In the PTP model we used the BI and ML trees of Cytb and COI genes, while in the ABGD model we used alignments (FASTA) of Cytb and COI genes.

New Zoological Taxonomic Names

The electronic version of this article in Portable Document Format (PDF) will represent a published work according to the International Commission on Zoological Nomenclature (ICZN), and hence the new names contained in the electronic version are effectively published under that Code from the electronic edition alone. This published work and the nomenclatural acts it contains have been registered in ZooBank, the online registration system for the ICZN. The ZooBank LSIDs (Life Science Identifiers) can be resolved and the associated information viewed through any standard web browser by appending the LSID to the prefix <http://zoobank.org/>. The LSID for this publication is: urn:lsid:zoobank.org:pub:22604A8F-0472-43EB-8D9F-9503C7AE4419. The online version of this work is archived and available from the following digital repositories: PeerJ, PubMed Central and CLOCKSS.

Results

This study was originally envisioned to produce a complete revision of the genus *Chilomys* following an integrative approach. The Covid19 pandemic hampered the possibility to inspect crucial American collections, in particular those of the FMNH and Smithsonian Institution (Washington DC) containing important samples from Colombia and Venezuela. Under these circumstances, we opted to redesign the scope to be limited to Ecuadorian populations which are currently included in *Chilomys instans* (see *Tirira, 2017*).

In the first specimens obtained, we detected noticeable external differences between them, not only in terms of general body size or coloration, but especially in the morphology of manus and pes (e.g., hairiness, distance among pads, patterns of scales). These field observations triggered our interest to conduct an extensive analysis of Cytb sequences of the collected specimens. In addition, the large sample collected in Reserva Dracula (about 50 individuals) allowed us to expand the knowledge of morphological non-geographic variability. Combining the topology of the Cytb marker, the genetic distances, and accounting for ontogenetic and sexual variation, we concluded that *C. instans* represents a species complex. In the following sections, the main results of the phylogenetic and metric analyses are presented, while the morphological evidence is restricted to taxonomic accounts to avoid redundancy.

Phylogeny

The genus *Chilomys* was recovered as monophyletic (Cytb, PP: 1.00 / BS: 96; COI, 1.00 / 100; Figure 1; Supplementary S3) and embedded in a clade with *Rhipidomys*, and *Thomasomys*, all recognized members of Thomasomyini. The relationships among these genera differ among the individual genes used. The Cytb gene recovered (*Rhipidomys* (*Thomasomys* + *Chilomys*)) with high supports (PP > 0.90 / BS > 70; Figure 1), COI recovered (*Rhipidomys* (*Thomasomys* + *Chilomys*)) in some cases the supports were high (0.98/100; Supplementary S3).

Within the *Chilomys* clade several minor clades were recovered. Cytb topology is resolved in five subclades (Figure 1): A group of samples from northern Ecuador, from the Provincia de Carchi, were grouped into two sister clades (1.00 / 93), one from Reserva Dracula (1.00 / 98), the other including a sample from Colombia (AF108679) and a group from the Reserva Ecológica El Angel (1.00 / 96); another group of samples are from the Provincia de Cotopaxi from the Reserva Integral Otonga (1.00 / 100); and the two remaining clades included samples from the

north and south east, two sister clades, one with samples from the Provincias de El Oro and Zamora Chinchipe (1.00 / 100), and the other with samples from the Provincias de Napo and Morona Santiago (1.00 / 100). COI recovered four of the five clades found in the phylogenetic tree of Cytb (Supplementary S3): Reserva Ecológica El Angel (1.00 / 100; Figure 1), Reserva Integral Otonga (1.00 / 100), Napo and Morona Santiago (0.97 / 70), and two separate samples, from Zamora Chinchipe and El Oro; for the samples from the Reserva Dracula, no sequences were obtained for COI. The clade of the genus *Chilomys* presented an intraspecific distance of $6.56\% \pm 0.49\%$, while in clades of the phylogenetic tree of Cytb, genetic distance values ranged from 4.88% (Reserva Dracula versus Reserva Ecológica El Angel) to 10.17 % (Napo-Morona Santiago versus Colombia AF108679); all pairwise distances are presented in Table 1.

Species delimitation

The PTP model identified nine putative species (PS): the sample from Colombia and those from Reserva El Angel were identified as different PS1 (1.00) and PS2 (0.98); the Reserva Dracula samples were identified as PS3 (0.99) and PS4 (1.00); the samples from El Oro and Zamora Chinchipe were identified as PS5 (0.84) and PS6 (0.84), respectively; the samples from Napo and Morona Santiago were identified as a single putative species PS8 (0.87), with the exception of the sample QCAZ 8876 which was identified as a different putative species PS7 (1.00); finally, the samples from the Reserva Integral Otonga were identified as PS9 (0.98). The ABGD model identified the samples into groups of 6, 7 and 10 species, with 6 species being the most frequent grouping (Figure 2).

Morphometric analysis

The new species of *Chilomys* named immediately below is the largest in our sample, and it is evident that most of the PCA variation is driven by size along PC1 explaining 68.03% of the variation (Figure

3A). Among the remaining species there is a large overlap particularly between *C. instans* and the new species *C. percequilloi*. The DFA shows that it is possible to differentiate the six species of *Chilomys* analyzed, with DF1 explaining 30.54% of the variation (Figure 3B). The loadings of the first two PCs and the two DFs are presented in Table 2.

Systematic accounts

Family Cricetidae Fischer, 1817

Subfamily Sigmodontinae Wagner, 1843

Tribe Thomasomyini Steadman and Ray, 1982

Genus *Chilomys* Thomas, 1897

Chilomys carapazi sp. nov. Brito and Pardiñas

urn:lsid:zoobank.org:act:A12AF0E7-4465-4A9F-99B0-7E09DBDD5BBA

Carapaz's Forest Mouse, Ratón del bosque de Carapaz (in Spanish)

Holotype: MECN 5291 (field number JBM [Jorge Brito Molina] 1453), an adult male captured 27 September, 2016, by J. Brito, J. Robayo, L. Recalde, T. Recalde and C. Reyes, preserved as a cleaned skull and the rest of the body in ethanol, and muscle and liver biopsies in 95% ethanol.

Type locality: Ecuador, Provincia de Carchi, Reserva Dracula, Gualpi Km 18 (0.849796°, -78.234767°, WGS84 coordinates taken by GPS at the site of collection; elevation 2,350 m).

Etymology: Named in honor of Richard Carapaz Montenegro, an Ecuadorian professional cyclist born in the Provincia de Carchi. The species epithet is formed from the surname "Carapaz," taken as a noun in the genitive case, adding the Latin suffix "i" (ICZN 31.1.2).

Diagnosis: A species of *Chilomys* which can be identified by the following combination of characters: Head and body length ~ 95 mm; dorsal surface of foot covered with round scales and

without interspaces; long nasal (~ 8.5 mm); long diastema (~ 8.2 mm); M2 with broad hypoflexus (similar in width to mesoflexus); m1 without anteromedian flexid.

Morphological description of the holotype: Large body size for the genus (head and body length combined 95 mm). Brown color (color 277) dorsal fur; short hairs (medium length on back = 9 mm) with medium neutral gray (color 298) base and ground cinnamon (color 270) tips. Smoke gray (color 267) ventral coat, with hairs (medium length = 7 mm) with dark neutral gray (color 299) base and smoke gray (color 266) tips. Olive-brown (color 278) periocular ring. Postauricular patch absent. Mystacial vibrissae long, thick at base and thin towards tip, exceeding shoulder when tilted backwards; superciliary vibrissae 1 present, genal vibrissae 1 present (sensu *Pacheco, 2003*). Ears (11 mm from notch to margin) externally covered by short smoke gray (color 266) hairs, and with pale buff (color 1) inner surface and pale neutral gray (color 296) margin.

Narrow and ground cinnamon drab (color 259) metatarsal patch, which extends to the base of the phalanges; dorsal surface of the foot with round scales and without interspaces (Figure 4A). Plantar surface with 6 pads, including 4 interdigitals of similar size, thenar and hypothenar pads large and with ample interspace; sole between pads smooth (Figure 4B). Short digit I reaches base of digit II; digit II slightly smaller than digit III and digit III same size as digit IV; short digit V (apparently somewhat opposable) reaches middle of digit IV. Long tail (95 mm; 134% of HB), unicolor fawn (color 258) except for apex, which is white (up to 10 mm). Tail with 16 rows of scales per cm on axis; rectangular scales with three hairs each, which extend over 1-1.5 rows of scales; naked-looking tail except for tip, where it presents a small brush of up to 5 mm. Prominent anus.

Cranium large for the genus (26.35 mm of CIL). Short and narrow rostrum, with nasal bones that do not extend to incisors; poorly developed gnathic process. Posterior margin of nasal bone not surpassing plane of lacrimal bone. Shallow zygomatic notch. Large and rounded lacrimal bones. Wide interorbital region with smooth outer edges, without exposing alveolar maxillary processes in dorsal view (Figure 5A). Supraorbital region with diverging posterior borders. Frontoparietal suture U-shaped. Broad, rounded and not inflated braincase, concave at outer edges. Broad zygomatic plate, comparatively longer than length of M1, leaning forward and with posterior edge not reaching maxillary row. Zygomatic arches sturdy with jugals spanning a large segment of each mid-arch. Small supraorbital foramen with posterior border in line with M3 (Figure 6B). Alisphenoid strut present but narrow. Carotid circulatory pattern type 3 (sensu *Voss, 1988*); carotid canal large, stapedia foramen small, without alisphenoid squamous groove and with sphenofrontal foramen. Subsquamosal fenestra four times larger than postglenoid foramen; hamular process of squamosal thin and long, and distally applied on mastoid capsule. Slightly triangular tegmen tympanic, superimposed with suspensory process of squamous. Lateral expressions of parietals present; bullae small; pars flaccida of tympanic membrane present; orbicular apophysis of malleus well-developed. Paraoccipital process small. Hill foramen small; short and wide incisive foramina with curved edges, not reaching plane defined by anterior faces of M1. Premaxillary capsule narrow, parallel-sided and narrow at rear ends; maxillary septum of incisive foramen slim and long. Long and wide palate (sensu *Herskovitz, 1962*). Posterolateral palatal pit small. Wide mesopterygoid fossa, with by a medium palatal process present. Inconspicuous sphenopalatine vacuities covered by roof of palate. Basisphenoid wide. Large foramen ovale, similar in size to transverse canal. Middle

lacerate foramen narrow. Auditory bullae small and uninflated with large and narrow eustachian tube (Figure 7B).

Dentary with short and wide coronoid process (not extending beyond upper edge of condylar process); short and thin mental foramen ~~of jaw~~.

Proodont upper incisors (Thomas angle $\sim 95^\circ$; Figure 6B) with orange and smooth ~~front~~ enamel; lower incisors with sharp tip; crested and pentalophodont molars (sensu *Hershkovitz, 1962*), with noticeably thick enamel. Maxillary molar rows converging slightly backwards; main cusps opposite (Figure 8A) and sloping backwards when viewed from side. M1 rectangular in outline; without anteromedian flexus; deep paraflexus; short and wide anteroloph; short and wide mesoloph; reduced posteroloph. M2 squared in outline; mesoloph showing same condition as in M1; broader hypoflexus (similar in width to mesoflexus); internal fosseta larger than fosseta of M1. M3 less than half the size of M2; M3 rounded in outline with conspicuous anteroloph; central fosseta small. Lower molars with opposite main cusps (Figure 8B) and sloping forwards when viewed from side. First lower molar (m1) without anteromedian flexus; large anterolabial cingulum; short mesolophid; mesolophid of m2 showing same condition as in m1; noticeable anterolabial cingulum; hypoflexid of m3 long and wide.

Comparisons

Chilomys carapazi sp. nov. is the largest species recognized for the genus (Figure 3). As it occurs in sympatry with *C. georgeledecii* sp. nov. at Reserva Dracula it could be confused with this species ~~in the first instance~~. Nevertheless, beside metric characteristics (see Table 3) it differs from *C. georgeledecii* (states in parenthesis) by the following traits: Thomas angle $\sim 95^\circ$ (Thomas angle $\sim 102^\circ$); M1 without anteromedian flexus (with anteromedian flexus); M2 with broader hypoflexus, similar in width to mesoflexus (with narrowed hypoflexus, distinctly

narrower than mesoflexus); m1 without anteromedian flexus (m1 with anteromedian flexus). A detailed comparison with all species of *Chilomys* is presented in Table 3.

Distribution: Known only from the type locality at Reserva Dracula (Carchi, Ecuador), on the western flank of the Andes (Figure 9), at an elevation of 2,350 m. The climate at this locality has an average annual temperature of 15.5°C and a precipitation of 1,520 mm per year. The climate is relatively stable during the first months of the year and between July and October the differences between minimum and maximum temperatures increase, with the lowest temperatures in August (9.3°C) and the highest in September (21.8°C). The highest precipitation occurs in October with an average of 190 mm per month, the lowest in August with 46 mm per month (*Hijmans et al., 2005*).

Natural history: The type locality is located in the headwaters of the Gualpi River in the lower montane ecosystem (*Cerón et al., 1999*). The local expression of the montane cloud forest is characterized by a tree canopy that reaches 30 m high. The understory is luxurious and mostly composed of species belonging to Araceae, Melastomataceae, Cyclanthaceae, Bromeliaceae, and ferns. From the same pit falls where *Chilomys carapazi* sp. nov. was obtained, we also collected the sigmodontines *C. georgeledecii*, *Pattonimus ecominga*, *Melanomys caliginosus*, *Microryzomys minutus*, *Nephelomys* cf. *pectoralis*, and *Thomasomys bombycinus*, the heteromyid *Heteromys australis*, the marsupials *Caenolestes convelatus*, *Mamosops cauae*, and the soricid *Cryptotis equatoris*.

***Chilomys georgeledecii* sp. nov.** Brito, Tinoco, García, Koch and Pardiñas

urn:lsid:zoobank.org:act:BDEFF98C-5ED9-4DC7-8EC9-6ADE8BB297C1

Ledeci Forest Mouse, Ratón del bosque de Ledeci (in Spanish)

Holotype: MECN 6024 (field number JBM 1955), an adult male captured 8 November, 2018, by J. Brito, J. Curay and R. Vargas, preserved as dry skin, skull, postcranial skeleton and muscle and liver biopsies in 95% ethanol.

Paratypes: MECN 4732, MECN 4751, and MECN 4752, adult males, and MECN 4761, adult female, all preserved as cleaned skulls and carcasses in ethanol, collected in Provincia de Carchi, Reserva Dracula, Cerro Oscuro (0.917274°, -78.187079°, 1,550 m) by J. Brito, J. Robayo, L. Recalde, T. Recalde and C. Reyes on 7 July, 2015. MECN 4983, MECN 4992, MECN 4993, MECN 4994, MECN 4995, MECN 4996, and MECN 4997, adult males, MECN 4925, MECN 4955, and MECN 4956, adult females, all preserved as dry skins and cleaned skulls, collected in Gualpi Km 14 (0.882408°, -78.223235°, 1,970 m) by J. Brito, J. Robayo, L. Recalde, T. Recalde and C. Reyes on 5 June, 2016. MECN 4968, MECN 4971 and MECN 5381, adult males preserved as dry skins and cleaned skulls, collected in Gualpi Km 18 (0.849796°, -78.234767°, 2,350 m) by J. Brito, J. Robayo, L. Recalde, T. Recalde and C. Reyes on 2 June, 2016. MECN 5301, MECN 5302, MECN 5303, adult males, MECN 5299, MECN 5300 adult females, all preserved as cleaned skulls and carcasses in ethanol, collected in Gualpi Km 18 (0.849796°, -78.234767°, 2,350 m) by J. Robayo, J. Brito and H. Yela on 27 September, 2016. MECN 5921, MECN 5925, and MECN 6205, adult males, MECN 5923 and MECN 5926, adult females, preserved as dry skins and cleaned skulls, collected in Guapilal (0.891944°, -78.20308°, 1,700 m) by J. Curay, R. Vargas and C. Bravo on 14 April, 2019. MECN 6323, MECN 6327, and MECN 6337, adult males, MECN 6303, an adult female, preserved as dry skins and cleaned skulls, collected in Bosque La Esperanza (0.929830°, -78.244860°, 1,912 m) by J. Brito, J. Castro, Z. Villacis and J. Guaya on 28 March, 2021.

Type locality: Ecuador, Provincia de Carchi, Reserva Dracula, Peñas Blancas-Pailón (-0.98259°, -78.22204°, WGS84 coordinates taken by GPS at the site of collection; elevation 1,502 m).

Etymology: Named in honor of Czech and US international conservationist George Campos Ledeci, who has worked to promote more environmentally friendly infrastructure development projects in Ecuador and other countries. The species epithet is formed from the surname “Ledeci,” taken as a noun in the genitive case, adding the Latin suffix “i” (ICZN 31.1.2).

Diagnosis: A species of *Chilomys* which can be identified by the following combination of characters: Head and body length ~83-90 mm; tail longer than head and body length combined (~144.4–177.7%); dorsal surface of foot with round scales and large interspaces; zygomatic plate slightly tilted backwards; M2 with narrow hypoflexus (distinctly narrower than mesoflexus); m1 with anteromedian flexus.

Morphological description of the holotype and variation: Small body size for the genus (head and body length combined range between 76 and 90 mm). Medium neutral gray (color 298) dorsal fur; short hairs (medium length on back = 5.5 mm). Pale neutral gray (color 296) venter coat, with hairs (medium length = 6.5 mm) with dark natural neutral gray (color 299) base. Jet black (color 300) periocular ring (Figure 10). Postauricular patch absent. Mystacial vibrissae short, thick at base and thin towards tip, slightly exceeding ears when are tilted backwards; superciliary vibrissae 1 present, genal vibrissae 1 present. Ears (11–16 mm from notch to margin) externally covered by short smoke gray (color 266) hairs, and with dark neutral gray (color 299) inner surface and light neutral gray (color 296) margin (Figure 10).

Metatarsal patch with whitish hairs, giving a naked; dorsal surface of foot with round scales and large interspaces. Plantar surface with 6 pads, including 4 interdigitals of similar size, thenar and hypothenar pads large and with small interspace; sole between pads is smooth (Figure

4D). Short digit I reaches base of digit II; digit II slightly smaller than digit III and digit III slightly smaller than digit IV; short digit V reaches middle of digit IV. Long tail (120–140 mm; ~144.44–177.78% of HB), unicolor fawn (color 258) except for apex, which is white (up to 12–20 mm). Tail with 16–18 rows of scales per cm on axis; square scales with three hairs each, which extend over 1.5 rows of scales; naked-looking tail except for tip, where it presents a small brush of up to 4 mm.

Cranium small for the genus (20.8–23.3 mm of CIL). Short and narrow rostrum, with nasal bones that extend to incisors; poorly developed gnathic process. Posterior margin of nasal bone does not exceed plane of lacrimal bone. Shallow zygomatic notch. Small and triangular outline of lacrimal bones, almost entirely welded to maxillae. Wide interorbital region with smooth outer edges, without exposing alveolar maxillary processes in dorsal view (Figure 11A). Supraorbital region with diverging posterior borders. Frontoparietal suture U-shaped. Broad rounded and inflated braincase, concave at outer edges. Developed ethmoturbinals (Figure 12F). Narrow zygomatic plate, comparatively same length as M1, leaning forward and with posterior edge not reaching maxillary row. Zygomatic arches thin with jugals spanning a large segment of each mid-arch. Large supraorbital foramen with posterior border in line with M2 (Figure 6C). Alisphenoid strut wide and robust. Carotid circulatory pattern type 3; carotid canal large, stapedial foramen very small, without alisphenoid squamous groove and without sphenofrontal foramen. Subsquamous fenestra three times smaller than postglenoid foramen (Figure 11C); hamular process of squamosal thin and long, and distally applied on mastoid capsule. Triangular tegmen tympanic, superimposed with suspensory process of squamous. Lateral expressions of parietals present; bullae small; pars flaccida of tympanic membrane present, large; orbicular apophysis of malleus well-developed. Paraoccipital process small. Hill foramen small (Figure

13C); short and narrow incisive foramina with curved edges without reaching plane defined by anterior faces of M1; a pair of ridges on either side of palatine foramina and in front of M1. Premaxillary capsule widened, parallel-sided and narrow at rear ends; maxillary septum of incisive foramen slim and long. Long and wide palate. Posterolateral palatal pits small. Wide mesopterygoid fossa, with by a medium palatal process present. Inconspicuous sphenopalatine vacuities covered by roof of palate. Basisphenoid narrow. Small foramen ovale, but larger than transverse canal. Middle lacerate foramen narrow. Auditory bullae small and uninflated with short and wide eustachian tubes (Figure 7C).

Dentary with short and narrow coronoid process (extends beyond upper edge of condylar process); short and thin mental foramen ~~of jaw~~.

Proodont upper incisors (Thomas angle $\sim 102^\circ$; Figure 6C) with orange and smooth ~~front~~ enamel; crested and pentalophodont molars, with noticeably thick enamel. Maxillary molar rows parallel; main cusps opposite (Figure 8C) and sloping backwards when viewed from side. M1 rectangular in outline with anteromedian flexus; conspicuous anteroloph; long and wide mesoloph; short posteroloph; internal closure of mesoflexus ends in a fosseta. M2 squared in outline; mesoloph showing same condition as in M1; narrow hypoflexus (distinctly narrower than mesoflexus); internal fosseta larger than fosseta of M1. M3 less than half the size of M2; M3 rounded in outline with conspicuous anteroloph; long paraflexus; central fosseta large, but smaller than in M2 (Figure 8C). Lower molars with main cusps opposite (Figure 8D) and sloping forwards when viewed from side. First lower molar (m1) with anteromedian flexus; small anterolabial cingulum; thin and long mesolophid. Mesolophid of m2 showing same condition as in m1; conspicuous cingulum m2. Hypoflexid of m3 long and wide; hypoflexid well-developed and deep in m1-m3 (Figure 8D).



Tuberculum of first rib articulates with transverse processes of seventh cervical. First and second thoracic vertebrae have differentially elongated neural spine. Vertebral column composed of 19 thoracolumbar, 16th with moderately developed anapophyses and 17th with little developed anapophyses, 4 sacrals (fused), and 37-43 caudal vertebrae; hemal arches in third and fourth caudal vertebra; 12 ribs.

Comparisons: *Chilomys georgeledecii* sp. nov., is one of the smallest species of *Chilomys* that inhabits Ecuador (Figure 3; Table 4). It occurs in sympatry with *C. carapazi* sp. nov. at Reserva Dracula and can be confused with this species ~~in the first instance~~. Nevertheless, beside metric characteristics (see Table 4) it differs from *C. carapazi* (states in parenthesis) by the following traits : **greater** Thomas angle $\sim 102^\circ$ (~~Thomas angle $\sim 95^\circ$~~); M1 with anteromedian flexus (~~without anteromedian flexus~~); M2 with narrow hypoflexus, distinctly narrower than mesoflexus (~~with broader hypoflexus~~, **broader and** similar in width to mesoflexus **in C. carapazi**); m1 with anteromedian flexus (~~without anteromedian flexus~~).

Another species that inhabits the western flank of Ecuador (Figure 9), ~~and is~~ similar in size to *C. georgeledecii*, is *Chilomys weksleri* sp. nov. (**named below**, see Table 4); *C. georgeledecii* differs from *C. weksleri* sp. nov. (states in parentheses) by the following traits: zygomatic plate comparatively same length as M1 and slightly tilted backwards (comparatively wider than M1 and leaning forwards); M2 with narrow hypoflexus, but distinctly narrower than mesoflexus (broader hypoflexus, similar in width to mesoflexus). Further comparison with all recognized species of *Chilomys* is provided in Table 3.

Distribution: Known from several neighbouring collecting sites in Reserva Dracula (Carchi, Ecuador), on the western flank of the Andes (Figure 9), at elevations ranging from 1,502 m to 2,350 m. The climate in the recorded localities has an annual mean temperature of 18°C and

precipitation of 1,720 mm per year. The greatest differences between minimum and maximum temperatures occur between June and October, with the lowest monthly average temperature in August (9.3°C) and the highest in September (25.2°C). The highest precipitation occurs in April with an average of 230 mm per month and the lowest in July and August with 30 mm per month each (Hijmans *et al.*, 2005).

Natural history: Reserva Dracula belongs to the subtropical and lower montane ecosystem (Cerón *et al.*, 1999). The local expression of the cloud montane forest is characterized by a tree canopy that reaches 30 m high. The understory is luxurious and mostly composed of species belonging to Araceae, Melastomataceae, Cyclanthaceae, Bromeliaceae, and ferns. Stomachs from six specimens were dissected to inspect content (Supplementary S4). Sampled *C. georgeledecii* sp. nov. were insectivorous, preying primarily on fly larva. Identifiable prey items were 50% Diptera, 28.5% Coleoptera, 7.1% Hymenoptera, 7.1% Blattodea, and 7.1% Annelida. From the same pit falls where *C. georgeledecii* sp. nov. was obtained, we also collected the sigmodontines *Chilomys carapazi* sp. nov., *Pattonimus ecominga*, *Melanomys caliginosus*, *Microryzomys minutus*, *Nephelomys* cf. *pectoralis*, *Oecomys* sp., *Rhipidomys latimanus*, *Tanyuromys thomasleei*, *Sigmodontomys alfari*, and *Thomasomys bombycinus*, the heteromyid *Heteromys australis*, the marsupials *Caenolestes convelatus*, *Mamosops cauae*, and *Marmosa isthmica*, and the soricid *Cryptotis equatoris*.

***Chilomys neisi* sp. nov.** Brito, Tinoco, García, Koch, and Pardiñas
urn:lsid:zoobank.org:act:F31C845C-DED1-4579-992D-9602FF14ADA6
Neisi Forest Mouse, Ratón del bosque de Neisi (in Spanish)

Holotype: MECN 6187 (field number JBM 2270), an adult male captured 4 October, 2020, by J. Brito and M. Herrera, preserved as dry skin, skull, postcranial skeleton, and muscle and liver biopsies in 95% ethanol.

Paratypes: MECN 3723, adult male, preserved as dry skin and cleaned skull, collected in Provincia de Zamora Chinchipe, Reserva Biológica Tapichalaca (-4.492083, -79.129778, 2,500 m) by F. Reid on 22 November, 2013. QCAZ 13175, adult male, preserved as dry skin and cleaned skull, collected in Provincia de Loja, La Libertad, Shucos (-3.82083, -79.1174619, 2,900 m) by S. Lobos on 28 January, 2012.

Type locality: Ecuador, Provincia de El Oro, Cantón Chilla, Ashigsho (-3.44785°, -79.61015°, WGS84 coordinates taken by GPS at the site of collection; elevation 2,539 m).

Etymology: Named in honor of Neisi Dajomes Barrera, an Ecuadorian weightlifting athlete born in the Provincia de Pastaza; Neisi is the first Ecuadorian female Olympic gold medalist. The species epithet is formed from the name “Neisi” taken as a noun in apposition.

Diagnosis: A species of *Chilomys* which can be identified by the following combination of characters: long nasal (~8.4–8.8 mm); zygomatic plate straight; M1 without anteromedian flexus; M1–M2 with indistinct mesoloph; M2 with narrowed hypoflexus (similar in width to mesoflexus); m1 without anteromedian flexus; hemal arches absent.

Morphological description of the holotype and variation: Small body size for the genus (head and body length combined range between 95 and 100 mm). Dark neutral gray (color 299) dorsal fur; short hairs (medium length on back = 6.5 mm) with dark neutral gray (color 299) base and olive-brown (color 278) tips. Dark neutral gray (color 299) venter coat, with hairs (medium length = 6.5 mm) with pale neutral gray (color 297) base and smoke gray (color 266) tips. Jet black (color 300) periocular ring. Postauricular patch present. Mystacial vibrissae long, thick at

base and thin towards tip, exceeding ears when tilted backwards; superciliary vibrissae 1 present, genal vibrissae 1 present. Ears (15–16 mm from notch to margin) externally covered by short smoke gray (color 266) hairs, dark neutral gray (color 299) inner surface, pale neutral gray (color 296) margin. Narrow and ground cinnamon drab (color 259) metatarsal patch, which extends to base of phalanges; dorsal surface of foot with round scales and small interspaces. Plantar surface with 6 pads, including 4 interdigitals of similar size, thenar and hypothenar pads small and with large interspace; space between pads is smooth (Figure 4F). Short digit I reaches base of digit II; digit II slightly smaller than digit III and digit III slightly smaller than digit IV; short digit V reaches middle of digit IV. Long tail (~128–136 mm; ~135% of HB), unicolor fawn (color 258) except for apex, which is white (up to 15–25 mm). Tail with 15–16 rows of scales per cm on axis; square scales with three hairs each, which extend over 1.5 rows of scales; naked-looking tail except for tip, where it presents a small brush of up to 4 mm.

Cranium small for the genus (~24.01–24.7 mm of CIL). Short and narrow rostrum, with nasal bones that extend to incisors; poorly developed gnathic process. Posterior margin of nasal bone does not exceed plane of lacrimal bone. Shallow zygomatic notch (deep in old specimen). Small and rounded lacrimal bones, almost entirely welded to maxillae. Wide interorbital region with smooth outer edges, exposing alveolar maxillary processes in dorsal view (Figure 14). Supraorbital region with diverging posterior borders. Frontoparietal suture V-shaped. Broad rounded and inflated braincase, concave at outer edges. Developed ethmoturbinals (Figure 12G). Wide zygomatic plaque, comparatively longer than length of M1, and posterior border reaches anterior face of M1. Zygomatic arches sturdy with jugals spanning a large segment of each mid-arch. Small supraorbital foramen with posterior border in line with M3 (Figure 6D). Alisphenoid strut wide and robust. Carotid circulatory pattern type 3; carotid canal large,

stapedial foramen small, without alisphenoid squamous groove and without sphenofrontal foramen. Subsquamous fenestra **one third size of** postglenoid foramen (Figure 14); hamular process of squamosal thin and long, and distally applied on mastoid capsule. Slightly triangular tegmen tympanic, superimposed with suspensory process of squamous. Lateral expressions of parietals present; bullae small; pars flaccida of tympanic membrane present, large; orbicular apophysis of malleus well-developed. Paraoccipital process small. Hill foramen long (Figure 13D); short and narrow incisive foramen with curved edges without reaching plane defined by anterior faces of M1; a pair of ridges on either side of palatine foramina and in front of M1. Premaxillary capsule widened, parallel-sided and narrow at rear ends; maxillary septum of incisive foramen slim and long. Long and wide palate, mesopterygoid fossa not reaching M3. Posterolateral palatal pit small. Wide mesopterygoid fossa, with by a medium palatal process present. Inconspicuous sphenopalatine vacuities covered by roof of palate. Basisphenoid narrow. Large D-shaped foramen ovale. Middle lacerate foramen narrow. Auditory bullae small and uninflated with large and wide eustachian tube (Figure 7D).

Dentary short, with short and wide coronoid process (not extending beyond upper edge of condylar process); short and thin mental foramen.

Proodont upper incisors (Thomas angle of $\sim 102^\circ$; Figure 6D) with orange and smooth ~~front~~ enamel; crested and pentalophodont molars, with noticeably thick enamel. Maxillary molar rows parallel; main cusps opposite (Figure 8E) and sloping backwards when viewed from side. M1 rectangular in outline without anteromedian flexus; thin and short anteroflexus; small anteroloph; indistinct mesoloph; reduced posteroloph; internal closure of mesoflexus ends in a fosseta. M2 squared in outline; mesoloph showing same condition as in M1; narrowed hypoflexus (distinctly narrower than mesoflexus); internal fosseta larger than fosseta of M1. M3 less than half the size

of M2; M3 rounded in outline with conspicuous anteroloph; central fosseta large but smaller than M2. Lower molars with main cusps opposite (Figure 8F) and sloping forwards when viewed from side. First lower molar (m1) without anteromedian flexus; large anterolabial cingulum; thin and short mesolophid. Mesoloph absent; noticeable anterolabial cingulum. Hypoflexid of m3 long and wide; hypoflexid well-developed and deep in m1–m3.

Tuberculum of first rib articulates with transverse processes of seventh cervical vertebra. First and second thoracic vertebrae have differentially elongated neural spine. Vertebral column is composed of 19 thoracolumbar, 16th with moderately developed anapophyses and 17th with little developed anapophyses, 4 sacrals (fused), and 39 caudal vertebrae without hemal arches; 12 ribs. Scapular notch extends to half of scapula and scapular spine not reaching caudal border; supratrochlear foramen of humerus absent; contact between tibia and fibula occurs in more medial part of these bones and fibula reaches 55% of length of tibia.

Comparisons: *Chilomys neisi* sp. nov., is a small *Chilomys* species that inhabits Ecuador (Figure 3; Table 4) and it can be confused with *C. percequilloi* sp. nov., but differs from *C. percequilloi* sp. nov. (states in parenthesis) by the following structures: Thomas angle $\sim 102^\circ$ (Thomas angle $\sim 92^\circ$); M1 without anteromedian flexus (with anteromedian flexus); M1–M2 with indistinct mesoloph (present); M2 with narrowed hypoflexus, similar in width to mesoflexus (broader hypoflexus, similar in width to mesoflexus); m1 without anteromedian flexus (with anteromedian flexus); hemal arches absent (present).

Chilomys instans, another small species that inhabits the eastern flank of Ecuador (Figure 9; and is of similar size (see Table 4) so that it could be confused with *C. neisi* sp. nov. However, it can be differentiated from *Chilomys instans* (states in parentheses) by the following structures: M1 without anteromedian flexus (with anteromedian flexus); M1–M2 indistinct mesoloph (distinct

mesoloph); M2 with narrowed hypoflexus, distinctly narrower than mesoflexus (broader hypoflexus, similar in width to mesoflexus). A detailed comparison with all *Chilomys* species is presented in Table 3.

Distribution: *Chilomys neisi* sp. nov., has the southernmost distribution of all species described in this work; it is known from two locations in the Provincias de Zamora Chinchipe and El Oro, Ecuador (Figure 9), at elevation around 2,500–2,900 m. To the north, *C. neisi* sp. nov. is recorded at Ashigsho, Chilla (Provincia de El Oro) at an elevation of 2,500 m; to the south, the species occurs at Reserva Tapichalaca (Provincia de Zamora Chinchipe) at an altitude of 2,900 m. The annual average temperature corresponds to 16.8°C. The coldest times are reached in August in Tapichalaca (minimum temperature of 9.6°C) and the warmest in September in Chilla (maximum temperature of 25.3°C). Average precipitation is 1,075 mm per year, the driest month (July and August) being in Chilla (23 mm per month) and the wettest in March in Tapichalaca, 190 mm per month (Hijmans et al., 2005).

Natural history: The zoogeographic area where *Chilomys neisi* sp. nov. occurs is Temperate (Albuja et al., 2012). The ecosystem corresponds to the montane forest (Ministerio del Ambiente del Ecuador, 2013), which is characterized by trees with abundant orchids, ferns, and bromeliads. *Chilomys neisi* sp. nov. was collected in mature forest where the undergrowth is visually dominated by herbaceous families such as Poaceae (*Chusquea* sp.), Araceae, and Melastomataceae. On the steep slopes, the palm (*Ceroxylon* sp.) predominates. Stomach content from one specimen revealed as preys Coleoptera (one larva), and Chrysomelidae (one adult). *Chilomys neisi* sp. nov., was collected in sympatry with the didelphids *Marmosops caucacae*, *Caenolestes caniventer* and *C. condorensis*, and the rodents *Akodon mollis*, *Nephelomys albigularis*, *Microryzomys minutus*, *Oreoryzomys balneator*, and *Thomasomys taczanowskii*.

630

631 *Chilomys percequilloi* sp. nov. Brito, Tinoco, García and Pardiñas

632 urn:lsid:zoobank.org:act:0985D3E1-87C6-4E2E-B95A-53FB0C1C81C2

633 Percequillo Forest Mouse, Ratón del bosque de Percequillo (in Spanish)

634 **Holotype:** MECN 5854 (field number JBM 1959), an adult male captured 26 January, 2018, by
635 J. Brito, and N. Tinoco, preserved as dry skin, skull, postcranial skeleton and muscle and liver
636 biopsies in 95% ethanol.

637 **Paratopotypes:** MECN 5822, adult female, preserved as dry skin and cleaned skull, collected by
638 J. Brito, J. Curay and R. Garcia on 12 September, 2017. MECN 5858, and MECN 5859, adult
639 males, QCAZ 17552, juvenile male, QCAZ 17555, and QCAZ 17557, adult males, all preserved
640 as dry skins and cleaned skulls, collected by J. Brito and N. Tinoco on 29 January, 2018.

641 **Paratypes:** MEPN 6921, adult male, preserved as dry skin and cleaned skull, collected in
642 Provincia de Napo, Laguna Guataloma (-0.28°, -78.13°, 4,000 m) by M. Cueva on 30 September,
643 1996. MEPN 5827, and MEPN 5828, juvenile males, preserved as dry skins and cleaned skulls,
644 collected in Laguna Loreto (-03°, -78.15°, 4,050 m) by W. Pozo and F. Trujillo on 29 November,
645 1996. MEPN 10063, adult male, preserved as dry skin and cleaned skull, collected in Cuyuja (-
646 0.402°, -78.018°, 2,775 m) by L. Albuja and F. Trujillo on 29 May, 2005. MEPN 9937, juvenile
647 male, preserved as dry skin and cleaned skull, collected in Río Azuela (-0.75555°, -77.59083°,
648 1,600 m) by L. Albuja and F. Trujillo on 23 June, 2004. QCAZ 4189, male adult, preserved as
649 dry skin and cleaned skull, collected in Papallacta (-0.33422°, -78.1455°, 3,570 m) by S. Burneo
650 on 2 June, 2001. MECN 6338, juvenile male, and MECN 6361, adult male, preserved as dry
651 skins and cleaned skulls, collected in Provincia de Tungurahua, Reserva Naturetrek Vizcaya (-
652 1.35871°, -78.39558°, 2,391 m) by J. Brito, R. Vargas, E. Pilozo, T. Recalde and E. Peña on 13

May, 2021. MECN 6362, adult male, preserved as dry skin and cleaned skull, collected in Parque Nacional Llanganates (-1.355580°, -78.379180°, 3,268 m) by J. Brito, R. Vargas, E. Pilozo, T. Recalde and E. Peña on 18 May, 2021. MECN 3796, juvenile male, preserved as dry skin and cleaned skull, collected in Provincia de Morona Santiago, Sardinayacu, Parque Nacional Sangay (-2.074306°, -78.211833°, 1,766 m) by J. Brito, H. Orellana and G. Tenecota on 21 June, 2014. MECN 4327, MECN 4329, adult females, and MECN 4328, adult male, preserved as dry skins and cleaned skulls, collected in Cerro Sambalán, Parque Nacional Sangay (-2.206139°, -78.452694°, 2,851 m) by J. Brito, G. Pozo, and R. Ojala-Barbour on 15 January, 2015.

Type locality: Ecuador, Provincia de Morona Santiago, Cantón Méndez, Parroquia Patuca, Cordillera de Kutukú (-2.78722°, -78.13166°, WGS84 coordinates taken by GPS at the site of collection; elevation 2,215 m).

Etymology: This species is named in honor of Alexandre Reis Percequillo (nickname PC), Brazilian contemporary biologist devoted to the study of Neotropical mammal fauna and a specialist in oryzomyine rodents. The species epithet is formed from the surname “Percequillo,” taken as a noun in the genitive case, with the Latin suffix “i” (ICZN 31.1.2).

Diagnosis: A species of *Chilomys* ~~which can be~~ identified by the following combination of characters: tail with 18–20 rows of scales per centimeter on axis; zygomatic plate sloping backwards; M1–M2 with mesoloph; M2 with broader hypoflexus (similar in width to mesoflexus); m1 with anteromedian flexus; hemal arches present.

Morphological description of the holotype and variation: Small body size for the genus (head and body length combined ~~with a range~~ between 76 and 90 mm). Light neutral gray (color 297) dorsal fur; short hairs (medium length on back = 7.1 mm) with dark neutral gray (color 299) base

and smoke gray (color 266) tips. Smoke gray (color 155) ventral coat, with hairs (medium length = 5.5 mm) with pale neutral gray (color 297) base and smoke gray (color 266) tips. Surface of throat and chest lighter than rest of belly. Jet black (color 300) periocular ring (Figure 15). Postauricular patch absent. Mystacial vibrissae long, thick at base and thin towards tip, exceeding shoulder when tilted backwards; superciliary vibrissae 1 present, genal vibrissae 1 present. Ears (14–17 mm from notch to margin) externally covered by short smoke gray (color 266) hairs, pale buff (color 1) inner surface, medium neutral gray (color 298) margin.

Narrow and ground cinnamon drab (color 259) metatarsal patch, which extends to base of phalanges. Plantar surface with 6 pads, including 4 interdigitals of similar size, hypothenar pad smaller than thenar pad and with space between them; space between pads is covered by scales (Figure 4H). Short digit I reaches base of digit II; digit II slightly smaller than digit III and digit III same size as digit IV; short digit V (apparently somewhat opposable) reaches middle of digit IV. Long tail (118–133 mm; ~146% of HB), unicolor fawn (color 258) (in some specimens ventral tail is slightly paler than back) except for apex, which is white (up to 15 mm). Tail with 18–20 rows of scales per cm on axis; rectangular scales with three hairs each, which extend over 1.5 rows of scales in dorsal basal sector; naked-looking tail except for tip, where it presents a small brush of up to 5 mm. Protruding anus. Three mammary pairs in females, one pectoral, one abdominal, one inguinal; females with a long white clitoris (~5 mm) that contrasts with color of belly.

Cranium small for the genus (22.8–24.3 mm of CIL). Short and narrow rostrum, with nasal bones that do not extend to incisors; poorly developed gnathic process (Figure 16). Posterior margin of nasal bone does not exceed plane of lacrimal bone. Shallow zygomatic notch. Small and rounded lacrimal bones. Wide interorbital region with smooth outer edges,

exposing alveolar maxillary processes in dorsal view. Supraorbital region with diverging posterior borders. Frontoparietal suture U-shaped. Broad, rounded and inflated braincase, concave at outer edges. Developed ethmoturbinals (Figure 12H). Wide zygomatic plaque, comparatively longer than length of M1, and with posterior edge not reaching maxillary row. Zygomatic arches sturdy with jugals spanning a large segment of each mid-arch. Large supraorbital foramen with posterior border in line with M3 mesoflexus (Figure 8G). Alisphenoid strut wide and robust, thin and delicate (MECN 3796) or absent (MECN 4327) in young individuals. Carotid circulatory pattern type 3; carotid canal large, stapedia foramen small, without alisphenoid squamous groove and without sphenofrontal foramen. Subsquamous fenestra twice smaller than postglenoid foramen (Figure 16); hamular process of squamosal thin and long, and distally applied on mastoid capsule. Slightly triangular tegmen tympanic, superimposed with suspensory process of squamous. Lateral expressions of parietals present; bullae small; pars flaccida of tympanic membrane present, large; orbicular apophysis of malleus well-developed. Paraoccipital process small. Hill foramen small; short and narrow incisive foramen with curved edges without reaching plane defined by anterior faces of M1. Premaxillary capsule widened, parallel-sided and narrow at rear ends; maxillary septum of incisive foramen slim and long. Long and wide palate. Posterolateral palatal pit small. Narrow mesopterygoid fossa produced by a medium process of short and blunt palatine. Inconspicuous sphenopalatine vacuities covered by roof of palate. Large D-shaped foramen ovale. Middle lacerate foramen narrow. Auditory bullae small and uninflated with large and narrow eustachian tube (Figure 7E).

Dentary short, with short and narrow coronoid process (not extending beyond upper edge of condylar process); short and thin mental foramen ~~of jaw~~.

Proodont upper incisors (Thomas angle $\sim 92^\circ$; Figure 6E) with orange and smooth ~~front~~ enamel; crested and pentalophodont molars, with noticeably thick enamel. Maxillary molar rows slightly convergent backwards and slightly hypsodont; coronal surfaces crested; main cusps opposite (Figure 8H) and sloping backwards when viewed from side. M1 rectangular in outline with procingulum divided by anteromedian flexus into subequal anterolabial and anterolingual conules (in young specimens); deep anteroflexus (in young specimens); short and wide anteroloph; slim and long mesoloph; reduced posteroloph; internal closure of mesoflexus ends in a fosseta. M2 squared in outline; mesoloph showing same condition as in M1; broader hypoflexus (similar in width to mesoflexus); internal fosseta larger than fosseta of M1. M3 less than half the size of M2; M3 rounded in outline with conspicuous anteroloph; central fosseta large but smaller than M2. Lower molars with main cusps opposite (Figure 8H) and sloping forwards when viewed from side; tip of incisors is sharp. First lower molar (m1) with anteromedian flexid inconspicuous that divides procingulum into subequal anterolabial and anterolingual conulids; large anterolabial cingulum; ectolophid present; thin and short mesolophid. Mesoloph of m2 showing same condition as in m1; ectostylid present; noticeable anterolabial cingulum; hypoflexid of m3 long and wide. Hypoflexid well-developed and deep in m1–m3.

Tuberculum of first rib articulates with transverse processes of seventh cervical vertebra. First and second thoracic vertebrae have differentially elongated neural spine. Vertebral column is composed of 19 thoracicolumbar, 16th with moderately developed anapophyses and 17th with little developed anapophyses, 4 sacrals (fused), and 36–40 caudal vertebrae; with complete hemal arches in second and third caudal vertebra; 12 ribs.

Comparisons: *Chilomys percequilloi* sp. nov. is one of the small *Chilomys* species that inhabits Ecuador (Figure 3; Table 4). However, this species could be confused with *C. neisi* sp. nov. (states in parenthesis) ~~in the first instance~~, but can be differentiated by the following traits: Thomas angle $\sim 92^\circ$ (Thomas angle $\sim 102^\circ$); M1 with anteromedian flexus (without anteromedian flexus); M1–M2 with distinct mesoloph (indistinct mesoloph); M2 with broader hypoflexus, similar in width to mesoflexus (narrow hypoflexus, similar in width to mesoflexus); m1 with anteromedian flexus (without anteromedian flexus); hemal arches present (hemal arches absent).

Another species that inhabits the eastern flank of Ecuador (Figure 9) which is of similar size (see Table 4) **and** could be confused with *Chilomys percequilloi* sp. nov. is *Chilomys instans*. However, the former can be differentiated from *C. instans* (states in parenthesis) by the following traits: Thomas angle $\sim 92^\circ$ (Thomas angle $\sim 100^\circ$); m1 with anteromedian flexus (without anteromedian flexus); hemal arches present (hemal arches absent). A detailed comparison with all species of *Chilomys* is presented in Table 3.

Distribution: Known from several localities in the provinces of Napo to Morona Santiago (Ecuador), on the eastern flank of the Andes (Figure 9), at an elevation between 1,600 to 4,050 m. *Chilomys percequilloi* sp. nov. has the widest range of the five species described in the present work, covering about 300 lineal kilometres between its northernmost (Azuela River, Provincia de Sucumbíos, MEPN 9937) and southernmost records (Cordillera de Kutukú, Provincia de Morona Santiago, MECN 5858). Likewise, it has the highest altitudinal range of all known species of *Chilomys*, since it is distributed in the eastern foothills of the Andes, in the Provincias de Sucumbíos, Napo, Tungurahua and Morona Santiago, although one would expect to find it also in the provinces of Cotopaxi and Chimborazo. Taking into account this altitudinal range **we can** suppose that *Chilomys percequilloi* sp. nov. has an ample tolerance to different

environmental conditions. The average temperature among the recording localities is 13.3°C, with a significant variation between 1.1°C as the minimum temperature in November for Loreto Lagoon (Provincia de Napo), to 25.6°C as the maximum temperature in November for Kutukú (Provincia de Morona Santiago). With respect to the precipitation, the annual average is 1,960 mm, also showing a significant variation ranging from 1,090 mm at Reserva Naturetrek Vizcaya (Provincia de Tungurahua) to 3,400 mm in Kutukú (*Hijmans et al., 2005*).

Natural history: The zoogeographic area where *C. percequilloi* sp. nov. occurs is Eastern Sub-Tropical, Temperate and Altoandino (*Albuja et al., 2012*). The ecosystem corresponds to the montane forest (*Ministerio del Ambiente del Ecuador, 2013*), which is characterized by trees with abundant orchids, ferns, and bromeliads. *Chilomys percequilloi* sp. nov. was collected in mature forest where the undergrowth is visually dominated by herbaceous families such as Poaceae (*Chusquea* sp.), Araceae, and Melastomataceae. On the steep slopes, the royal palm (*Dictyocaryum lamarckianum*) predominates. Stomach contents of three specimens were analysed. Identifiable prey items were composed of 25% Lepidoptera, 25% Blattodea, 25% Diptera, and 25% Acari (Supplementary S4). *Chilomys percequilloi* sp. nov. was collected in sympatry with the didelphids *Marmosa germana*, *Marmosops cauae* and *Monodelphis adusta*, and the rodents *Akodon aerosus*, *A. mollis*, *Nephelomys auriventer*, *N. nimbosus*, *Oreoryzomys balneator*, *Rhipidomys albujae*, *Thomasomys pardignasi*, *T. cinnameus*, *T. erro*, and *T. salazari*.

***Chilomys weksleri* sp. nov.** Brito, García, Pinto and Pardiñas

urn:lsid:zoobank.org:act:292D0BA6-BF28-4C0D-BF26-1433DE9AE423

Weksler Forest Mouse, Ratón del bosque de Weksler (in Spanish)

Holotype: MECN 6365, an adult female captured 5 October, 2020, by C. Niveló and J. Viera, preserved as skull and carcass in ethanol, and muscle and liver biopsies in 95% ethanol.

Paratopotypes: MECN 6363, juvenile male, and MECN 6364, adult female, preserved as cleaned skulls and carcasses in ethanol, collected 1 October, 2020, by C. Niveló and J. Vieira.

Paratypes: MEPN 9954, adult male, preserved as dry skin and cleaned skull, collected in Provincia de Pichincha, Mindo Nambillo (-0.051° , -78.54° , 2,600 m) by M. Cueva on 30 September, 1996. MECN 4925, adult male, preserved as dry skin and cleaned skull, collected in Reserva Geobotánica Pululahua (0.02025° , -78.493138° , 3,190 m) by J. Curay, J. Brito, R. Vargas and K. Valdivieso on 2 April, 2016. MECN 4171, adult male, preserved as dry skin and cleaned skull, collected in Hacienda Tambillo Alto (-0.4073917° , -78.565991° , 2,833 m) by R. García on 9 November, 2014. QCAZ 1787, adult male, preserved as ethanol, collected by P. Jarrín on 9 September, 1996. QCAZ 8693, QCAZ 8694, and QCAZ 8695, (sex and age indeterminate), preserved as cleaned skulls and carcasses in ethanol, collected in Provincia de Cotopaxi, Reserva Integral Otonga (-0.4189° , -79.0039° , 2,000 m) by K. Helgen and C. M. Pinto on 15 August, 2006.

Type locality: Ecuador, Provincia de Cotopaxi, Cantón Sigchos, Parroquia San Francisco de Las Pampas, Reserva Integral Otonga (-0.685367° , -78.995089° , WGS84 coordinates taken by GPS at the site of collection; elevation 1,654 m).

Etymology: This species is named in honor of Marcelo Weksler, Brazilian contemporary biologist devoted to the study of living and fossil Neotropical cricetids. The species epithet is formed from the surname “Weksler,” taken as a noun in the genitive case, with the Latin suffix “i” (ICZN 31.1.2).

Diagnosis: A species of *Chilomys* which can be identified by the following combination of characters: Head and body length ~74–85 mm; tail longer than head and body length combined (~143–153%); dorsal surface of foot with round scales and small interspaces; zygomatic plate leaning forward; M2 with broader hypoflexus (similar in width to mesoflexus); m1 with anteromedian flexus.

Morphological description of the holotype and variation: Small body size (head and body length combined range between 74 and 85 mm). Brown (color 277) dorsal fur; short hairs (medium length on back = 6.5 mm), dark neutral gray (color 299). Dark neutral gray (color 299) venter coat, with hairs (medium length = 6.5 mm) with pale neutral gray (color 297) base and smoke gray (color 266) tips. Jet black (color 300) periocular ring. Postauricular patch absent. Mystacial vibrissae long, thick at base and thin towards tip, exceeding ears when tilted backwards; superciliary vibrissae 1 present, genal vibrissae 1 present. Ears (~14–16 mm from notch to margin) externally covered by short smoke gray (color 266) hairs, with whitish inner surface, and pale neutral gray (color 296) margin.

Narrow and sayal brown (color 41) metatarsal patch, which extends to base of phalanges; dorsal surface of foot with round scales and small interspaces. Plantar surface with 6 pads, including 4 interdigitals of similar size, thenar and hypothenar pads large and with small interspace; space between pads is smooth (Figure 4J). Short digit I reaches base of digit II; digit II slightly smaller than digit III and digit III slightly smaller than digit IV; short digit V reaches middle of digit IV. Whitish unguals equal or slightly surpassing tip of claws. Long tail (103–121 mm; ~148% of HB), buff (color 15) and bicolor (dark above and whitish below) except for apex, which is white (up to 22.6 mm). Tail with ~22–23 rows of scales per cm on axis; square

scales with three hairs each, which extend over 1–1.5 rows of scales; naked-looking tail except for tip, where it presents a small brush of up to 3.5 mm.

Cranium small for the genus (~21.5–23.5 mm of CIL). Short and narrow rostrum, with nasal bones that extend to incisors; poorly developed gnathic process. Posterior margin of nasal bone does not reach plane of lacrimal bone. Shallow zygomatic notch. Small and elongated lacrimal bones, almost entirely welded to maxillae. Wide interorbital region with smooth outer edges, without exposing alveolar maxillary processes in dorsal view (Figure 17A). Supraorbital region with diverging posterior borders. Frontoparietal suture V-shaped. Broad rounded and inflated braincase, concave at outer edges. Wide zygomatic plaque, comparatively longer than length of M1, and with posterior edge not reaching maxillary row. Zygomatic arches sturdy with jugals spanning a large segment of each mid-arch. Large supraorbital foramen with posterior border in line with M2 (Figure 6F). Alisphenoid strut present. Carotid circulatory pattern type 3; carotid canal large, stapedia foramen small, without alisphenoid squamous groove and without sphenofrontal foramen. Subsquamous fenestra three times smaller than postglenoid foramen (Figure 17C); hamular process of squamosal thin and long, and in contact on mastoid capsule. Slightly triangular tegmen tympanic, superimposed with suspensory process of squamous. Lateral expressions of parietals present; bullae small; pars flaccida of tympanic membrane present; orbicular apophysis of malleus well-developed. Paraoccipital process small. Hill foramen small (Figure 13F); short and narrow incisive foramen with curved edges not reaching plane defined by anterior faces of M1; a pair of ridges on either side of palatine foramina and in front of M1. Premaxillary capsule widened, converging and narrow at rear ends; maxillary septum of incisive foramen slim and long. Long and wide palate, with mesopterygoid fossa not reaching M3. Posterolateral palatal pit small. Wide mesopterygoid fossa, with by a

medium palatal process present. Inconspicuous sphenopalatine vacuities covered by roof of palate. Basisphenoid narrow. Large D-shaped foramen ovale. Middle lacerate foramen very narrow. Auditory bullae small and slightly inflated with short and wide eustachian tube (Figure 7F).

Dentary short, with short and narrow coronoid process (not extending beyond upper edge of condylar process); elongated and thin mental foramen ~~of jaw~~.

Proodont upper incisors (Thomas angle of $\sim 92^\circ$; Figure 6F) with orange and smooth ~~front~~ enamel; crested and pentalophodont molars, with noticeably thick enamel. Maxillary molar rows parallel; main cusps opposite (Figure 8I) and sloping backwards when viewed from side. M1 rectangular in outline with procingulum divided by anteromedian flexus into subequal anterolabial and anterolingual conules; thin and short anteroflexus; long paraflexus; long anteroloph; long and thin mesoloph; reduced posteroloph; internal closure of mesoflexus ends in a fosseta; anterior mure long. M2 squared in outline; mesoloph showing same condition as in M1; broader hypoflexus (similar in width to mesoflexus); internal fosseta similar to fosseta of M1; long and thin protoflexus. M3 less than half the size of M2; M3 rounded in outline with conspicuous anteroloph; central fosseta large, similar to M2. Lower molars with main cusps opposite (Figure 8J) and sloping forwards when viewed from side. First lower molar (m1) with anteromedian flexus that divides procingulum into subequal anterolabial and anterolingual conulids; short and thin mesolophid; small anterolabial cingulum; ectostylid present. Mesolophid of m2 showing same condition as in m1; ectostylid present. Hypoflexid of m3 long and wide; hypoflexid well-developed and deep in m1-m3.

Comparisons: *Chilomys weksleri* sp. nov., ~~the smallest species of the genus~~, inhabits Ecuador (Figure 3; Table 4). However, it could be confused in the first instance with *C.*

georgeledecii sp. nov. (states in parenthesis), from which can be differentiated by the following traits: Thomas angle $\sim 102^\circ$ (Thomas angle $\sim 92^\circ$); zygomatic plate comparatively wider than M1 and leaning forward (comparatively similar to M1 and slightly tilted backwards); M2 with broader hypoflexus, similar in width to mesoflexus (narrowed hypoflexus, but distinctly narrower than mesoflexus); m1 with anteromedian flexus (without anteromedian flexus). See detailed comparison of all *Chilomys* species in Table 3.

Distribution: *Chilomys weksleri* sp. nov. is distributed in the foothills of the Western Cordillera of the central Andes of Ecuador, between the Provincias de Pichincha and Cotopaxi (Figure 9), at elevations between 1,600 and 3,200 m. The four recorded localities register a temperature average of 14.2°C with the greatest fluctuation between annual minimum and maximum temperatures in August, reaching a minimum temperature of 5.2°C and a maximum temperature of 23.6°C . The average precipitation is 1,500 mm per year, with the lowest monthly precipitation of 28 mm in July, and the highest precipitation of 225 mm occurring in March (Hijmans et al., 2005).

Natural history: The zoogeographic area where *Chilomys weksleri* sp. nov. occurs is Temperate (Albuja et al., 2012). The ecosystem corresponds to the montane forest (Ministerio del Ambiente del Ecuador, 2013), which is characterized by trees with abundant orchids, ferns, and bromeliads. *Chilomys weksleri* sp. nov. was collected in mature forest where the undergrowth is visually dominated by herbaceous families such as Poaceae (*Chusquea* sp.), Araceae, and Melastomataceae. The species was collected in sympatry with the didelphids *Marmosops caucuae*, *Caenolestes caniventer* and *C. fuliginosus*, and the rodents *Akodon mollis*, *Nephelomys moerex*, *Microryzomys minutus*, *Thomasomys aureus*, *T. baeops*, and *T. silvestris*.

DISCUSSION

1. Diagnosing *Chilomys*

Most of the history of the knowledge of *Chilomys* reflects the scarcity of specimens available for study. *Thomas (1895, 1897)* described the type species and the genus based on one skull, which was also studied by *Ellerman (1941: 372)*. *Osgood (1912)* erected *C. fumeus* based on two individuals. With the second decade of the past century the collection surveys developed by several American institutions in Ecuador, Colombia and Venezuela retrieved an important input of specimens. Especially, the field efforts of George H. H. Tate (during 1920–1924 in Ecuador), Philip Hershkovitz (around 1950 in Colombia), and Charles Handley (around 1969 in Venezuela) greatly enriched the number of collected *Chilomys* (e.g., https://collections-zoology.fieldmuseum.org/list?search_fulltext=Chilomys; Handley, 1976). In any case, the new material did not change the poor perception on this Andean form, which was reduced to a monotypic condition after the influential treatises of *Gyldenstolpe (1932)* and *Cabrera (1961)*. As was summarized by *Voss (2003: 23)* “The morphologically distinctive genus *Chilomys* *Thomas (1897a)* is currently thought to contain only a single valid species, *C. instans* (*Thomas, 1895b*); another nominal taxon, *C. fumeus* *Osgood (1912)* is either a subspecies or synonym according to *Cabrera (1961)* and *Musser & Carleton (1993)*... A revision of this long-neglected northern-Andean endemic genus is necessary...”

Pacheco (2015) deserves the merit to having produced the first generic description of *Chilomys* including aspects of mostly external (based on the examination of dry skins) and cranial morphology. Interesting to note, despite more than a century, *Chilomys* remained explicitly undiagnosed; when *Thomas (1897)* coined the generic the name, probably he judged enough the description already provided for *instans* advanced few years before (*Thomas, 1895*).

From a formal point of view, therefore, *Chilomys* lacks a diagnosis, although the list of generic features collated by *Gyldenstolpe* (1932: 37) can be considered as such.

We provide an improved diagnosis and present several morphological features for the first time.

Family Cricetidae Fischer, 1817

Subfamily Sigmodontinae Wagner, 1843

Tribe Thomasomyini Steadman and Ray, 1982

Genus *Chilomys* Thomas, 1897

Type species (by monotypy).—*Oryzomys instans* Thomas, 1895.

Etymology.— None originally, but Néstor Cazzaniga (in litteris) suggested that *Thomas* (1897) employed the Greek noun *τιλός* (*chilos*), meaning “grass” to distinguish *Chilomys* from *Oryzomys*, whose generic epithet is composed of *ὄρσζα* (*oryza*), meaning “rice.”

Geographic distribution.— Known from Andean montane forests and Páramo-forest ecotone from northwestern Venezuela in the north to northern Peru in the south, generally ranging between 1,000 and 4,050 m above sea level.

Chronological distribution.—Recent; no fossils are known.

Contents.—The type species (*C. instans*) and, in order of nomination, *C. fumeus* Osgood, 1912, *C. carapazi* sp. nov. Brito & Pardiñas, *C. georgeledecii* sp. nov. Brito, Tinoco, García, Koch & Pardiñas, *C. neisi* sp. nov. Brito, Tinoco, García, Koch, & Pardiñas, *C. percequilloi* sp. nov. Brito, Tinoco, García & Pardiñas, and *C. weksleri* sp. nov. Brito, García, Pinto & Pardiñas (this paper).

Emended diagnosis.— Small-bodied (head and body length ~85 mm; body weight ~18 grams; condylobasal length ~23 mm), long-tailed (~140% of head and body length)

949 thomasomyines distinguished by the following combination of characters: Fur soft and straight,
 950 dark gray to gray-brown with venter not countershaded; ears medium sized; eyes small and
 951 rimmed by very short hair; mystacial vibrissae numerous and somewhat rigid, typically not
 952 surpassing auricular pinna when pressed backwards; pollex very small; hindfeet narrow and
 953 relatively long, dorsally unusually scaly and scarcely haired and ventrally typically smooth and
 954 having six well-defined pads; pes claws medium sized, moderately hooked and basally covered
 955 by whitish ungual tufts; protuberant but not prominent anus; large clitoris; tail unicolored thinly
 956 haired and typically having fleshy-colored distal inch; three pairs of mammae in inguinal,
 957 abdominal, and thoracic positions; cranium with markedly domed profile with comparatively
 958 short rostrum and large, rounded, deep braincase; nasals narrow, shorter than premaxillae, evenly
 959 converging backwards; shallow zygomatic notches; interorbital region broad and smooth;
 960 coronal suture U or V-shaped; large interparietal; nasolacrima capsules inflated; zygomatic
 961 plates narrow and high; zygomatic arches robust but not broadened and with their ventral
 962 margins placed distinctly above orbital floor; jugal long; large supraorbital foramina;
 963 conspicuous lateral expression of parietals; carotid circulation representing pattern 3 (sensu *Voss*,
 964 1988); alisphenoid struts typically present; tegmen tympanic overlaps suspensory processes of
 965 squamosals; hamular processes of squamosals large and distally applied to well-developed
 966 mastoid capsules; dorsal aperture of ectotympanic ring open; gnathic process absent; medium
 967 and large Hill foramen; incisive foramina short distantly placed from first upper molars;
 968 posterior parts of upper diastema marked by swollen ridges lying on either sides of incisive
 969 foramina, combined with masseteric scars distinctly placed anterior to root of zygomatic plates;
 970 palate broad, uncomplicated and typically long; parapterygoid plates well-defined and large,
 971 perforated by conspicuous ovale foramina and transverse canals; hamular processes of

pterygoids large; otic bullae flasked-shaped; upper incisors ungrooved and markedly proodont exhibiting Thomas' angles between 92–102° and in some species clearly visible in front of nasals in a vertical view of skull; molars noticeably small (microdont condition) and brachydont with thick enamel; mesolophs present in M1–M2 but tending to disappear with wear, closed remnants of mesoflexus persistent as fossettes in M1–M3; M3 markedly smaller than M2; m3 sigmoid-shaped; lower incisors slender and pointed; lower diastema flat and almost horizontal but markedly broad; lower border of dentary tending to flat; coronoid processes well-developed and hooked; condyles broad; capsular process well-developed; angular processes short; stomach unilocular-hemiglandular with subequal distribution of cornified and glandular epithelia; caecum small and single; gall bladder present; baculum with thin and sinoid-curved shaft and deeply concave and narrow base; complex penis with lateral cartilaginous digits thick and pointed and medial digit slim and blunter; one pair of preputials and larger medial and ventral prostates than lateral ones (after *Thomas, 1895; Osgood, 1912; Gyldenstolpe, 1932; Ellerman, 1941; Carleton, 1973; Steppan, 1995; Voss, 1991; Pacheco, 2015; Calderón-Capote et al., 2016; this paper*).

Description.— *Pacheco (2015)* provided a description of external and cranial features of *Chilomys*. We have elaborated here the anatomical fields that have been scarcely explored or not mentioned so far. Externally, *Chilomys* is characterized by a prominent head in comparison to body, with eyes of large size, beautifully rimmed in black and magnified by periocular rings of very short hairs. Mystacial vibrissae are numerous, blackish and whitish, of moderate length (not surpassing posterior margin of pinna when pressed against body) and inserted in a partially naked field, extended to both sides of nose and confluent with periocular ring (Figure 18A). *Chilomys* has a simple rhinarium characterized by a naked and broad dorsal integumental fold, non-sculptured nasal pads with almost undiscernibly horizontal grooves, ventral integumental

folds flanking lower external angle, nostrils of moderate size and a marked median sulcus. Both upper and lower lips are covered by short hairs (Figure 18B). Ears are noticeable although partially hidden in dorsal fur, appearing naked but covered by very short hairs. Pinnae are pinkish due to subjacent blood irrigation and characterized by a well-developed antihelix and antitragus and closed up by marked crura of antihelix delimiting a patent fossa triangularis and a recessed concha (Figure 18A).

Osgood (1912: 53) emphasized the unusually scaly nature of the dorsal surface of the pes in *C. fumeus*, a common condition in other species of *Chilomys* (Figure 4A-I). With a minor degree of variation, shortness and scarcity of hairs in upperparts of fore and hind foot contribute to make evident scales. The latter are subrectangular in shape, disposed in tight rows or sometimes appearing as disordered and extending scaly lining to fingers (i.e., first and second phalanx are dorsally covered by about 8 rows of scales). In addition, another peculiarity of cheiridia scales is the coloration, described as “...being dark colored with lighter margins” (*Osgood, 1912: 53*), a characteristic not seen in dry skins but very vivid in fresh or ethanol-preserved specimens. Finally, each digit is apically embellished with a dense tuft of ungual vibrissae, mostly expressed over third phalanx and scarcely reaching end of claw. The latter condition is highlighted by hallux, whose claw seems to be naked. The tip of each finger is covered basally with a turgid, deep callus and distally with an acute, moderately broad, medium-length, and ventrally open claw. The sole of the hind foot has been described as lacking imbrications, a statement coined by *Osgood (1912)* and quoted by contemporary authors (see *Pacheco, 2015*). Surely *Osgood (1912)* emphasized the naked nature of the undersurface, without scales but having a varying number of “granules” (a term used herein to denote and expand interspaces between interdigital pads and between first interdigital and thenar pads).

Both digit and metatarsal pads, **bulging**, rounded and roughly subequal in size and shape, even the hypothenar, which is typically smaller than the other plantar structures. Regarding the manus, *Osgood* (1912: 53) highlighted the minute condition of the pollex, **only** an excrescence related to the thenar pad (Figure 18C). The remainder four digits are subequal in length, markedly stocky and ringed, ending in deep calluses and topped off with broadened, but hooked claws. Almost the entire palm is occupied by the pads, being the interspaces smooth but crossed by a visible stria separating the digital group from the palmar group.

A protuberant anus is not prominent, according to *Pacheco* (2015), but appears as a noticeable orifice produced at the top of a fleshy bulbous structure (Figure 18D). The clitoris is decidedly large (Figure 18D), well haired and whitish and the mammae are disposed in three pairs, including an inguinal one.

Although the cranium of *Chilomys* was characterized by a short rostrum and the development of the braincase strongly dominated, the most impressive characteristic of the genus is clearly its microdonty. Viewed from below, the diastemal portion is capable of containing twice the molar series. More indeed, the diastemic palate anterior to the incisive foramina shows almost the same length as the latter mentioned structures and bears a well-enlarged Hill foramen. An additional unusual trait with occurrence in the diastemal portion was described by *Osgood* (1912: 54) as “... a pair of swollen ridges lying on either side of the palatine foramina and in front of M1” (Figure 13). These ridges, plus marked “scars” for the origin of the masseter superficialis and serrated premaxillary-maxillary sutures conform a set of characteristics presumably associated to a powerful masticatory musculature. Despite being described as narrow (*Pacheco*, 2015), the zygomatic plate **is** a solid and tall structure, with a short free upper border and far from the degenerative type that characterizes several small Andean

sigmodontines (*Thomas, 1927*). This is in line with robust zygomatic arches and well-developed jugals. Even having a long palate (according to the definition of *Herskovitz, 1962*), the parapterygoid region is also impressive in *Chilomys*, and the same can be said for the unusually large pterygoids. Finally, the braincase is firmly globular, giving the cranium a noticeable depth in lateral view, as there is no perceptible basicranial deflection. Several bony structures associated to this region appear magnified such as the infraorbital foramen, the hamular process of the squamosal, the dorsally produced tegmen tympani, etc.

The soft diastemal palate is very ample, and surpasses the interdental palate in this respect. It is crossed by three entire rugae, which are well separated from each other (Figure 18E). Five interdental rugae complete the dotation of the soft palate being partially bowed and well divided middorsally by a perceptible longitudinal sulcus. It is interesting to note how fixed the number of diastemic ridges appears to be, since three, if the anterior most bearing the incisive papilla is counted as one (*sensu Quay, 1954: fig. 1*), are widespread in cricetids. Thus, even the diastemal palate is large in *Chilomys*, there is no enlargement of the ridges but an enlargement of the rugae interspaces. The tongue fills the mouth closely when the molars are near occlusion. Its length comprises three times the molar series and its width is not greatly enlarged in the distal portion with respect to the intermolar portion. A shallow median sulcus dissects the dorsal surface of the distal 1/3 of the tongue, and an indistinct semilunar sulcus defines the anterior limit of the torus linguae. From the apex to a short distance anterior to the epiglottis, the surface is lined with filiform papillae resembling horny denticles. A single circumvallate papilla is located on the dorsal midline of the tongue, shortly anterior to the epiglottis (Figure 18F).

The stomach gross morphology was previously assessed based on three specimens of *C. weksleri* sp. nov. from Pichincha, Ecuador and typified as unilocular-hemiglandular (*Carleton,*

1973: fig. 3A, mentioned as *C. instans*). We here reaffirm this characterization after the dissection of more than 10 individuals representing several of the described species. No morphological differences attributable to taxonomy have been detected. A uniform unilocular-hemiglandular pattern with roughly equivalent distribution of cornified and glandular epithelia was registered; the walls of the corpus are thin and the internal surface moderately smooth to the naked eye, while the antrum has thicker walls; the bordering fold looks like a thick cord and probably acts effectively to produce a functional bicamerality in this kind of the unilocular stomach; very close to the esophageal opening the bordering fold bends strongly to the right, forming a narrow and definitive esophageal channel; finally, the stomach has a well-defined and broadened prepyloric part (Figure 19). We also confirm the widespread occurrence of a gallbladder in *Chilomys* (detected in *C. georgeledecii* sp. nov. MECN 5381, 5387, 6303, 6315, 6337, 6364; *C. instans* MECN 4769; *C. percequilloi* sp. nov. MECN 5593, 6338; *C. neisi* sp. nov. MECN 6187; and *C. weksleri* sp. nov. MECN 4171, 6365), which was first reported by Voss (1991: table 4) based on five specimens originally assigned to *C. instans* (AMNH 63370-63372; UMMZ 155619, 155620). In four species (*C. georgeledecii* sp. nov., *C. percequilloi* sp. nov., *C. neisi* sp. nov. and *C. weksleri* sp. nov.) examined to assert the general morphology of the intestine, the post-caecum portion was noticeably short (about 40 mm), while the pre-caecum intestine accounted for a medium length of about 180 mm. The gross morphology of the caecum was subequal among the species studied, consisting mostly of a single sac with two main constrictions, no appendix, and a rather simple colonic region (Figure 20). This general configuration is consistent with a fiber-free, enriched-protein diet free (Vorontsov, 1982).

Very little has been reported about the postcranial skeleton of *Chilomys* (see Steppan, 1995). The tuberculum of the first rib articulates with the transverse processes of the seventh

cervical; the first thoracic and the second thoracic vertebra have differentially elongated neural spine. The remainder ~~portion~~ of the axial skeleton is composed of 19 thoracolumbar, the 16th with moderately developed anapophyses and the 17th with little developed anapophyses, 4 sacrals (fused), and 36–40 caudal vertebrae with/without hemal arches. The recorded number of ribs is 12. The scapular notch extends to half of the scapula and the scapular spine does not reach the caudal border. A cursory inspection of the main long bones did not show the supratrochlear foramen of the humerus. The contact between the tibia and fibula occurs in the more medial part of these bones and the fibula reaches 50–60% of the length of the tibia.

2. Dental key traits: incisor procumbence and microdonty



After more than a century, and despite the considerable diversity added to the universe of sigmodontine rodents, *Thomas's* (1895) keen perception of the incisor procumbence in *Chilomys* is sustained (Figure 6). He stated “Upper incisors unusually thrown forwards, so that in a vertical view of the skull they are clearly visible in front of the nasals” (*Thomas, 1895: 369*). This condition was later termed as proodont (or pro-odont) by the same author (*Thomas, 1919*), who also typified orthodont and opisthodont to describe angular variations of the upper (unusually also applied to lower) incisors in rodents. To avoid any confusion, this author has illustrated how to take the angle formed by the upper incisor (*Thomas, 1919: fig. 1*), a descriptor today known as the “angle of Thomas” and employed for taxonomic differentiation (e.g., *Myers, 1989*). Interesting to note, *Herskovitz* (1962: 101-102) adopted Thomas’s terminology (and meaning) but introduced different vertical and horizontal planes to assess the procumbence of the incisors. While *Thomas* (1919) measured the angle formed by the chord of the incisor arc against the molar plane, *Herskovitz* (1962: fig. 19) used the interception between a “vertical

incisive-plane” with the “basal-incisive plane.” Although the latter was clearly defined (*HersHKovitz, 1962*: fig. 21), the former was illustrated but not described; intuitively, the “incisive-plane” should be the plane crossing the upper incisors by the centroid of the exposed (i.e., extralveolar) portion (*HersHKovitz, 1962*: fig. 21). More recent authors followed mostly the definitions of *HersHKovitz (1962)* (e.g., *Steppan, 1995, Pacheco, 2003*) but also introduced subtle variations in how planes are defined and/or interpreted. For example, *Weksler (2006: 43)* explained “The degree of upper incisor procumbency is defined by the position of the cutting edge of the incisor relative to the vertical-incisive plane (*HersHKovitz, 1962; Steppan, 1995*).” Therefore, this author introduced a new element compared to *Thomas (1919)*, the cutting edge, and eliminated one of the planes employed by *HersHKovitz (1962)*, the “basal-incisive plane.” In this context, it is clear that no angle can be calculated because a plane is missing, and the perception of incisor orientation is limited to a more or less subjective appreciation of the way these dents protrude forward or not. Although the original proposition of *Thomas (1919)* was criticized (see discussion in *Akersten, 1973*), it still seems to be the most objective way to assess incisor **procumbency** independently if the character is scrutinized for phylogenetical scoring or taxonomical/functional interpretation.

A **cursory** revision of the 90 living genera included within Sigmodontinae is conclusive **regarding** that the widespread condition is ~~the~~ opisthodonty (including the extreme state called hyper-opisthodont; see *Steppan, 1995: 17*). Orthodonty is much less frequent and proodonty is extremely rare. Regarding the latter two conditions, genus assignments varied between different authors, probably due to anarchy in estimating **procumbency** (vide supra). As such, *Ellerman (1941)* designated some species of *Necromys* (Akodontini), two genera of Phyllotini (*Auliscomys* and *Galenomys*), one Oryzomyini (*Scolomys*), and *Chilomys* as proodont, the latter being

designated as strongly proodont. *Herskovitz (1962)* agrees with the proodont condition of *Galenomys*, but limits the case of *Auliscomys* to the species *boliviensis*. However, *Steppan (1995: 19)* explicitly opposed the conclusion of *Herskovitz's (1962)* and typified both genera as orthodont, thus eradicating the proodonty of Phyllotini and the associated high-crowned sigmodontines (i.e., Andinomyini, Euneomyini, and Reithrodontini). *Weksler (2006: 43)* did the same, but with respect to Oryzomyini, apart from the impossibility of finding perpendicularity between two vertical planes, he concluded that “*Amphinectomys, Handleyomys, Melanomys, Oryzomys [= Mindomys] hammondi, Scolomys, and Sigmodontomys [= Tanyuromys] aphaerastus* have orthodont incisors with the cutting edge perpendicular to the vertical-incisive plane.” *Pacheco (2003)* restricted proodonty to *Abrawayamys, Chilomys*, and a few species of *Thomasomys*, while *Pardiñas, Teta & D’Elia (2009: table 2)* showed variation in upper incisor angles in *Abrawayamys*, implying a transition from opisthodontic to proodontic conditions. More recently, *Teta et al. (2017)* indicated **orthodont or slightly proodont** upper incisors in *Abrothrix* and *Chelemys*.

Apparently, extreme proodonty is not exclusive to *Chilomys*, as envisioned by *Thomas (1985)*, but it clearly deserves attention because this trait distinguishes the genus among the thomasomyines. The orientation of the upper incisors takes on a new meaning when combined with another dental characteristic of *Chilomys*: microdonty. The latter is applied here according to *Schmidt-Kittler (2006)*, implying that the molar tooth-row is comparatively short judged against the entire skull length. No previous authors mentioned this condition for *Chilomys*, but it is evident based on a direct inspection of the materials, or the ratio obtained dividing condyle-incisive length/upper molars tooth-row length (Table 4). Micro- and macrodonty are virtually unexplored traits of sigmodontines (*Ronez et al. 2020*). At least intuitively, however, the

diminution in molar size can be linked to insectivory, a relationship that has been discussed and demonstrated for other groups of mammals (e.g., *Freeman, 2000; Ungar, 2010*). There is no published information on the diet of *Chilomys*, although the genus has been categorized as insectivorous (*Maestri et al., 2017*: appendix S1). The examined stomach contents dissected here exclusively revealed insect and other invertebrate (Supplementary S3) remains including entire animals or large pieces of exoskeletons. This highly animal-protein diet is in agreement with the single caecum morphology displayed by *Chilomys* (*Vorontsov, 1982*; Figure 20). Having all these elements at hand, we can advance the hypothesis that this thomatomyine is an invertebrate-eater and its diet triggered two dental characteristics already discussed: proodonty and microdonty. Partially in contrast to a more widespread phenotype in the morphological evolution of sigmodontines that involves the “long-nosed” condition associated to insectivory (see *Martinez et al., 2018; Missagia & Perini 2018; Pardiñas et al., 2021*), specialization in short-rostrum *Chilomys* is a privilege of incisor procumbency. It is not known if this thomatomyine uses these teeth to pick and/or pinch invertebrates, or if they serve as digging tools when foraging. Two additional dental traits deserve mention here, as they are probably related to both non-exclusive strategies. *Thomas (1895)* described the lower incisors of *C. instans* as long and very slender, and we can confirm this characterization, but also emphasizing their acute tips (in fact, we pricked our fingers several times while working with the mandibles during the ~~conduction~~ of this study). In addition, the enamel of the molars of *Chilomys* looks unusually thick considering their minute size. In the context of the brachydont condition of the genus, the thickening of the enamel can be interpreted as a positively selected trait to counteract excessive wear caused by ingestion of soil particles (*Madden, 2015*).

3. Facing hidden Andean diversity in cricetids

The ~~new~~ speciose condition of *Chilomys* is not necessarily surprising. This thomasomyine genus is widespread in northern Andes and covers more than 10 degrees of latitude from western Venezuela to northern Peru (*Medina et al., 2016*). As a typical inhabitant of the montane forest belt that developed on both Andean slopes, *Chilomys* is not only exposed to the selection pressure of the moderate ecological gradient imposed by altitudinal variation (roughly from 1,600 to 4,050 m), but its range is also strongly fragmented by mountain discontinuity and fluvial systems (e.g., Táchira Depression, Huancabamba Depression, Mira and Jubones rivers). If we add to this current context the historical dimension, all the necessary elements are present to favor active speciation.

Our knowledge of the real diversity of *Chilomys* is still incipient. There is virtually no data for huge portions of its range, including almost all Colombian and Peruvian populations, but also for the southern Ecuadorian Andes. Therefore, nothing solid can be said about the history of diversification of the genus. However, focusing on the Ecuadorian diversity sampled, one could probably propose an allopatric speciation model (e.g., *Smith and Patton, 1992*). Time estimates derived from molecular phylogenies, although probably biased by poor fossil control, suggest the *Chilomys* originated in the Pleistocene (i.e., no older than 2.5 MA) and is considered sister to another rare thomasomyine, *Aepeomys* (see *Schenk & Steppan, 2018*).

Chilomys would have been exposed to numerous contractions and expansions of Andean vegetation belts triggered by the impact of glacial-interglacial cycles. Even admitting the high degree of regional variability, the multivariate local conditions, the occurrence of non-analogue vegetational assemblages, and likely? volcanic events,

1202 ~~etc.~~, from the pioneering studies to the recent most contributions on Quaternary paleoecology a
 1203 clear picture emerges: montane forests have been fragmented, compressed, expanded, and/or
 1204 isolated many times (e.g., *Van der Hammen, 1974; Marchant et al., 2002; Hooghiemstra and*
 1205 *Van der Hammen, 2004; Bakker et al., 2008; Cárdenas et al., 2011; Loughlin et al., 2018*).
 1206 Classical palynological long-term profiles, such as those of the High Plain of Bogota (western
 1207 side of the Cordillera Oriental in Colombia), ~~are eloquent to point to~~ several replacements between
 1208 Páramo-type vegetation and Andean forests during most of the Plio-Pleistocene (e.g.,
 1209 *Hooghiemstra, 1984; Clapperton, 1993* and the references cited therein). We are convinced that
 1210 the diversification of *Chilomys* was in part the result of Pleistocene expansion and contraction
 1211 cycles that led to geographic isolation and/or secondary contact of species, as has been suggested
 1212 for several other Andean animal and plant species (e.g., *Rull 2011; Nevado et al., 2018*).

1213 Numerous cricetids occurring in northern Andes are currently treated as mono- or
 1214 paucispecific genera (*Patton et al., 2015*). These are, among others, members of the tribes
 1215 Ichthyomyini (e.g., *Neusticomys*), Oryzomyini (e.g., *Microroryzomys, Oreoryzomys*),
 1216 Neomicroxini (e.g., *Neomicroxus*), etc. They share large geographical ranges with *Chilomys* and
 1217 are exposed to a variety of environmental gradients and topographical discontinuities. More
 1218 indeed, preliminary studies published or not, are revealing unexpected geographical variability.
 1219 Hence, *Chilomys* is surely not a unique case of an Andean sigmodontine with hidden diversity.
 1220 An important degree of genetic variation, partially coincident with different geographic Andean
 1221 units was recently reported for populations traditionally referred to *Neomicroxus latebricola*, a
 1222 Páramo sigmodontine (*Cañón et al., 2020*). Ongoing research is revealing that *Oreoryzomys*,
 1223 supposedly monotypic and even a plausible synonym of *Microroryzomys* (see *Percequillo, 2015*),
 1224 is not only a valid genus, but also consists of at least three species (*Brito et al., unpubl. data*).

Coupled with the extensive sampling being done by several teams of scientists (e.g., Instituto Nacional de Biodiversidad, Pontificia Universidad Católica del Ecuador) and the refinement of molecular studies and other kind of approaches, it is not unlikely that numerous species will be described or resurrected from nominal forms during this decade.

We began by stating that this addition to the specific diversity of *Chilomys* is not surprising, but challenging, and we would like to end this contribution with a brief elaboration on this second aspect of our findings. The impact of hidden diversity in several fields of our comprehension of the evolutionary biology is a candent (?) topic (see *Richter et al., 2021* and the references cited therein). Thomasomyines are probably one of the most remarkable expressions of the sigmodontine radiation in Andean habitats. However, their convoluted history as a tribe (e.g., mixed with the oryzomyines for many years), their supposed moderate diversity, and a perceptible stasis in their study, have led to a poor participation when the evolution of the subfamily is addressed (e.g., *Parada, D'Elia & Palma, 2015; Schenk & Steppan, 2018*). Extirpating *Rhagomys*, incorporated to Thomasomyini by *D'Elia et al. (2006)* but removed by *Pardiñas et al. (2021b)*, the tribe is currently composed of the living genera *Aepeomys*, *Chilomys*, *Rhipidomys* and *Thomasomys*, and the extinct *Megaoryzomys* being also in question of its tribal affiliation (*Ronez et al., 2020*). To date, our knowledge of *Aepeomys* and *Chilomys* is so scarce that attention to this suprageneric group has focused almost exclusively on *Rhipidomys* and *Thomasomys*. Although the latter is the most diverse living sigmodontine, with at least 47 species recognized as valid (*Brito et al., 2021; Ruelas & Pacheco, 2021*), this is not enough to make a clear impact in evolutionary explorations, since much of this diversity is not represented in molecular phylogenies (e.g., the most extensive contributions cover < 35% of the species, see *Brito et al., 2021; Ruelas & Pacheco 2021*). In addition, and judged generically, is a fact that the

diversity of Thomasomyini is pale in comparison with even minor groups such as Abrotrichini or Ichthyomyini. Reached to this point we are persuaded that thomasomyines represent a suitable example of the negative effect of hidden diversity. After the present contribution, the diversity of *Chilomys* is raised to seven species and therefore the genus now integrates the group of those with moderate specific richness (between five to ten species, e.g., *Abrothrix*, *Eligmodontia*, *Necomys*, *Nephelomys*). However, the real issue is whether *Thomasomys* does not represent a complex of genera, as strongly suggested by the morphological and molecular data collected by several scholars (e.g., Pacheco, 2003; Voss, 2003). The division of *Thomasomys* into eight genera, the number of species groups proposed by Pacheco (2015) and refined in subsequent studies (Brito et al., 2019; Brito et al., 2021), probably seems to cause over splitting. However, this scenario is not very different to the division of *Oryzomys* in several units of generic rank, as was proposed by Weksler et al. (2006) and widely accepted (e.g., Patton et al., 2015). There is still much to learn about the radiation of the thomasomyines, and unraveling their systematics is crucial to illuminating Andean biotic evolution and the history of the entire subfamily.

CONCLUSIONS

After more than a century of stasis in alpha taxonomy an integrative approach supported by extensive field sampling reveals that the poorly-known Andean thomasomyine *Chilomys instans* constitutes a complex of species. Five new species are described here, from Ecuadorian populations inhabiting montane forests on both sides of the Andes. Preliminarily, the newly revealed diversity can be attributed to allopatric speciation associated with the effect of Quaternary glacial-interglacial cycles on vegetation belts. *Chilomys* emerges as a

morphologically distinctive Andean thomomyine that exhibits unique specializations related to the procumbent incisors and probably related to an invertebrate feeding strategy.

ACKNOWLEDGEMENTS

To J. Robayo, J.P. Reyes, L. Jost, and H. Schneider of Basel Botanical Garden and Rainforest Trust; to the graduate biologists J. Curay, R. Vargas, C. Bravo, S. Pozo, K. Cuji, Z. Villacis, J. Guaya, J. Castro and E. Piloza (the ‘Minion’ team), and G. Pozo and R. Ojala-Barbour for invaluable field assistance; to the rangers of EcoMinga, especially H. Yela, T. Recalde, E. Peña, R. Peña, and M. Canticus for their deep efforts with field logistics; to D. Inclán and F. Prieto of INABIO, for their sponsorship and permanent support, to Roberto Portela Miguez (NHMUK) for access to collections and type material. M. Herrera (INABIO) kindly collaborated by identifying the stomach content. We are deeply indebted to the above-mentioned persons and institutions. This is an Initiative Vorontsov 2030’s contribution # 2.

REFERENCES

- Ade M. 1999. External morphology and evolution of the rhinarium of Lagomorpha, with special reference to the Glires hypothesis. *Mitteilungen aus dem Museum für Naturkunde in Berlin, Zoologische Reihe* 75:191–216.
- Akersten WA. 1973. Upper incisor grooves in the Geomyinae. *Journal of Mammalogy* 54:349–355.
- Albuja L, Almendáriz A, Barriga R, Montalvo LD, Cáceres F, Román JL. 2012. *Fauna de Vertebrados del Ecuador*. Quito: Instituto de Ciencias Biológicas, Escuela Politécnica Nacional.

- 1293 Anderson RP, Gutiérrez EE, Ochoa-G J, García FJ, Aguilera M. 2012. Faunal nestedness and
1294 species-area relationship for small non-volant mammals in “sky islands” of northern
1295 Venezuela. *Studies on Neotropical Fauna and Environment* 47:157–170 DOI
1296 [10.1080/01650521.2012.745295](https://doi.org/10.1080/01650521.2012.745295).
- 1297 Arana M, Ramírez O, Santa María S, Kunimoto C, Velarde R, de la Cruz C, Ruiz ML. 2002.
1298 Population density and reproduction of two Peruvian leaf-eared mice (*Phyllotis* spp.).
1299 *Revista Chilena de Historia Natural* 75:751–756.
- 1300 Bakker J, Moscol Olivera M, Hooghiemstra H. 2008. Holocene environmental change at the
1301 upper forest line in northern Ecuador. *Holocene* 18:877–893 DOI
1302 [10.1177/0959683608093525](https://doi.org/10.1177/0959683608093525).
- 1303 Bilton DT, Jaarola M. 1996. Isolation and purification of vertebrate DNAs. In: CLAPP, JP. ed.
1304 Species diagnostics protocols: PCR and other nucleic acid methods in molecular biology.
1305 Humana Press, Totowa, New Jersey 25–37 DOI [10.1385/0-89603-323-6:25](https://doi.org/10.1385/0-89603-323-6:25).
- 1306 Bonvicino C, Moreira M. 2001. Molecular phylogeny of the genus *Oryzomys* (Rodentia:
1307 Sigmodontinae) based on cytochrome b DNA sequences. *Molecular*
1308 *Phylogenetics and Evolution* 18:282–292 DOI [10.1006/mpev.2000.0878](https://doi.org/10.1006/mpev.2000.0878).
- 1309 Brito J, Batallas RB. 2014. Vocalizaciones de los ratones *Reithrodontomys soderstromi* y
1310 *Thomasomys paramorum* (Rodentia: Cricetidae) de la Provincia de Carchi, Ecuador
1311 *Avances en Ciencias e Ingenierías* 6:B13–B16 DOI [10.18272/aci.v6i2.173](https://doi.org/10.18272/aci.v6i2.173).
- 1312 Brito J, Pardiñas UFJ. 2017. Genus *Chilomys* Thomas, 1897. In: Wilson DE, Lacher TE Jr,
1313 Mittermeier RA, eds. *Handbook of the Mammals of the World-Volume 7: Rodents II*, 205–
1314 206.

- 1315 Brito J, Tinoco N, Curay J, Vargas R, Reyes-Puig C, Romero V, Pardiñas UF. 2019. Diversidad
1316 insospechada en los Andes de Ecuador: filogenia del grupo “cinereus” de *Thomasomys* y
1317 descripción de una nueva especie (Rodentia, Cricetidae). *Mastozoología Neotropical*
1318 26:308–330 DOI [10.31687/saremMN.19.26.2.0.04](https://doi.org/10.31687/saremMN.19.26.2.0.04).
- 1319 Brito J, Vaca-Puente S, Koch C, Tinoco N. 2021. Discovery of the first Amazonian *Thomasomys*
1320 (Rodentia, Cricetidae, Sigmodontinae): a new species from the remote Cordilleras del
1321 Cóndor and Kutukú in Ecuador. *Journal of Mammalogy* 102:615–635 DOI
1322 [10.1093/jmammal/gyaa183](https://doi.org/10.1093/jmammal/gyaa183).
- 1323 Cabrera A. 1961. Catálogo de los mamíferos de América del Sur. *Revista del Museo Argentino*
1324 *de Ciencias Naturales “Bernardino Rivadavia” e Instituto Nacional de Investigación de*
1325 *Ciencias Naturales* 4:309–732.
- 1326 Calderón-Capote MC, Jerez A, Sánchez Palomino P, Fernando López-Arévalo HF. 2016.
1327 Bacular morphology of seven species of high andean rodents from Colombia (Rodentia:
1328 Sigmodontinae). *Mastozoología Neotropical* 23:25–37.
- 1329 Cañón C, Curay J, Brito J, Colmenares-Pinzón JE, Pardiñas UFJ. 2020. Alpha-taxonomy in the
1330 cricetid rodent *Neomicroxus*, a first assessment *Therya* 11:374–389 DOI [10.12933/therya-](https://doi.org/10.12933/therya-20-983)
1331 [20-983](https://doi.org/10.12933/therya-20-983).
- 1332 Cárdenas ML, Gosling W, Sherlock SC, Poole I, Pennington RT, Mothes P. 2011. The Response
1333 of Vegetation on the Andean Flank in Western Amazonia to Pleistocene Climate Change.
1334 *Science* 331(6020):1055–1058 DOI [10.1126/science.1197947](https://doi.org/10.1126/science.1197947).
- 1335 Carleton MD, Musser CG. 1989. Systematic studies of Oryzomyine rodents (Muridae,
1336 Sigmodontinae): A synopsis of *Microryzomys*. *Bulletin of the American Museum of*
1337 *Natural History* 191:1–83.

- 1338 Carleton MD. 1973. A survey of gross stomach morphology in New World Cricetinae (Rodentia,
1339 Muroidea), with comments on functional interpretations. *Miscellaneous Publications,*
1340 *Museum of Zoology, University of Michigan* 146:1–43.
- 1341 Cerón C, Palacios W, Valencia R, Sierra R. 1999. Las formaciones naturales de la Costa del
1342 Ecuador. In: Sierra R. ed. *Propuesta preliminar de un sistema de clasificación de*
1343 *vegetación para el Ecuador continental*. Quito: Proyecto INEFAN/GERF-BIRF and
1344 Ecociencia.
- 1345 Clapperton C. 1993. Quaternary Geology and Geomorphology of South America.
1346 Amsterdam: Elsevier Science Publishers.
- 1347 Clavel J, Merceron G, Escargue G. 2014. Missing data estimation in morphometrics: how much
1348 is too much?. *Systematic Biology* 63:203–218 DOI [10.1093/sysbio/syt100](https://doi.org/10.1093/sysbio/syt100).
- 1349 Costa BMA, Geise L, Pereira LG, Costa LP. 2011. Phylogeography of *Rhipidomys* (Rodentia:
1350 Cricetidae: Sigmodontinae) and description of two new species from southeastern Brazil.
1351 *Journal of Mammalogy* 92:945–962 DOI [10.1644/10-MAMM-A-249.1](https://doi.org/10.1644/10-MAMM-A-249.1).
- 1352 D’Elía G, Luna L, González EM, Patterson BD. 2006. On the Sigmodontinae radiation
1353 (Rodentia, Cricetidae): an appraisal of the phylogenetic position of *Rhagomys*. *Molecular*
1354 *Phylogenetics and Evolution* 38:558–564 DOI [10.1016/j.ympev.2005.08.011](https://doi.org/10.1016/j.ympev.2005.08.011).
- 1355 Ellerman JR. 1941. The families and genera of living rodents. Trustees of the British Museum,
1356 London, United Kingdom.
- 1357 Freeman PW. 2000. Macroevolution in Microchiroptera: Recoupling morphology and ecology
1358 with phylogeny. *Evolutionary Ecology Research* 2:317–335.
- 1359 Gyldenstolpe N. 1932. A manual of Neotropical sigmodont rodents. *Kungliga Svenska*
1360 *Vetenskapsakademiens Handlingar*, ser. 3, band 11(3):1–164.

- 1361 Haidarliu S, Kleinfeld D, Ahissar E. 2013. Mediation of muscular control of rhinarial motility in
1362 rats by the nasal cartilaginous skeleton. *The Anatomical Record* 296:1821–1832 DOI
1363 [10.1002/ar.22822](https://doi.org/10.1002/ar.22822).
- 1364 Handley CO Jr. 1976. Mammals of the Smithsonian Venezuelan project. *Brigham Young*
1365 *University Science Bulletin, Biological Series* 20:1– 89.
- 1366 Hershkovitz P. 1962. Evolution of Neotropical cricetine rodents (Muridae) with special reference
1367 to the Phyllotine group. *Fieldiana: Zoology* 46:1–524.
- 1368 Hijmans RJ, Cameron SE, Parra JL, Jones PG, Jarvis A. 2005. Very high resolution interpolated
1369 climate surfaces for global land areas. *International Journal of Climatology* 25:1965–1978
1370 DOI [10.1002/joc.1276](https://doi.org/10.1002/joc.1276).
- 1371 Honaker J, King G, Blackwell M. 2011. Amelia II: A Program for Missing Data. *Journal of*
1372 *Statistical Software* 45:1–47. URL <http://www.jstatsoft.org/v45/i07/>.
- 1373 Ivanova NV, Zemlak T, Hanner RH, Hebert PDN. 2007. Universal primer cocktails for DNA
1374 fish barcoding. *Molecular Ecology Notes* 7:544–548 DOI [10.1111/j.1471-](https://doi.org/10.1111/j.1471-8286.2007.01748.x)
1375 [8286.2007.01748.x](https://doi.org/10.1111/j.1471-8286.2007.01748.x).
- 1376 Köhler G. 2012. Color catalogue for field biologists. Herpeton, Offenbach, 49 pp.
- 1377 Koutecký P. 2015. MorphoTools: a set of R functions for morphometric analysis. *Plant*
1378 *Systematics and Evolution* 301:1115–1121 DOI [10.1007/s00606-014-1153-2](https://doi.org/10.1007/s00606-014-1153-2).
- 1379 Kumar S, Stecher G, Li M, Knyaz C, Tamura K. 2018. MEGA X: Molecular Evolutionary
1380 Genetics Analysis across computing platforms. *Molecular Biology and Evolution* 35:1547–
1381 1549 DOI [10.1093/molbev/msy096](https://doi.org/10.1093/molbev/msy096).
- 1382 Lanfear R, Frandsen PB, Wright AM, Senfeld T, Calcott B. 2017. PartitionFinder 2: new
1383 methods for selecting partitioned models of evolution for molecular and morphological

- 1384 phylogenetic analyses. *Molecular Biology and Evolution* 34:772–773 DOI
- 1385 [10.1093/molbev/msw260](https://doi.org/10.1093/molbev/msw260).
- 1386 Loughlin Nicholas JD, Gosling WD, Coe AL, Gulliver P, Mothes P, Montoya E. 2018.
- 1387 Landscape-scale drivers of glacial ecosystem change in the montane forests of the eastern
- 1388 Andean flank, Ecuador. *Palaeogeography, Palaeoclimatology, Palaeoecology* 489:198–
- 1389 208 DOI [10.1016/j.palaeo.2017.10.011](https://doi.org/10.1016/j.palaeo.2017.10.011).
- 1390 Madden, R. H. 2015. Hypsodonty in mammals: Evolution, geomorphology and the role of earth
- 1391 surface processes. Cambridge University Press. Cambridge, United Kingdom.
- 1392 Maestri R, Monteiro LR, Fornel R, Upham NS, Patterson BD, de Freitas TRO. 2017. The
- 1393 ecology of a continental evolutionary radiation: Is the radiation of sigmodontine rodents
- 1394 adaptive?. *Evolution* 71:610–632 DOI [10.1111/evo.13155](https://doi.org/10.1111/evo.13155).
- 1395 Marchant R, Boom A, Hooghiemstra H. 2002. Pollen-based biome reconstructions for the past
- 1396 450,000 yr from the Funza-2 core, Colombia: comparisons with model-based vegetation
- 1397 reconstructions. *Palaeogeography, Palaeoclimatology, Palaeoecology* 177:29–45
- 1398 Mark. 2017. Program avg.py. Available at
- 1399 <https://stackoverflow.com/questions/42934340/taking-average-from-multiple-text-files-in-r>
- 1400 (accessed 6 July 2021).
- 1401 Martínez JJ, Sandoval ML, Carrizo LV. 2016. Taxonomic status of large- and middle-sized
- 1402 *Calomys* (Cricetidae: Sigmodontinae) from the southern central Andes inferred through
- 1403 geometric morphometrics of the skull. *Journal of Mammalogy* 97:1589–1601 DOI
- 1404 [10.1093/jmammal/gyw123](https://doi.org/10.1093/jmammal/gyw123).

- 1405 Martinez Q, Lebrun R, Achmadi AS, Esselstyn JA, Evans AR, Heaney LR, Miguez RP, Rowe
1406 KC, Fabre PH. 2018. Convergent evolution of an extreme dietary specialisation, the
1407 olfactory system of worm-eating rodents. *Scientific Reports* 8(1):17806 DOI
1408 [10.1038/s41598-018-35827-0](https://doi.org/10.1038/s41598-018-35827-0).
- 1409 Medina CE, Medina YK, Pino K, Pari A, López E, Zeballos H. 2016. Primer registro del ratón
1410 colombiano del bosque *Chilomys instans* (Cricetidae: Rodentia) en Cajamarca:
1411 actualizando el listado de mamíferos del Perú. *Revista Peruana de Biología* 23:315–320
1412 DOI [10.15381/rpb.v23i3.12868](https://doi.org/10.15381/rpb.v23i3.12868).
- 1413 Ministerio del Ambiente del Ecuador. 2013. Sistema de clasificación de los ecosistemas del
1414 Ecuador continental. Subsecretaría de Patrimonio Natural, Quito, Ecuador.
- 1415 Missagia RV, Perini FA. 2018. Skull morphology of the Brazilian shrew mouse *Blarinomys*
1416 *breviceps* (Akodontini; Sigmodontinae), with comparative notes on Akodontini rodents.
1417 *Zoologischer Anzeiger* 277:148–161 DOI <https://doi.org/10.1016/j.jcz.2018.09.005>.
- 1418 Musser GG, Carleton MD 2005. Superfamily Muroidea. In: Wilson DE, Reeder DM, eds.
1419 *Mammal Species of the World: A Taxonomic and Geographic Reference*. The Johns
1420 Hopkins University Press, Baltimore.
- 1421 Musser GG, Carleton MD, Brothers E, Gardner AL. 1998. Systematic studies of oryzomyine
1422 rodents (Muridae, Sigmodontinae): diagnoses and distributions of species formerly
1423 assigned to *Oryzomys* “capito.” *Bulletin of the American Museum of Natural History*
1424 236:1–376.
- 1425 Musser GG, Carleton MD. 1993. Family Muridae. In: Wilson DE, Reeder DM, eds. *Mammal*
1426 *species of the world: a taxonomic and geographic reference*. Smithsonian Institute,
1427 Washington, DC.

- 1428 Myers P. 1989. A preliminary revision of the various group of *Akodon* (*A. dayi*, *dolores*, *molinae*,
1429 *neocenus*, *simulator*, *toba* and *varius*). In: Redford KH, Eisenberg JF, eds. Advances in
1430 Neotropical Mammalogy. Gainesville, Florida: Sandhill Crane Press, Inc., pp. 5–54.
- 1431 Nevado B, Contreras-Ortiz N, Hughes C, Filatov DA. 2018. Pleistocene glacial cycles drive
1432 isolation, gene flow and speciation in the high-elevation Andes. *New Phytologist* 219: 779–
1433 793 DOI [10.1111/nph.15243](https://doi.org/10.1111/nph.15243).
- 1434 Osgood WH. 1912. Mammals from western Venezuela and eastern Colombia. *Field Museum of*
1435 *Natural History* 10:33–66.
- 1436 Pacheco V. 2003. Phylogenetic analyses of the Thomasomyini (Muroidea: Sigmodontinae) based
1437 on morphological data. Dissertation, City University New York.
- 1438 Pacheco V. 2015a. Genus *Chilomys* Thomas, 1897. In: Patton JL, Pardiñas UFJ, D’Elía G, eds.
1439 *Mammals of South America, Vol. 2: Rodents*, 577–580.
- 1440 Pacheco V. 2015b. Genus *Thomasomys* Coues, 1884. In: Patton JL, Pardiñas UFJ, D’Elía G, eds.
1441 *Mammals of South America, Vol. 2: Rodents*, 617–682.
- 1442 Parada A, D’Elía G, Palma RE. 2015. The influence of ecological and geographical context in
1443 the radiation of Neotropical sigmodontine rodents. *BMC Evolutionary Biology* 15:1–17
1444 DOI [10.1186/s12862-015-0440-z](https://doi.org/10.1186/s12862-015-0440-z).
- 1445 Pardiñas UF, Curay J, Brito J, Cañón C. 2021a. A unique cricetid experiment in the northern
1446 high-Andean Páramos deserves tribal recognition. *Journal of Mammalogy* 102:155–172
1447 DOI [10.1093/jmammal/gyaa147](https://doi.org/10.1093/jmammal/gyaa147).
- 1448 Pardiñas UF, Teta P, D’Elía G. 2009. Taxonomy and distribution of *Abrawayaomys* (Rodentia:
1449 Cricetidae), an Atlantic Forest endemic with the description of a new species. *Zootaxa*
1450 2128:39–60.

- 1451 Pardiñas UFJ, Tinoco N, Barbière F, Ronez C, Cañón C, Lessa G, Koch C, Brito J. 2021b.
1452 Morphological disparity in a hyper diverse mammal clade: A new morphotype and tribe of
1453 Neotropical cricetids. *Zoological Journal of the Linnean Society* (in press).
- 1454 Pearson OP. 1957. Additions to the mammalian fauna of Peru and notes on some other Peruvian
1455 mammals. *Brevoria* 73:1–7.
- 1456 Pinto CM, Ojala-Barbour R, Brito J, Menchaca A, Carvalho ALG, Weksler M, Amato G, Lee Jr
1457 TE. 2018. Rodents of the eastern and western slopes of the Tropical Andes: phylogenetic
1458 and taxonomic insights using DNA barcodes. *Therya* 9:15–27 DOI [10.12933/therya-18-](https://doi.org/10.12933/therya-18-430)
1459 [430](https://doi.org/10.12933/therya-18-430).
- 1460 Puillandre N, Lambert A, Brouillet S, Achaz GJME. 2012. ABGD, Automatic Barcode Gap
1461 Discovery for primary species delimitation. *Molecular Ecology* 21:1864–1877 DOI
1462 [10.1111/j.1365-294X.2011.05239.x](https://doi.org/10.1111/j.1365-294X.2011.05239.x).
- 1463 R Core Team. 2019. R: A language and environment for statistical computing. R Foundation for
1464 Statistical Computing, Vienna, Austria. URL <https://www.R-project.org/>.
- 1465 Reig OA. 1977. A proposed unified nomenclature for the enameled components of the molar
1466 teeth of the Cricetidae (Rodentia). *Journal of Zoology* 181:227–241.
- 1467 Richter A, Nakamura G, Iserhard CA, Duarte LDS. 2021. The hidden side of diversity: Effects of
1468 imperfect detection on multiple dimensions of biodiversity. *Ecology and Evolution* DOI
1469 [10.1101/2021.06.02.446400](https://doi.org/10.1101/2021.06.02.446400).
- 1470 Ronez C, Barbière F, De Santis L, Pardiñas UF. 2020. Third upper molar enlargement in
1471 sigmodontine rodents (Cricetidae): morphological disparity and evolutionary convergence.
1472 *Mammalia* 84:278–282 DOI [10.1515/mammalia-2019-0031](https://doi.org/10.1515/mammalia-2019-0031).

- 1473 Ronquist F, Teslenko M, Van Der Mark P, Ayres D, Darling AA, Höhna S, Larget B, Liu L,
1474 Suchard MA, Huelsenbeck JP. 2012. MrBayes 3.2: Efficient Bayesian phylogenetic
1475 inference and model choice across a large model space. *Systematic Biology* 61:539–542 DOI
1476 [10.1093/sysbio/sys029](https://doi.org/10.1093/sysbio/sys029).
- 1477 Ruelas D, Pacheco V. 2021. A new species of *Thomasomys* Coues, 1884 (Rodentia:
1478 Sigmodontinae) from the montane forests of northern Peru with comments on the "aureus"
1479 group. *Revista peruana de biología* 28(3):e19912 DOI [10.15381/rpb.v28i3.1991](https://doi.org/10.15381/rpb.v28i3.1991).
- 1480 Rull V. 2011. Neotropical biodiversity: timing and potential drivers. *Trends in Ecology and*
1481 *Evolution* 26:508–513 DOI [10.1016/j.tree.2011.05.011](https://doi.org/10.1016/j.tree.2011.05.011).
- 1482 Sahley CT, Cervantes K, Pacheco V, Salas E, Paredes D, Alonso A. 2015. Diet of a
1483 sigmodontine rodent assemblage in a Peruvian montane forest. *Journal of Mammalogy*
1484 96:1071–1080 DOI [10.1093/jmammal/gyv112](https://doi.org/10.1093/jmammal/gyv112).
- 1485 Sahley CT, Cervantes K, Salas E, Paredes D, Pacheco V, Alonso A. 2016. Primary seed dispersal
1486 by a sigmodontine rodent assemblage in a Peruvian montane forest. *Journal of Tropical*
1487 *Ecology* 32:125–134 DOI [10.1017/S026646741600](https://doi.org/10.1017/S026646741600).
- 1488 Salazar-Bravo J. 2015. Genus *Calomys* Waterhouse, 1837. In: Patton JL, Pardiñas UFJ, D’Elia
1489 G, eds. *Mammals of South America, Vol. 2: Rodents*, 481–507.
- 1490 Schenk JJ, Steppan S J. 2018. The role of geography in adaptive radiation. *The American*
1491 *Naturalist* 192:415–431.
- 1492 Schmidt-Kittler, N. 2006. Microdonty and macrodonty in herbivorous mammals.
1493 *Palaeontographica Abteilung A* 278:163–179 DOI [10.1127/pala/278/2006/163](https://doi.org/10.1127/pala/278/2006/163).

- 1494 Sikes RS, & Animal Care and Use Committee of the American Society of Mammalogists. 2016.
1495 Guidelines of the American Society of Mammalogists for the use of wild mammals in
1496 research and education. *Journal of Mammalogy* 97:663–688 DOI
1497 [10.1093/jmammal/gyw078](https://doi.org/10.1093/jmammal/gyw078).

- 1498 Smith MF, Patton JL. 1993. The diversification of South American murid rodents: evidence from
1499 mitochondrial DNA sequence data for the akodontine tribe. *Biological Journal of the*
1500 *Linnean Society* 50:149–177 DOI [10.1111/j.1095-8312.1993.tb00924.x](https://doi.org/10.1111/j.1095-8312.1993.tb00924.x).

- 1501 Smith MF, Patton JL. 1999. Phylogenetic relationships and the radiation of sigmodontine rodents
1502 in South America: evidence from cytochrome b. *Journal of Mammalian Evolution* 6:89–
1503 128 DOI [10.1023/A:1020668004578](https://doi.org/10.1023/A:1020668004578).

- 1504 Soriano PJ, Díaz de Pascual A, Ochoa-G J, Aguilera M. 1999. Biogeographic analysis of the
1505 mammal communities in the Venezuelan Andes. *Interciencia* 24:17–25.

- 1506 Stamatakis A. 2014. RAxML version 8: a tool for phylogenetic analysis and post analysis of
1507 large phylogenies. *Bioinformatics* 30:1312–1313 DOI [10.1093/bioinformatics/btu033](https://doi.org/10.1093/bioinformatics/btu033).

- 1508 Steppan S. 1995. Revision of the tribe Phyllotini (Rodentia: Sigmodontinae), with a
1509 phylogenetic hypothesis for the Sigmodontinae. Revisión de la tribu Phyllotini (Rodentia:
1510 Sigmodontinae), con una hipótesis filogenética para los Sigmodontinae. *Fieldiana*
1511 *Zoology* 1464:1–112.

- 1512 Steppan SJ, Ramirez O. 2015. Genus *Phyllotis* Waterhouse, 1837. In: Patton JL, Pardiñas UFJ,
1513 D’Elia G, eds. *Mammals of South America, Vol. 2: Rodents*, pp. 535–555.

- 1514 Strauss RE, Atanassov MN, de Oliveira JA. 2003. Evaluation of the principal-component and
1515 expectation-maximization methods for estimating missing data in morphometric studies.

- 1516 *Journal of Vertebrate Paleontology* 23:284–296 DOI [10.1671/0272-](https://doi.org/10.1671/0272-4634(2003)023[0284:EOTPAE]2.0.CO;2)
- 1517 [4634\(2003\)023\[0284:EOTPAE\]2.0.CO;2](https://doi.org/10.1671/0272-4634(2003)023[0284:EOTPAE]2.0.CO;2).

- 1518 Teta P, Cañón C, Patterson BD, Pardiñas UF. 2017. Phylogeny of the tribe Abrotrichini
- 1519 (Cricetidae, Sigmodontinae): integrating morphological and molecular evidence into a new
- 1520 classification. *Cladistics* 33:153–182 DOI [10.1111/cla.12164](https://doi.org/10.1111/cla.12164).

- 1521 Thomas O. 1895. Description of four small Mammals from South America, including one
- 1522 belonging to the peculiar Marsupial Genus “*Hyracodon*,” Tomes. *Annals and Magazine of*
- 1523 *Natural History serie 6* 16:367–370.

- 1524 Thomas O. 1897. Notes on some S. American Muridae. *Annals and Magazine of Natural*
- 1525 *History, Series 6*, 19:494–501.

- 1526 Thomas O. 1919. The method of taking the incisive index in rodents. *Annals and Magazine of*
- 1527 *Natural History* 4:289–290.

- 1528 Thomas O. 1927. The Godman-Thomas Expedition to Peru.—V. On mammals collected by Mr.
- 1529 R. W. Hendee in the Province of San Martin, N. Peru, mostly at Yurac Yacu. *Annals and*
- 1530 *Magazine of Natural History* 9th Series 19:361–375.

- 1531 Tirado C, Cortés A, Bozinovic F. 2008. Water balance in two South American *Phyllotis* desert
- 1532 rodents, *P. xanthopygus rupestris* and *P. darwini darwini*. *Journal of Arid Environments*
- 1533 72:664–670.

- 1534 Tirira, D. 2017. Guía de campo de los mamíferos del Ecuador. Editorial Murciélagos Blanco,
- 1535 Quito, Ecuador.

- 1536 Tribe CJ. 1996. The neotropical rodent genus *Rhipidomys* (Cricetidae: Sigmodontinae): a
- 1537 taxonomic revision. Ph.D. Dissertation, University College London. London, United
- 1538 Kingdom.

- 1539 Ungar PS. 2010. Mammal teeth: origin, evolution, and diversity. JHU Press, Baltimore. pp. 288.
- 1540 Van der Hammen T. 1974. The Pleistocene changes of vegetation and climate in tropical South
1541 America. *Journal of Biogeographic* 1:3–26.
- 1542 Vorontsov NN. 1982. [The hamsters (Cricetidae) of the world fauna. Part 1. Morphology and
1543 ecology]. *Fauna of the USSR, New Series M° 125, Mammals* 3: 1–452 [in Russian].
- 1544 Voss R. 1993. A revision of the Brazilian muroid rodent genus *Delomys* with remarks on
1545 “thomatomyine” characters. *American Museum Novitates* 3073:1–44.
- 1546 Voss RS. 1991. An introduction to the Neotropical muroid rodent genus *Zygodontomys*. *Bulletin*
1547 *of the American Museum of Natural History* 210:1–120.
- 1548 Voss RS. 2003. A new species of *Thomasomys* (Rodentia: Muridae) from eastern Ecuador, with
1549 remarks on mammalian diversity and biogeography in the Cordillera Oriental. *American*
1550 *Museum Novitates* 3421:1–47.
- 1551 Weksler M. 2006. Phylogenetic relationships of oryzomine rodents (Muroidea: Sigmodontinae):
1552 separate and combined analyses of morphological and molecular data. *Bulletin of the*
1553 *American Museum of Natural History* 296:1–149 DOI [10.1206/0003-](https://doi.org/10.1206/0003-0090(2006)296[0001:PROORM]2.0.CO;2)
1554 [0090\(2006\)296\[0001:PROORM\]2.0.CO;2](https://doi.org/10.1206/0003-0090(2006)296[0001:PROORM]2.0.CO;2).
- 1555 Zeballos H, Palma RE, Marquet PA, Ceballos G. 2014. Phylogenetic relationships of *Calomys*
1556 *sorellus* complex (Rodentia: Cricetidae), with the description of two new species. *Revista*
1557 *Mexicana de Mastozoología Nueva época* 4:1–23.
- 1558 Zhang J, Kapli P, Pavlidis P, Stamatakis A. 2013. A general species delimitation method with
1559 applications to phylogenetic placements. *Bioinformatics* 29:2869–2876 DOI
1560 [10.1093/bioinformatics/btt499](https://doi.org/10.1093/bioinformatics/btt499).
- 1561

1562

1563

1564

1565

1566

1567 **Supplemental files**

1568

1569 **Supplementary S2:** List of studied **specimens belonging** to the following

1570 mammal collections: FMNH, Field Museum of Natural History, USA; MECN, Instituto Nacional
1571 de Biodiversidad, Quito, Ecuador; NHMUK, Natural History Museum, London, United Kingdom;
1572 MEPN, Museo de la Escuela Politécnica Nacional, Quito, Ecuador; QCAZ, Museo Pontificia
1573 Universidad Católica del Ecuador, Quito, Ecuador; specimens marked with an * are holotypes.

1574 **Supplementary S2:** Sequences used in the analysis genetic.

1575 **Supplementary S3:** Maximum likelihood tree of the mitochondrial cytochrome oxidase I (COI).

1576 In colors the species described within the genus *Chilomys*: gene. *C. georgeledecii* sp. nov.
1577 (Reserva Dracula), *C. instans* (Reserva Ecológica El Angel), *C. neisi* sp. nov. (El Oro – Zamora
1578 Chinchipe), *C. percequilloi* sp. nov. (Napo – Morona Santiago), *C. weksleri* sp. nov. (Reserva
1579 Integral Otonga). The values above and below **the branches represent bootstrap** and
1580 posterior probability.

1581 **Supplementary S4:** Stomach content composition of *Chilomys*.

Table 1(on next page)

Genetic distances.

Matrix of corrected genetic distances (expressed as %, below the diagonal) of Cytochrome b (Cytb) gene sequences among clades of the genus of rodent *Chilomys*; values above the diagonal are the standard deviation.

1

	1	2	3	4	5	6
1 Colombia		0.78	1.06	0.70	0.89	0.91
2 Reserva Ecológica El Ángel - Carchi	6.97		1.01	0.67	0.87	0.85
3 El Oro - Zamora Chinchipe	9.01	7.75		0.88	0.76	0.88
4 Reserva Dracula - Carchi	4.96	4.88	6.12		0.79	0.66
5 Napo - Morona Santiago	10.17	8.72	6.25	7.41		0.75
6 Reserva Integral Otonga - Cotopaxi	9.35	8.09	7.12	5.85	7.79	

2

Table 2 (on next page)

Loadings and percentage of the explained variation of the principal component analysis.

Loadings and percentage of the explained variation of the Principal Component Analysis (first three principal components) and of the Discriminant Function Analysis (first three discriminant functions) performed on five species of the genus of rodent *Chilomys*. Acronyms of variables are explained in the main text (Materials and Methods section).

1

	Character	PC1	PC2	PC3	DF1	DF2	DF3
1	CIL	0.229	0.042	0.077	0.411	-0.110	0.011
2	LM	0.068	0.071	0.335	0.277	-0.175	-0.056
3	LR	0.199	0.033	0.178	0.352	-0.068	-0.109
4	HR	0.161	-0.126	0.084	0.344	-0.065	0.266
5	LN	0.294	0.199	0.231	0.547	0.183	0.001
6	HC	0.065	0.084	0.158	0.356	0.038	-0.152
7	BM1	0.130	-0.029	0.380	0.258	-0.058	0.027
8	LIF	0.246	-0.227	0.112	0.266	-0.175	0.000
9	BIF	0.110	-0.255	0.328	0.263	-0.453	0.319
10	BPB	0.060	-0.251	-0.054	0.074	-0.244	0.236
11	BZP	0.473	0.337	0.000	0.520	0.058	0.116
12	LIB	0.085	-0.046	0.060	0.329	-0.567	-0.032
13	ZB	0.151	-0.008	0.024	0.345	-0.104	0.243
14	MB	0.064	-0.477	0.192	0.060	0.003	-0.007
15	DI	0.434	0.007	-0.397	0.283	-0.090	0.058
16	BIT	0.396	-0.478	-0.336	0.345	-0.056	0.031
17	MMR	0.082	0.048	0.407	0.374	-0.090	-0.105
18	GLM	0.194	0.032	0.020	0.357	-0.131	0.078
19	DR	0.217	0.416	-0.142	0.309	0.103	0.372
	% Variation	68.03	5.45	4.87	30.54	23.69	20.48

2

Table 3(on next page)

Morphological comparisons.

Morphological comparisons of selected traits among species of the genus of rodent *Chilomys*.

1

<i>C. carapazi</i>	<i>C. georgeledecii</i>	<i>C. percequilloi</i>	<i>C. neisi</i>	<i>C. weksleri</i>	<i>C. instans</i>	<i>C. fumeus</i>
Head and body length ~95 mm	Head and body length range 83–90 mm	Head and body length range 76–90 mm	Head and body length range 95–100 mm	Head and body length range 74–85 mm	Head and body length range 78–98 mm	Head and body length range 86–90 mm
Tail ~134 % head-body length	Tail ~144,44–177.78 % head-body length	Tail ~137–155% head-body length	Tail ~134–136% head-body length	Tail ~143–153 head-body length	Tail ~112–146% head-body length	Tail ~134–139% head-body length
Tail with 16 rows of scales per cm on the axis	Tail with 16-18 rows of scales per cm on	Tail with 18-20 rows of scales per cm on the axis	Tail with 15-16 rows of scales per cm on the axis	Tail with 16 rows of scales per cm on the axis	Tail with 17-19 rows of scales per cm on the axis	Tail with 16 rows of scales per cm on the axis
Dorsal surface of the foot with round scales and without interspaces	Dorsal surface of the foot with round scales and large interspaces	Dorsal surface of the foot with round scales and small interspaces	Dorsal surface of the foot with round scales and small interspaces	Dorsal surface of the foot with round scales and small interspaces	-	Dorsal surface of the foot with round scales and small interspaces
Large thenar and hypothenar pads, ample interspace	Large thenar and hypothenar pads, small interspace	Hypothenar smaller than thenar pad	Small thenar and hypothenar pads, ample interspace	Large thenar and hypothenar pads, small interspace	Large thenar and hypothenar pads, small interspace	-
Interspace between pads smooth	Interspace between pads smooth	Interspace between pads scaly	Interspace between pads smooth	Interspace between pads smooth	Interspace between pads smooth	Interspace between pads smooth
Nasals long 8.55 mm	Nasals short 6.1–7.5 mm	Nasal long 7.2–8.8 mm	Nasals long 8.4–8.8 mm	Nasals long 7.2–7.7 mm	Nasals long 7.4–8.76 mm	Nasals short 6.41–7.39 mm
Broad zygomatic plates 2.60 mm	Narrowed zygomatic plates 1.66–2.09 mm	Broad zygomatic plates 2.03–2.3 mm	Broad zygomatic plates 2.1–2.4 mm	Narrowed zygomatic plates 1.8–2.1 mm	Broad zygomatic plates 2.05–2.41 mm	Narrowed zygomatic plates 1.34–1.96 mm
Diastema long 8.23 mm	Diastema long 6.5–7.4 mm	Diastema long 7–7.58 mm	Diastema long 7.33 mm	Diastema long 6.8–7.39 mm	Diastema long 7.0–7.91 mm	Diastema short 6.14–6.96 mm

Thomas angle 95°	Thomas angle 102°	Thomas angle 92°	Thomas angle 102°	Thomas angle 92°	Thomas angle 100°	Thomas angle 94°
M1 without flexus anteromedian	M1 with flexus anteromedian	M1 with flexus anteromedian	M1 without flexus anteromedian	M1 with flexus anteromedian	M1 with flexus anteromedian	M1 with flexus anteromedian
M1-M2 present Mesoloph	M1-M2 present Mesoloph	M1-M2 present Mesoloph	M1-M2 indistinct Mesoloph	M1-M2 present Mesoloph	M1-M2 present Mesoloph	M1-M2 present Mesoloph
M2 with broader hypoflexus (similar in width to mesoflexus)	M2 with narrowed hypoflexus (distinctly narrower than mesoflexus)	M2 with broader hypoflexus (similar in width to mesoflexus)	M2 with narrowed hypoflexus (distinctly narrower than mesoflexus)	M2 with broader hypoflexus (similar in width to mesoflexus)	M2 with broader hypoflexus (similar in width to mesoflexus)	M2 with narrowed hypoflexus (distinctly narrower than mesoflexus)
Maxillary tooththrow large 3.4 mm	Maxillary tooththrow large <3.2 mm	Maxillary tooththrow large <3.4 mm	Maxillary tooththrow large <3.2 mm	Maxillary tooththrow large <3.3 mm	Maxillary tooththrow large >3.1 mm	Maxillary tooththrow short <3.1 mm
m1 without flexus anteromedian	m1 with flexus anteromedian	m1 with flexus anteromedian	m1 without flexus anteromedian	m1 with flexus anteromedian	m1 without flexus anteromedian	m1 without flexus anteromedian
-	Hemal arches present	Hemal arches present	Hemal arches absent	Hemal arches present	Hemal arches Absent	Hemal arches present
This study	This study	This study	This study	This study	Pacheco, 2015; this study	Osgood, 1912; Pacheco, 2015; this study

Table 4 (on next page)

Comparative statistic.

Univariate statistics (\bar{x} = mean; SD = standard deviation; max = maximum; min = minimum; N = number of specimens) and external and craniodental measurements (in mm), and weight in grams for each species of the genus *Chilomys*; measured specimens are listed in Appendix 1; acronyms are explained in the main text.

1

<i>C. carapazi</i> sp. nov.		<i>C. georgeledecii</i> sp. nov.						<i>C. percequilloi</i> sp. nov.						<i>C. neisi</i> sp. nov.		<i>C. weksleri</i> sp. nov.						<i>C. instans</i>					
Holotype		Holotyp e		Paratypes				Holotyp e		Paratypes				Holotyp e		Paratyp e		Holotyp e		Paratypes				Holotype			
MECN 5291		MECN 6024		□	SD	max	min	N	MECN 5854		□	SD	max	min	N	MECN 6187		MECN 6365		□	SD	max	min	N	NHMUK 1895.10.14 .1		
HBL	95	80		78	8.37	90	63	24	95		86	6.94	95	70	18	95		100	75		75.8	8.46	85	65	5	99	
LT	128	122		119	9.50	140	100	24	133		114	9.53	132	96	18	128		136	103		110	7.68	121	105	5	130	
HF	24	24		23.4	1.44	25	19	24	26		23.1	2.31	28	20	18	25		27	21		23	2.45	26	20	5	22.70	
E	11	14		13.4	1.53	16	10	24	16		15.1	1.96	17	8	18	16		15	14		14.8 0	0.96	16	14	5	14.10	
CIL	26.35	22.23		21.7	1.11	23.3	19.3	24	24.24		23.4	1.07	24.6	20.8	18	24.05		24.70	21.88		22.1 0	1.41	23.55	20	5	24.16	
CBL	26.31	22.31		21.9	1.01	23.6	19.8	24	24.66		23.6	1.09	25	21	18	24.24		24.90	22.15		22.3 0	1.36	23.62	20.3 0	5	22.93	
LD	8.23	6.93		6.72	0.41	7.40	5.86	24	7.58		7.20	0.36	7.70	6.39	18	7.33		7.30	6.81		6.88	0.48	7.39	6.12	5	7.15	
LM	3.43	3.19		3.11	0.08	3.30	2.99	24	3.33		3.24	0.10	3.40	3	18	3.24		3.20	3.11		3.09	0.19	3.30	2.80	5	3.47	
LR	7.87	7.09		6.84	0.30	7.26	6.01	24	7.92		7.34	0.37	7.80	6.60	18	7.04		7.90	6.73		7.01	0.44	7.61	6.53	5	6.60	
HR	5.18	4.3		4.28	0.21	4.80	3.90	24	4.93		4.52	0.16	4.79	4.10	18	4.58		4.90	4.03		4.29	0.19	4.54	4.04	5	4.31	
LN	8.55	6.55		6.87	0.43	7.55	6.04	24	8.41		7.88	0.55	8.80	6.30	18	8.41		8.80	7.35		7.31	0.35	7.76	6.99	5	7.41	
HC	11.71	11.57		11.2	0.26	11.7	10.7	24	12.14		11.7	0.24	12.15	11.2 0	18	11.87		11.80	11.08		11.3	0.44	12.10	11	5	11.26	
BM1	1.12	1.07		0.98	0.04	1.07	0.90	24	1.20		1.05	0.06	1.14	1	18	1.19		1	0.93		0.98	0.07	1.07	0.90	5	1.11	
LIF	4.03	3.73		3.37	0.27	3.70	2.81	24	3.73		3.53	0.27	3.90	2.90	18	3.96		3.90	3.31		3.30	0.14	3.53	3.18	5	3.69	
BIF	1.77	1.32		1.35	0.08	1.50	1.21	24	1.37		1.37	0.06	1.50	1.29	18	1.32		1.50	1.29		1.23	0.09	1.33	1.09	5	1.64	
BPB	2.75	2.66		2.46	0.09	2.66	2.30	24	2.68		2.43	0.09	2.60	2.20	18	2.55		2.70	2.22		2.43	0.16	2.70	2.30	5	2.46	
BZP	2.60	1.69		1.66	0.17	2.09	1.31	24	2.10		2.03	0.14	2.30	1.70	18	2.12		2.40	1.66		1.86	0.19	2.10	1.57	5	1.72	
LIB	5.29	4.76		4.69	0.10	4.89	4.56	24	4.78		4.79	0.13	5.10	4.60	18	4.80		4.80	4.37		4.53	0.18	4.70	4.23	5	4.70	
ZB	14.98	13.17		12.6	0.44	13.23	11.8	24	13.9		13.1	0.39	13.6	12.2	18	13.4		14.10	12.34		12.8	0.63	13.35	11.8 0	5	13.22	
MB	1.34	1.35		1.33	0.09	1.50	1.18	24	1.54		1.35	0.11	1.54	1.14	18	1.38		1.40	1.38		1.29	0.08	1.40	1.20	5	1.71	
DI	1.65	1.16		1.17	0.12	1.34	0.90	24	1.44		1.30	0.13	1.50	1	18	1.35		1.50	1.07		1.24	0.19	1.40	0.94	5	1.23	
BIT	1.54	1.17		1.19	0.11	1.45	0.95	24	1.52		1.34	0.14	1.50	1	18	1.65		1.60	1.11		1.21	0.16	1.40	0.96	5	1.31	

MM R	3.54	3.29	3.24	0.07	3.40	3.12	24	3.54	3.43	0.14	3.70	3.10	18	3.43	3.40	3.01	3.22	0.10	3.35	3.10	5	3.36
GLM	15.89	13.77	13.4	0.68	14.4	11.7 0	24	14.8	14.1	0.57	15	12.4 0	18	14.55	15.4	13.28	13.5 0	0.65	14.07	12.7 0	5	13.72
DR	3.30	2.43	2.43	0.12	2.70	2.28	24	2.70	2.63	0.16	3	2.40	18	2.83	2.90	2.60	2.74	0.28	3.03	2.44	5	2.32
W	-	18.50	19.07	4.21	24	13	7	23	18	2.54	23	15	11	16	27	-	18.5 0	4.95	22	15	2	-

2

3

4

Figure 1

Phylogenetic tree of Bayesian inference (left) and maximum likelihood (right) based on the mitochondrial gene Cytochrome b (Cytb).

The dashed line indicates the closest genera: [*Rhipidomys* + (*Thomasomys* + *Chilomys*)], in colors the species described within the genus *Chilomys*: *C. georgeledecii* sp. nov. (Reserva Dracula), *C. instans* (Reserva Ecológica El Ángel), *C. neisi* sp. nov. (El Oro – Zamora Chinchipe), *C. percequilloi* sp. nov. (Napo – Morona Santiago), *C. weksleri* sp. nov. (Reserva Integral Otonga). The values above and below the branches represent the values of bootstraps and posterior probability.

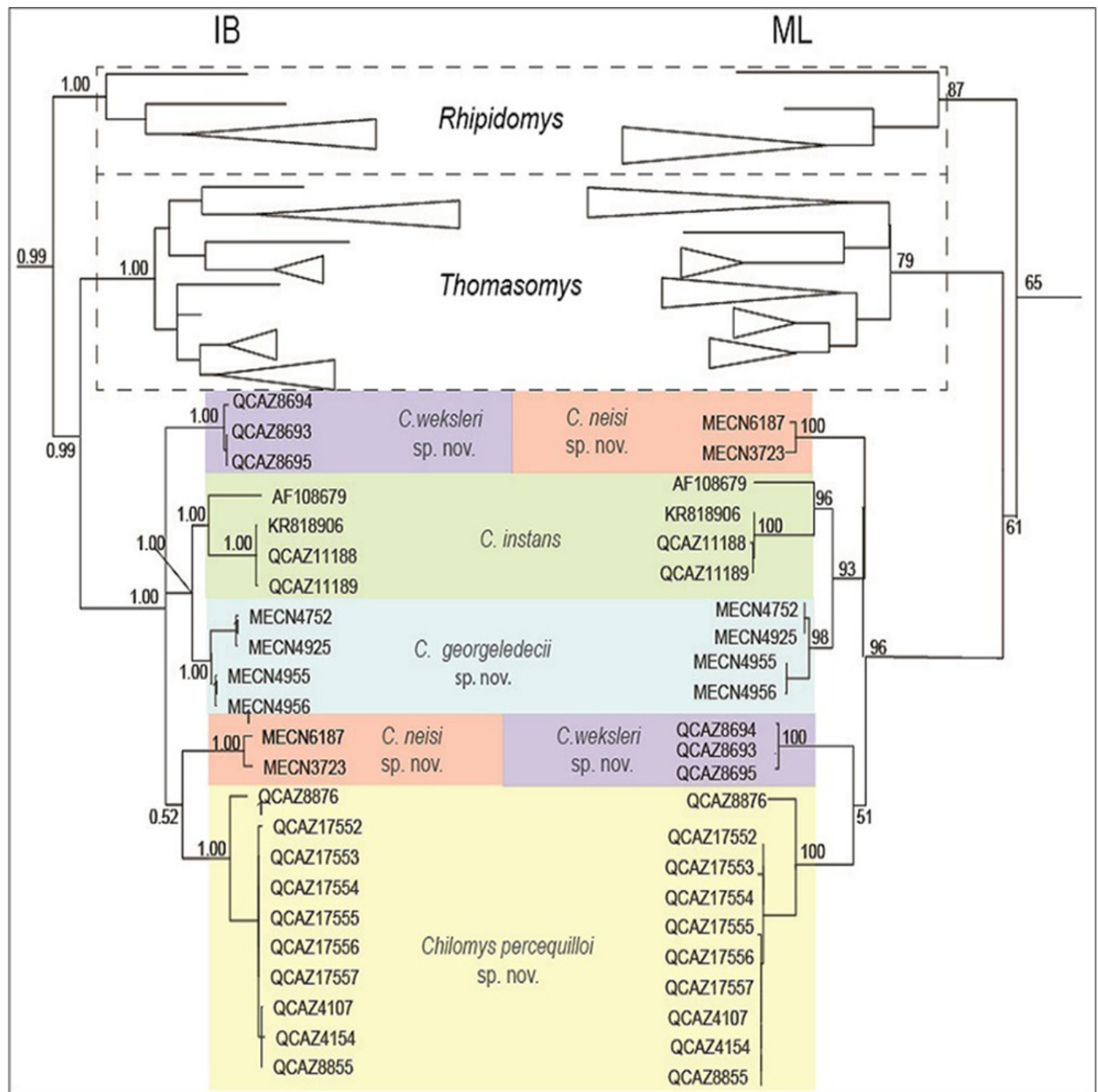


Figure 2

Delimitation of the Poisson Tree Process (PTP) model based on the Cytb maximum likelihood phylogenetic tree for the genus *Chilomys*.

Lineages (putative species) are identified with blue vertical bars; individuals of the same putative species are denoted in red. The values on the branches represent the posterior probability values (> 0.90 values are considered as high support).

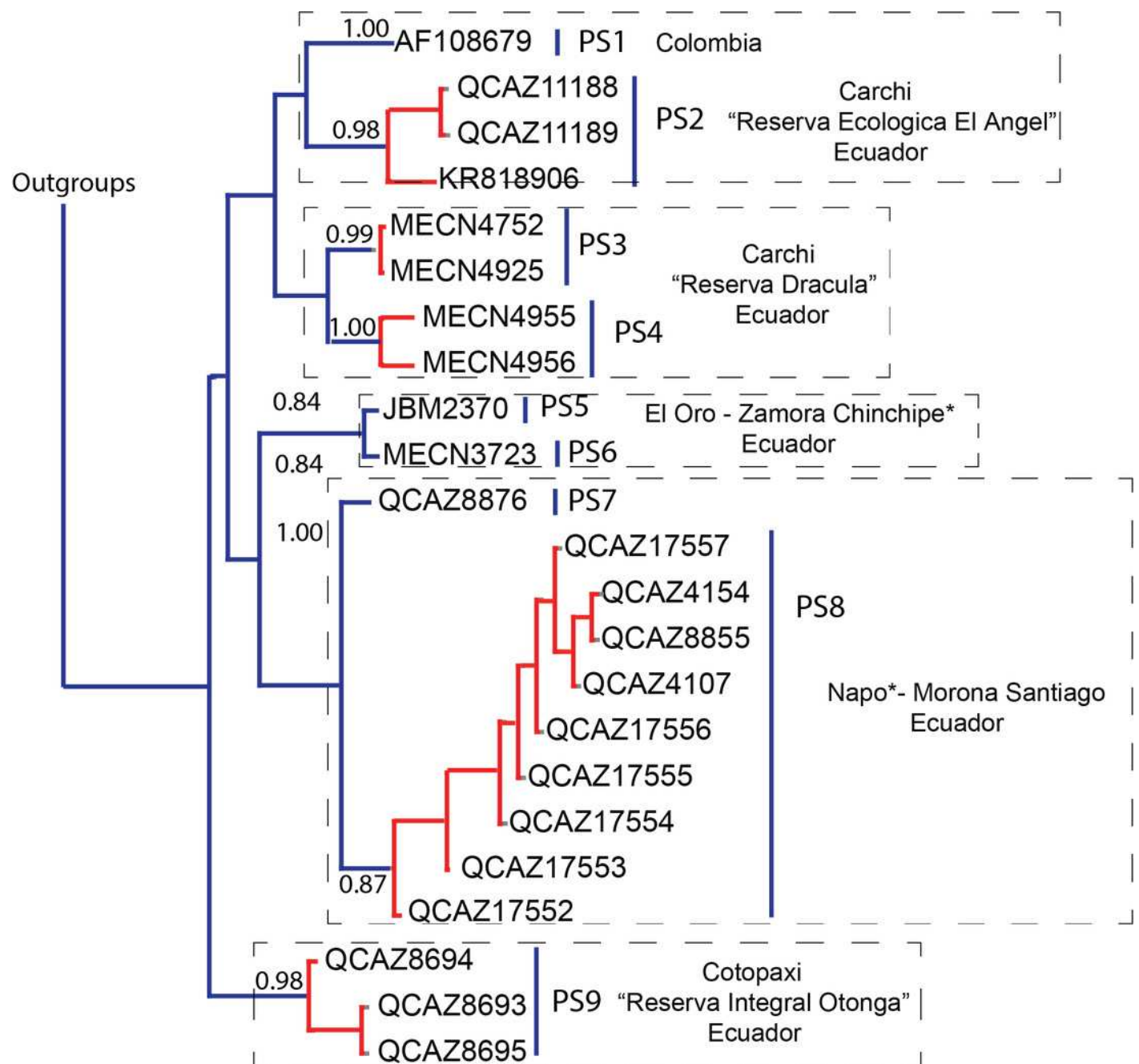
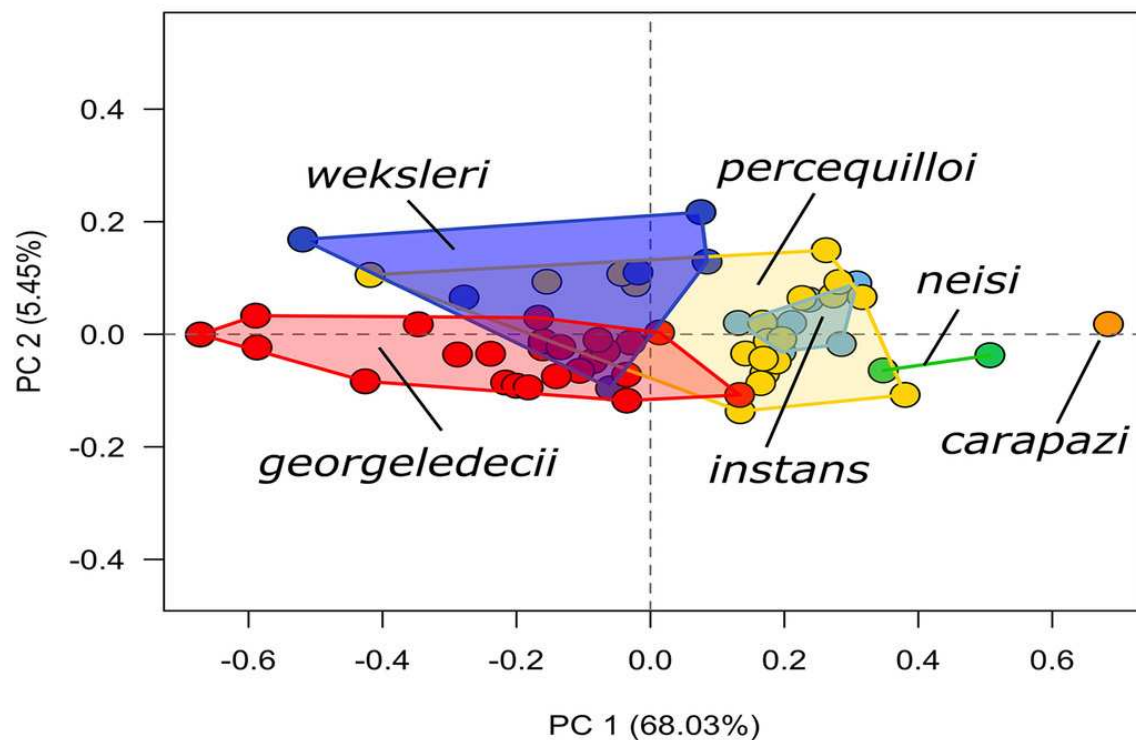


Figure 3

Morphometric analyse.

Morphometric analyses of six species of the genus *Chilomys*. (A) Scatter plot of the principal component analysis (PCA); (B) Scatter plot of the discriminant function analysis (DFA).

A



B

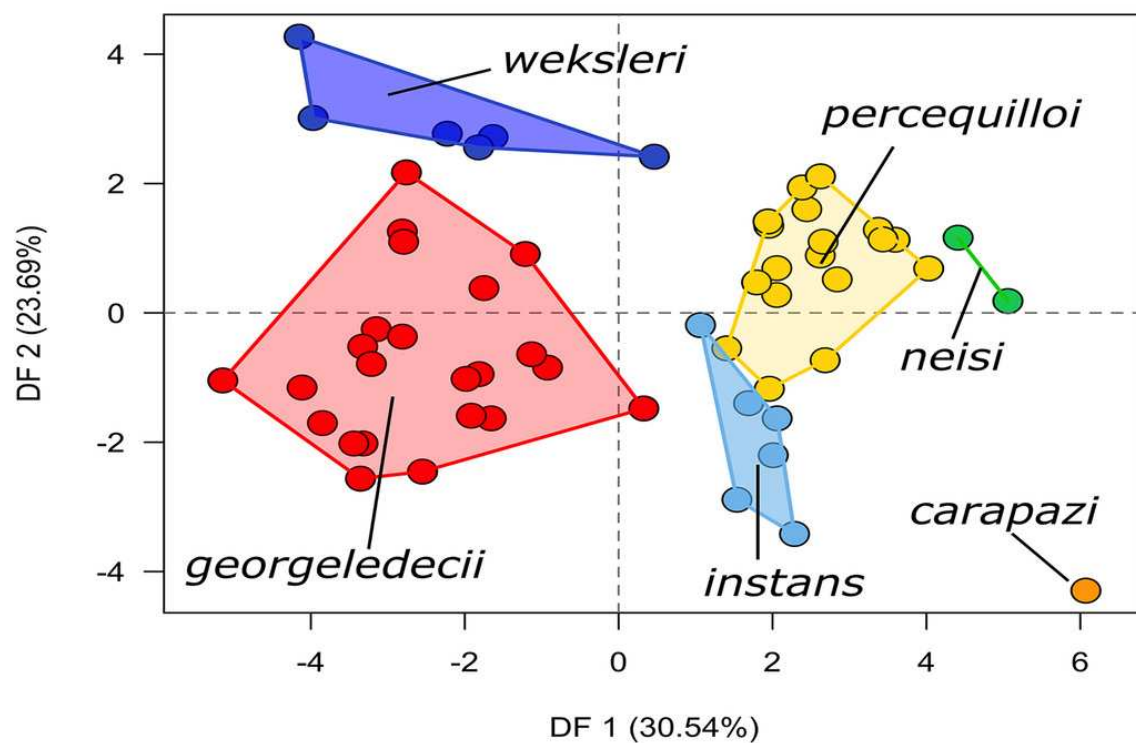


Figure 4

Morphology comparisons.

Morphology of the dorsal (upper row) and ventral (lower row) surface of the right hind foot in species of *Chilomys*. (A, B) *Chilomys carapazi* sp. nov. (MECN 5291, holotype; Reserva Drácula, Carchi, Ecuador); (C, D) *C. georgeledeci* sp. nov. (MECN 6337, paratype; Reserva Drácula, Carchi, Ecuador); (E, F) *C. neisi* sp. nov. (MECN 6187, holotype; Ashigsho, Chilla, El Oro, Ecuador); (G, H) *C. percequilloi* sp. nov. (MECN 6362, paratype; Parque Nacional Llanganates, Tungurahua, Ecuador); (I, J) *C. weksleri* sp. nov. (MECN 6365, holotype; Reserva Geobotánica Pululahua, Pichincha, Ecuador). Approximately scaled to the same length.

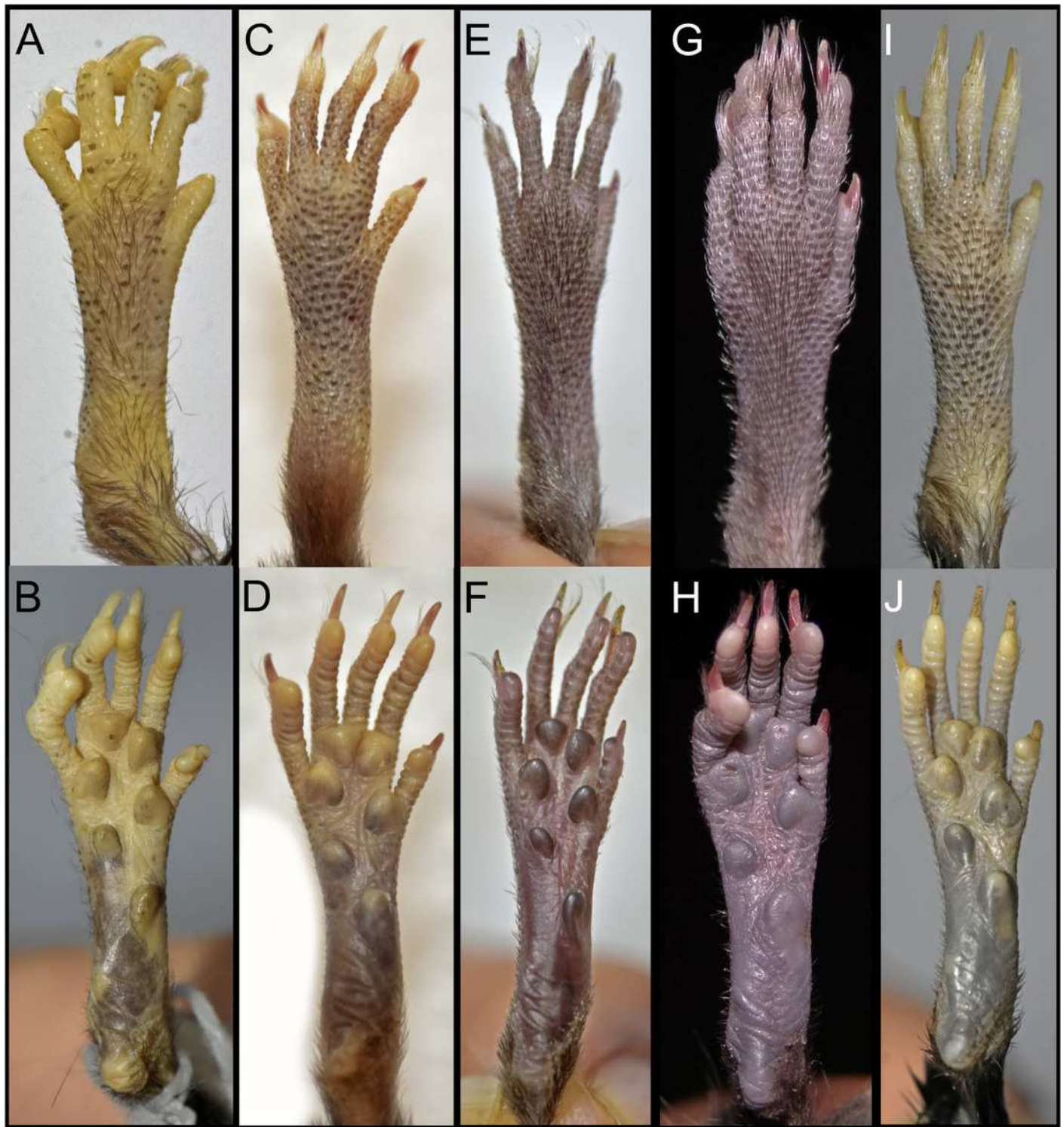


Figure 5

Chilomys carapazi sp. nov.

Chilomys carapazi sp. nov. (Reserva Dracula, Carchi, Ecuador): cranium in (A) dorsal, (B) ventral, and (C) lateral views, and mandible in (D) labial view (MECN 5291 holotype).

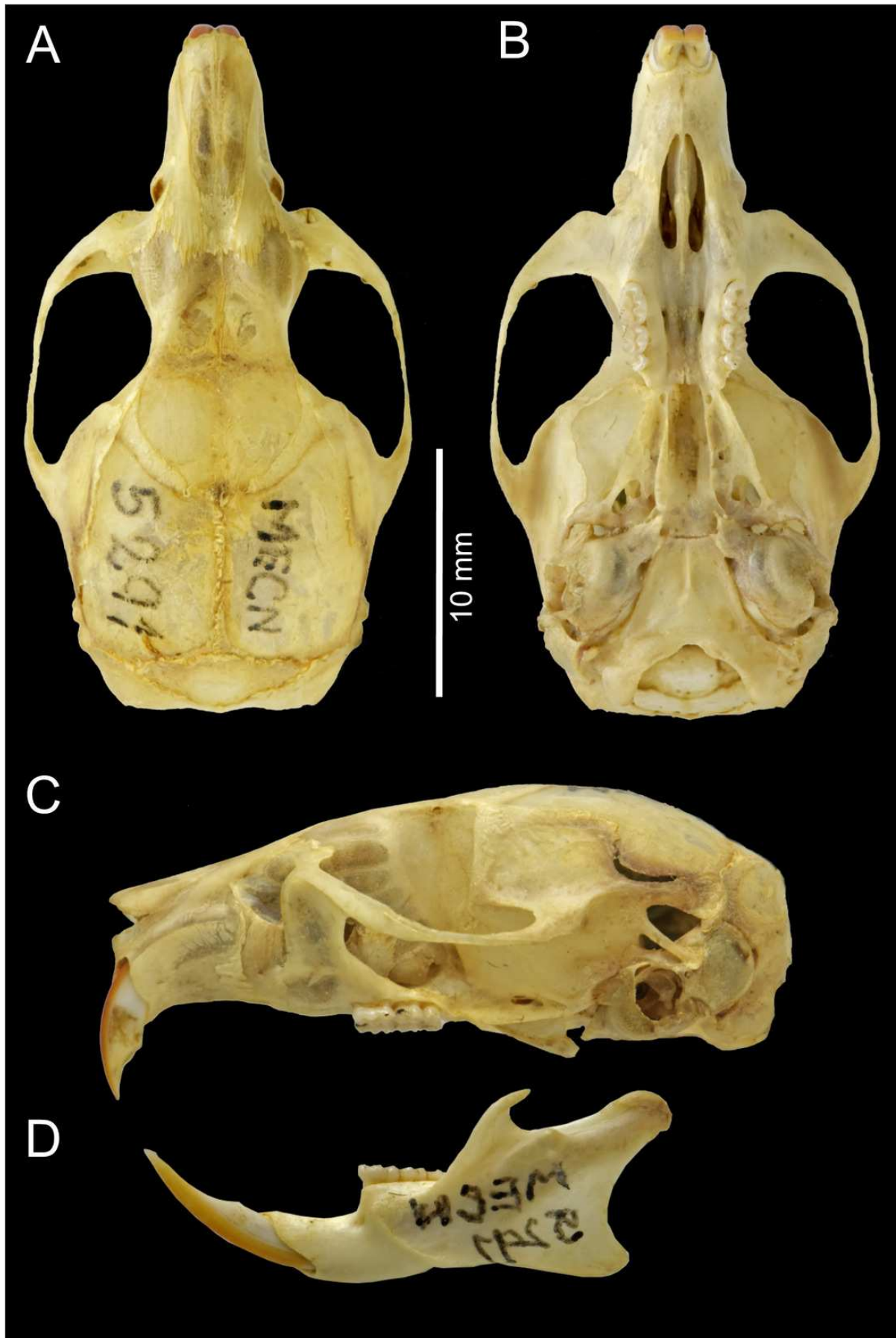


Figure 6

Morphological comparisons.

Comparison of the left anterior portion of the cranium, viewed from the side, in several species of *Chilomys*: (A) *C. instans* (NHMUK 1895.10.14.1, holotype); (B) *C. carapazi* sp. nov. (MECN 5291, holotype); (C) *C. georgeledecii* sp. nov. (MECN 6024, holotype); (D) *C. neisi* sp. nov. (MECN 6187, holotype); (E) *C. percequilloi* sp. nov. (MECN 5854, holotype); and (F) *C. weksleri* sp. nov. (MECN 6365, holotype). Thomas' angles according to incisive and basal planes are indicated as well as the extension of the molar series. Abbreviations: nc = nasolacrima capsule; m = masseteric scar; nlf = nasolacrima fissure; sf = supraorbital foramen; sm = supramaxillary foramen, zp = zygomatic plate.

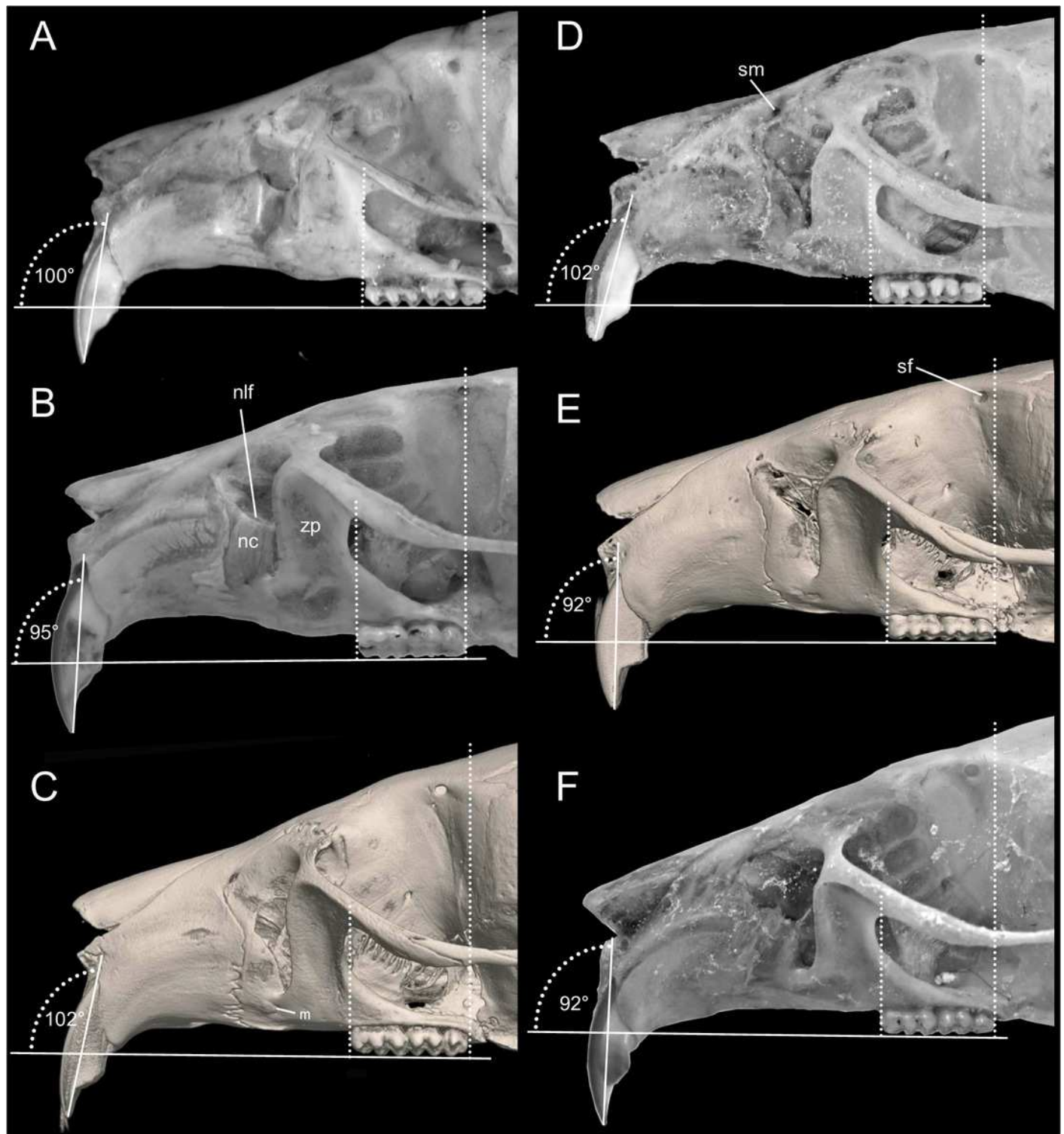


Figure 7

Morphological comparisons.

Comparison of right auditory capsule in ventral view in several species of *Chilomys*: (A) *C. instans* (NHMUK 1895.10.14.1, holotype); (B) *C. carapazi* sp. nov. (MECN 5291, holotype); (C) *C. georgeledecii* sp. nov. (MECN 6024, holotype); (D) *C. neisi* sp. nov. (MECN 3723, paratype); (E) *C. percequilloi* sp. nov. (MECN 5854, holotype); and (F) *C. weksleri* sp. nov. (MECN 6365, holotype). Abbreviations: bet = bony eustachian tube; cc = carotid canal; e = ectotympanic; mlf = middle lacerate foramen; pt = petrosal; sft = stapedial foramen.

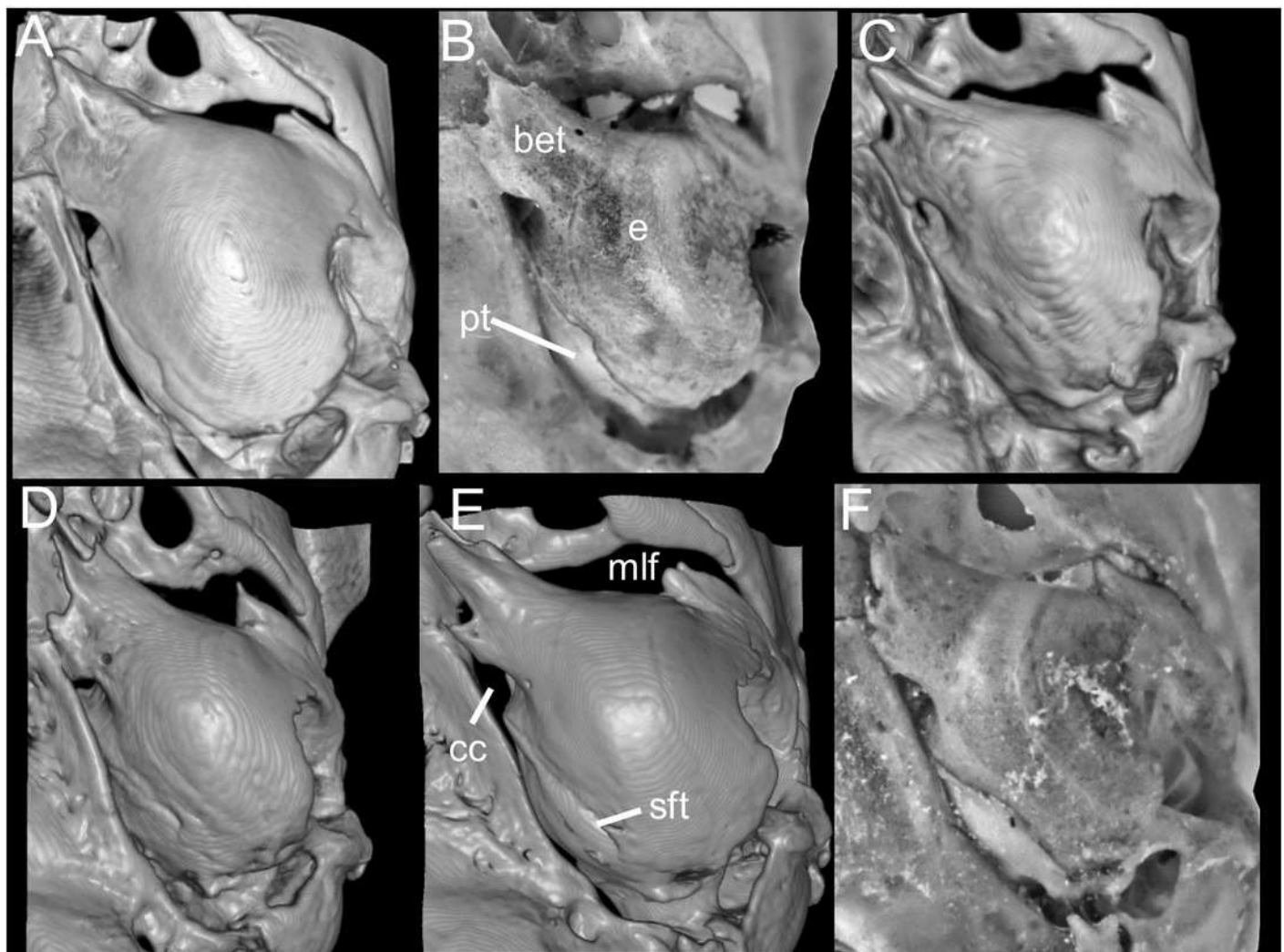


Figure 8

Morphological comparisons.

Comparison of upper (A, C, E, G, I) and lower (B, D, F, H, J) right molar series in occlusal view among species of *Chilomys*: (A, B) *C. carapazi* sp. nov. (MECN 5291, holotype); (C, D) *C. georgeledecii* sp. nov. (MECN 6024, holotype); (E, F) *C. neisi* sp. nov. (MECN 6187, holotype); (G, H) *C. percequilloi* sp. nov. (MECN 6338, paratype); and (I, J) *C. weksleri* sp. nov. (MECN 6363, paratype). Abbreviations: al = anterolabial cingulum; am = anterior mure; af = anteromedian flexus/id; h = hypoflexid; m = mesoloph/id; mm = median murid; p = protoflexus.

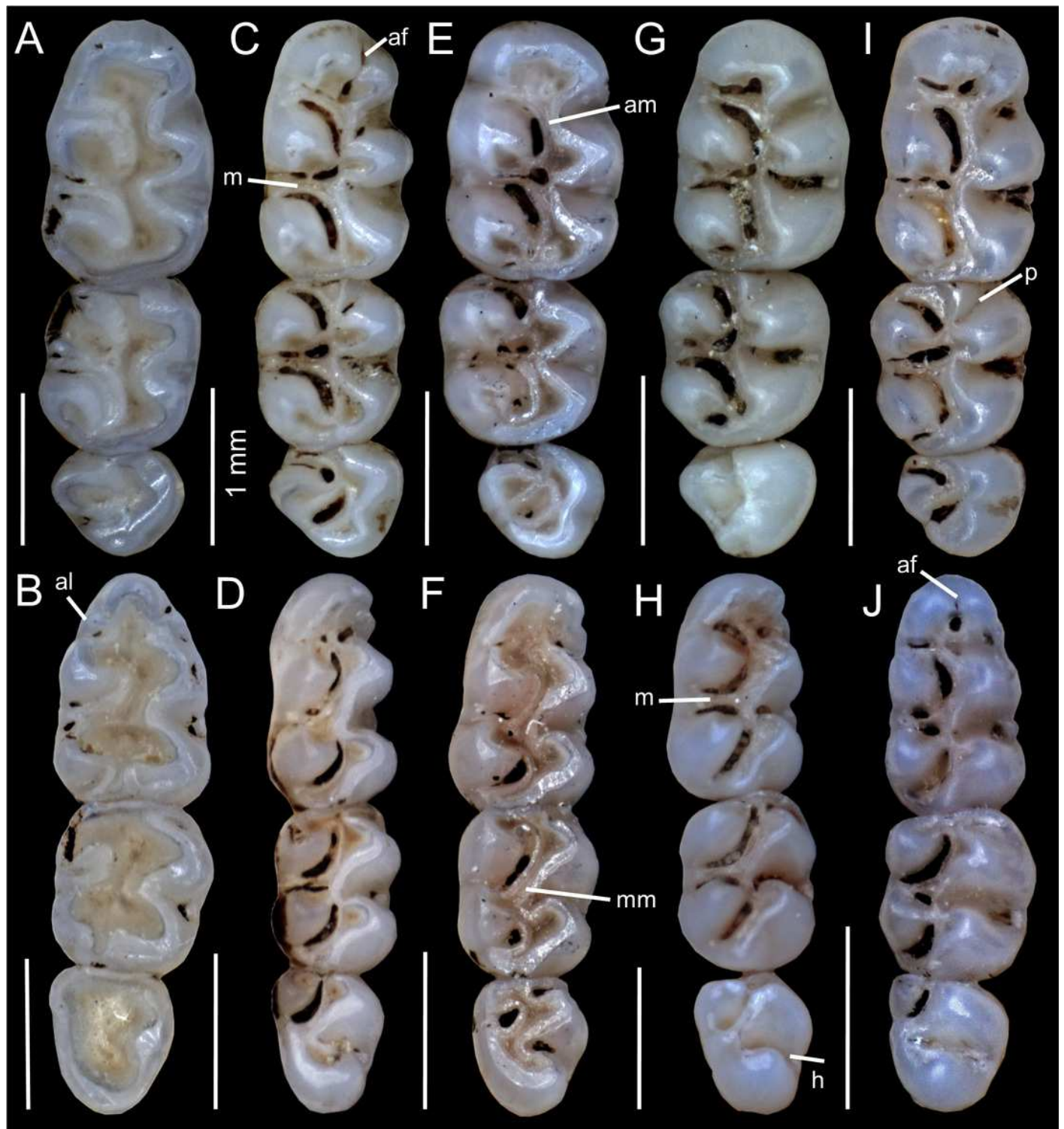


Figure 9

Chilomys in Ecuador.

Localities for the species of *Chilomys* recognized in Ecuador. Symbols with a black dot in the center represent type localities.

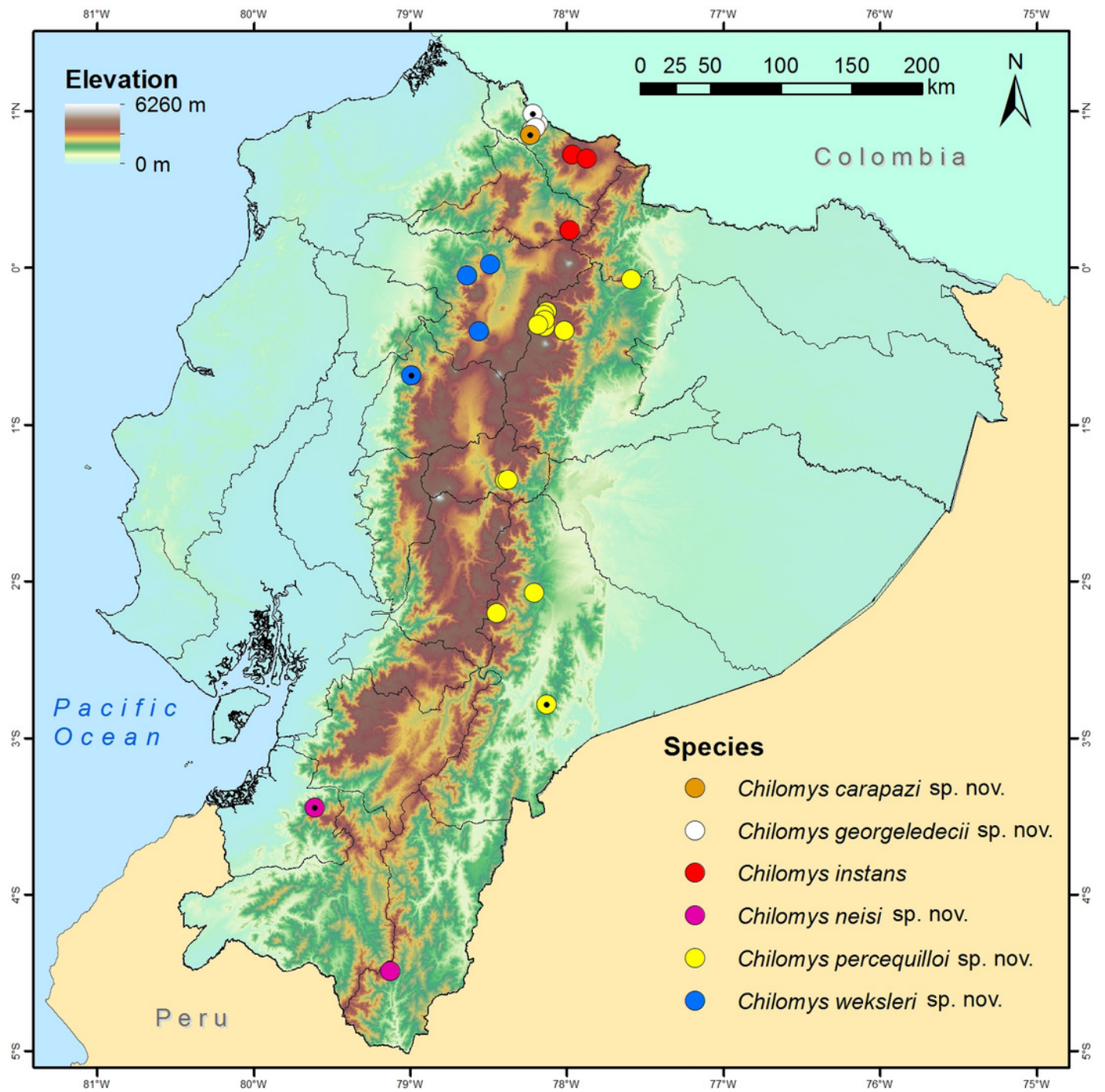


Figure 10

External aspect of *Chilomys georgeledecii* sp. nov.

External aspect of *Chilomys georgeledecii* sp. nov. (MECN 6024, holotype), an adult male from Reserva Dracula, Carchi, Ecuador.



Figure 11

Chilomys georgeledecii sp. nov.

(Reserva Dracula, Carchi, Ecuador): cranium in (A) dorsal, (B) ventral, and (C) lateral views, and mandible in (D) labial view (MECN 6024, holotype).

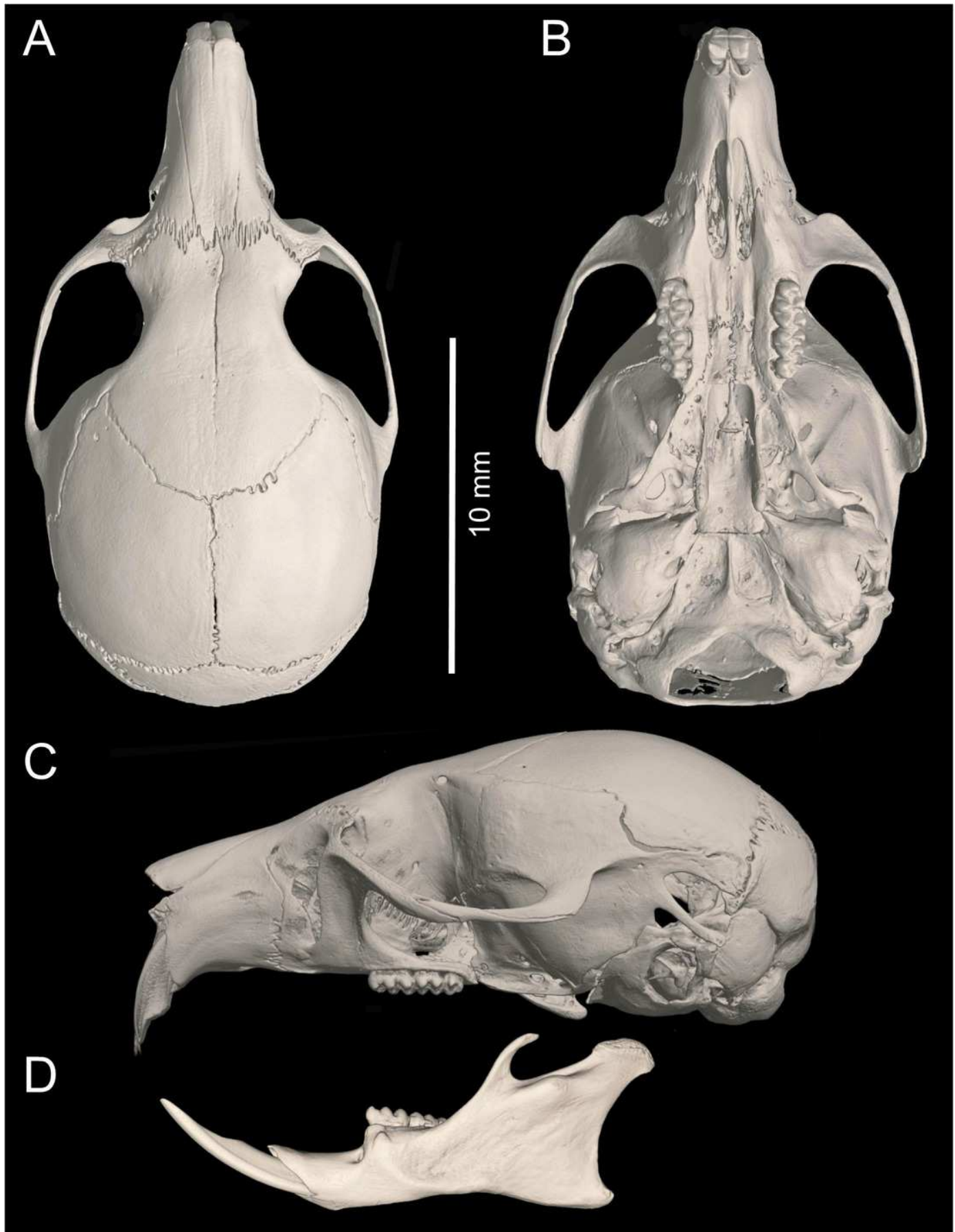


Figure 12

Morphological comparisons.

Comparison of selected regions of the cranium in several species of *Chilomys*, including the basicranial region (upper row; roofing bones of braincase removed) in dorsal view and the cross section at the frontal sinuses plane (lower row): (A, E) *C. instans* (NHMUK 1895.10.14.1, holotype); (B, F) *C. georgeledecii* sp. nov. (MECN 6024, holotype); (C, G) *C. neisi* sp. nov. (MECN 3723, paratype), and (D, H) *C. percequilloi* sp. nov. (MECN 5854, holotype).

Abbreviations: bo = basioccipital; bs = basisphenoid; cc = carotid canal; etl-III = ethmoturbinals; fo = foramen ovale; ft1-2 = frontoturbinals; it = interturbinal; lc = lamina cribosa; ls = lamina semicircularis; pet = petrosal; ps = presphenoid; sacg = groove for secondary arterial connection; sact = tunnel-like medial entrance to alisphenoid canal for secondary arterial connection.

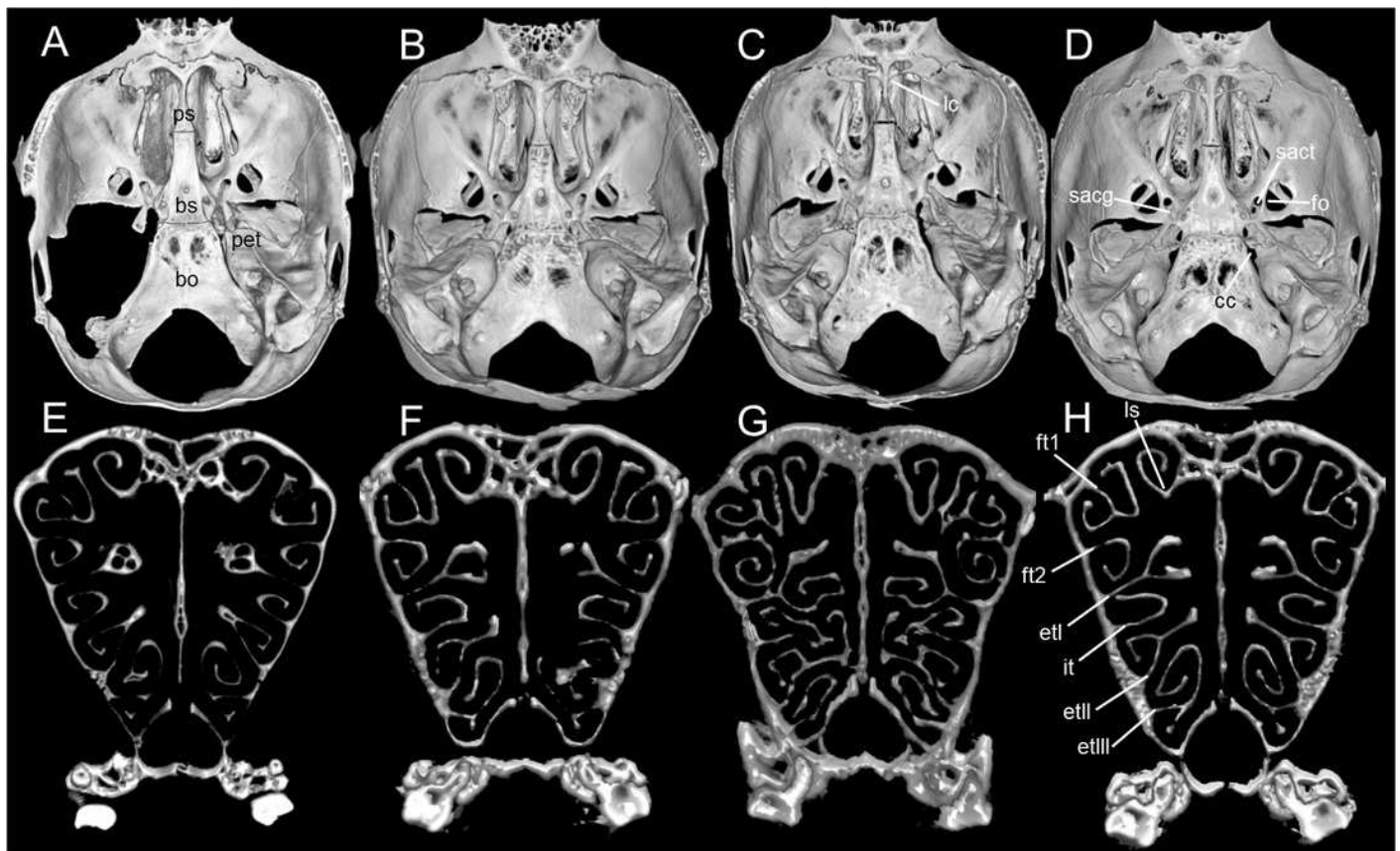


Figure 13

Morphological comparisons.

Comparison of diastemal palate in several species of *Chilomys*: (A) *C. instans* (NHMUK 1895.10.14.1, holotype); (B) *C. carapazi* sp. nov. (MECN 5291, holotype); (C) *C. georgeledecii* sp. nov. (MECN 6024, holotype); (D) *C. neisi* sp. nov. (MECN 3723, paratype); (E) *C. percequilloi* sp. nov. (MECN 5854, holotype); and (F) *C. weksleri* sp. nov. (MECN 6365, holotype). Arrows in (D) point to masseteric ridges; abbreviations: hf = Hill foramen; m = masseteric scar.

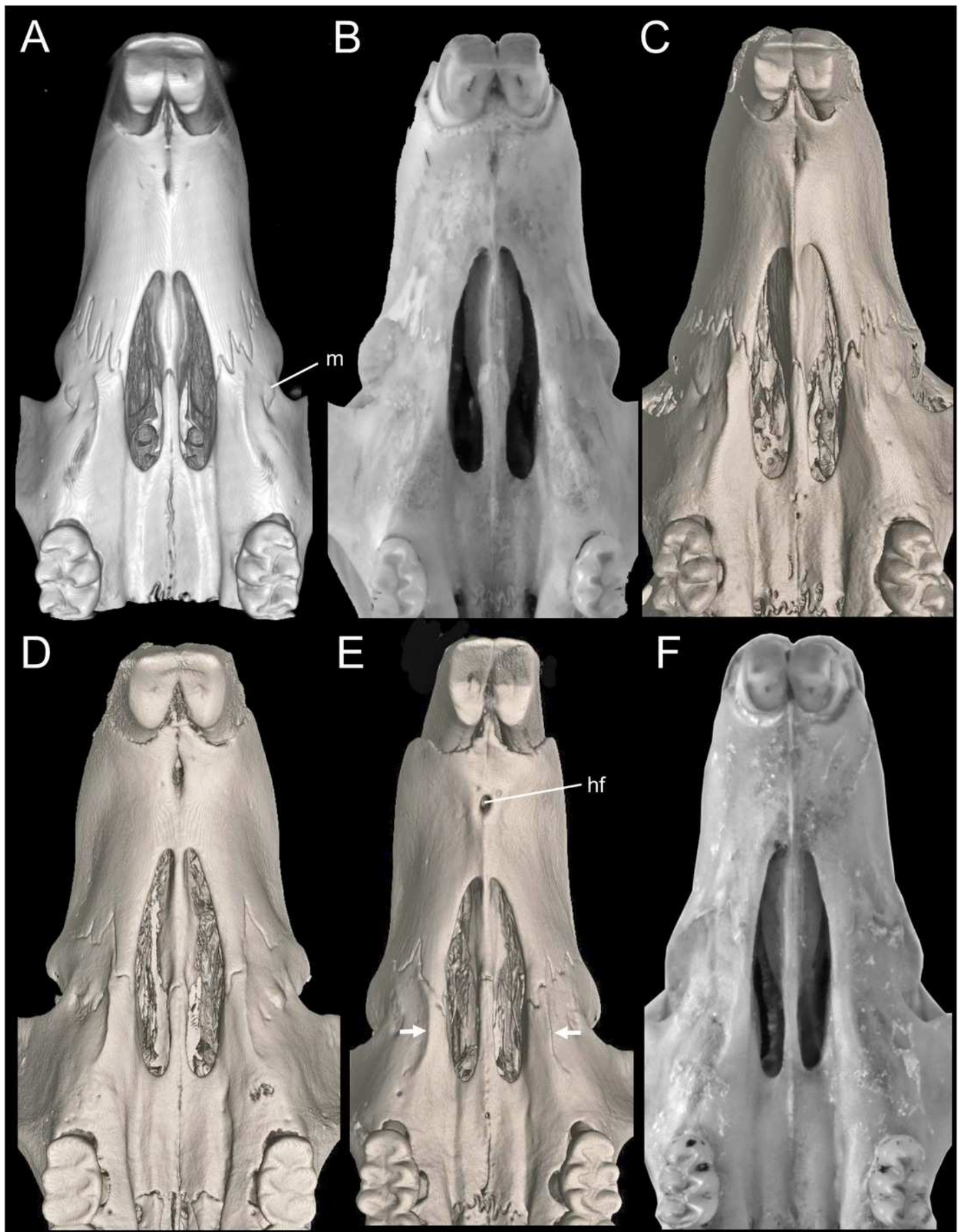


Figure 14

Chilomys neisi sp. nov.

Chilomys neisi sp. nov. (Ashigsho, Chilla, El Oro, Ecuador): cranium in (A) dorsal, (B) ventral, and (C) lateral views, and mandible in (D) labial view (MECN 6187, holotype).

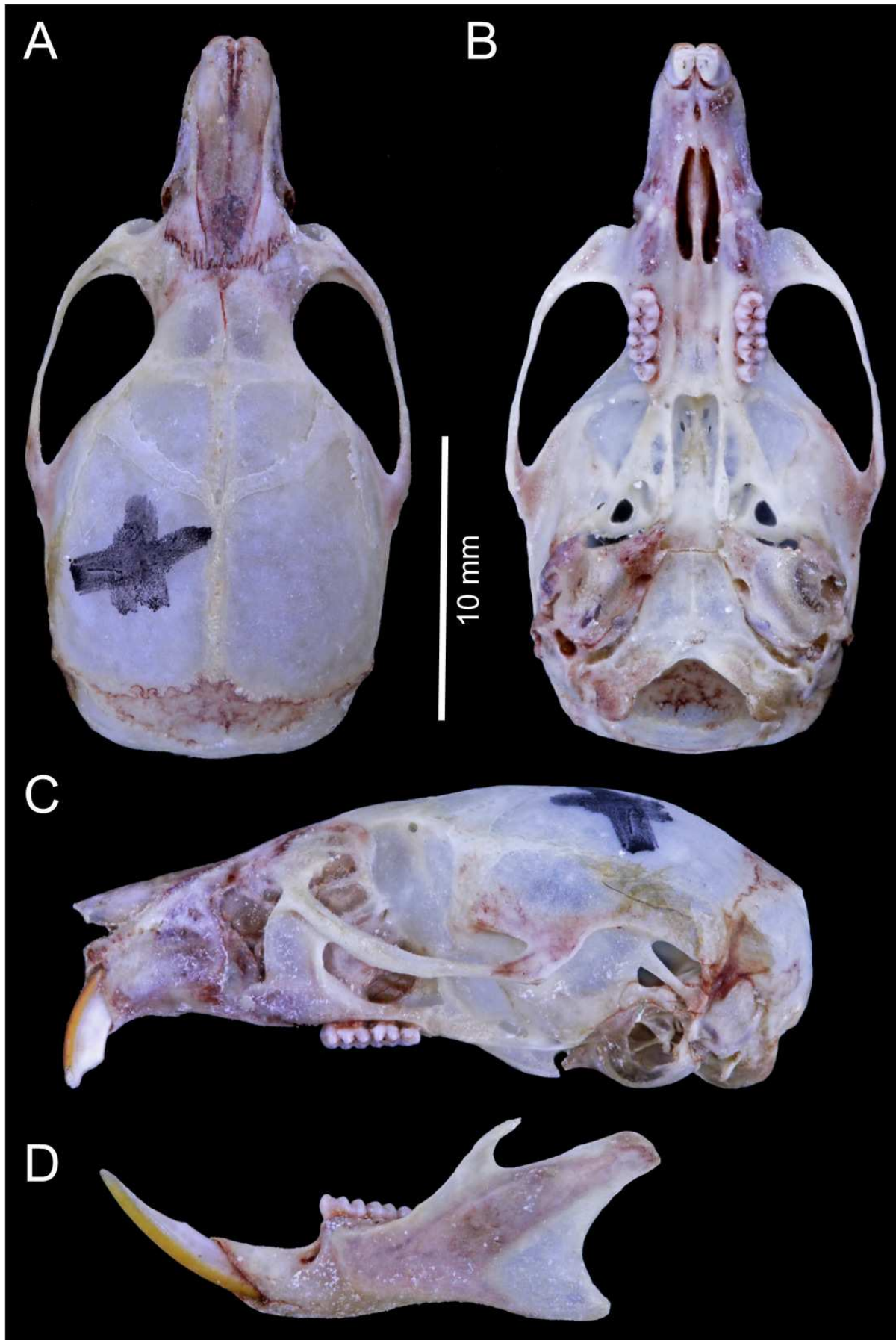


Figure 15

External aspect of *Chilomys percequilloi* sp. nov.

External aspect of *Chilomys percequilloi* sp. nov. (MECN 5854, holotype), an adult male from Cordillera de Kutukú, Morona Santiago, Ecuador.



Figure 16

Chilomys percequilloi sp. nov.

Chilomys percequilloi sp. nov. (Cordillera de Kutukú, Morona Santiago, Ecuador): cranium in (A) dorsal, (B) ventral, and (C) lateral views, and mandible in (D) labial view (MECN 5854, holotype).

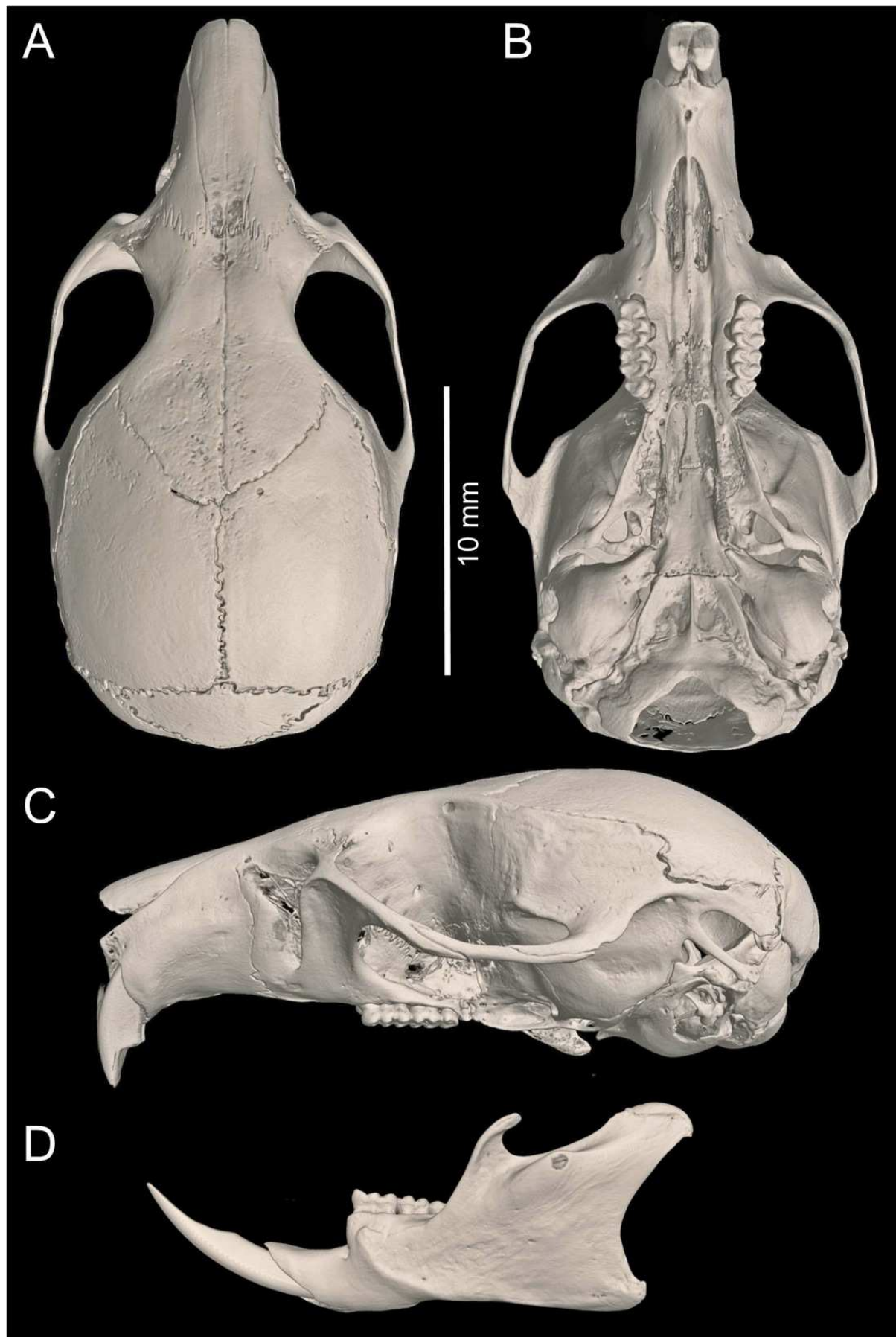


Figure 17

Chilomys weksleri sp. nov.

Chilomys weksleri sp. nov. (Reserva Intergral Otonga, Cotopaxi, Ecuador): cranium in (A) dorsal, (B) ventral, and (C) lateral views, and mandible in (D) labial view (MECN 6365, holotype).

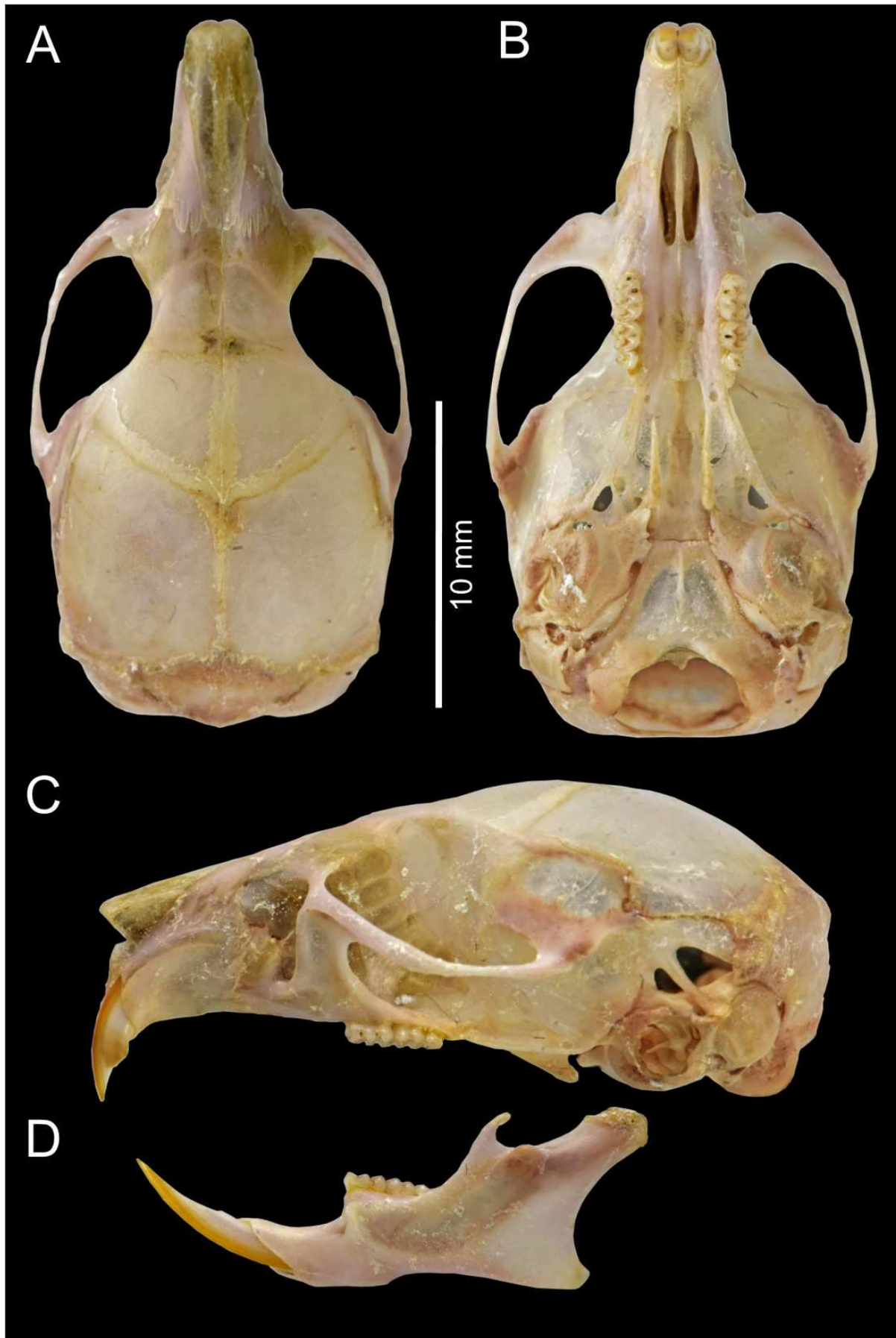


Figure 18

Selected external and soft anatomical traits of *Chilomys*.

Selected external and soft anatomical traits of *Chilomys*: (A) external aspect of an individual in wild (*C. georgeledecii* sp. nov.; MECN 5381, paratype); (B) rhinarium in anterior view (*C. georgeledecii*; MECN 6205, paratype); (C) ventral surface of right front foot (*C. georgeledecii* sp. nov.; MECN 5381, paratype); (D) genital region (*C. georgeledecii* sp. nov.; MECN 5381, paratype); (E) soft palate (*C. weksleri* sp. nov.; MECN 6364, paratopotype); and (F) tongue in dorsal view (*C. weksleri* sp. nov.; MECN 6364, paratopotype). Abbreviations: 1-5 = digits; a = anus; ah = antihelix; at = antitragus; c = clitoris; ch = concha; cv = circumvallate papilla; d1-d3 = diastemal rugae; ft = fossa triangularis; he = helix; if = lower integumental fold; i1-15 = interdental rugae; my = mystacial vibrissae; n = nostril; np = nasal pad; pe = periocular ring; ph = philtrum; su = semilunar sulcus; uf = upper integumental fold; v = vagina.

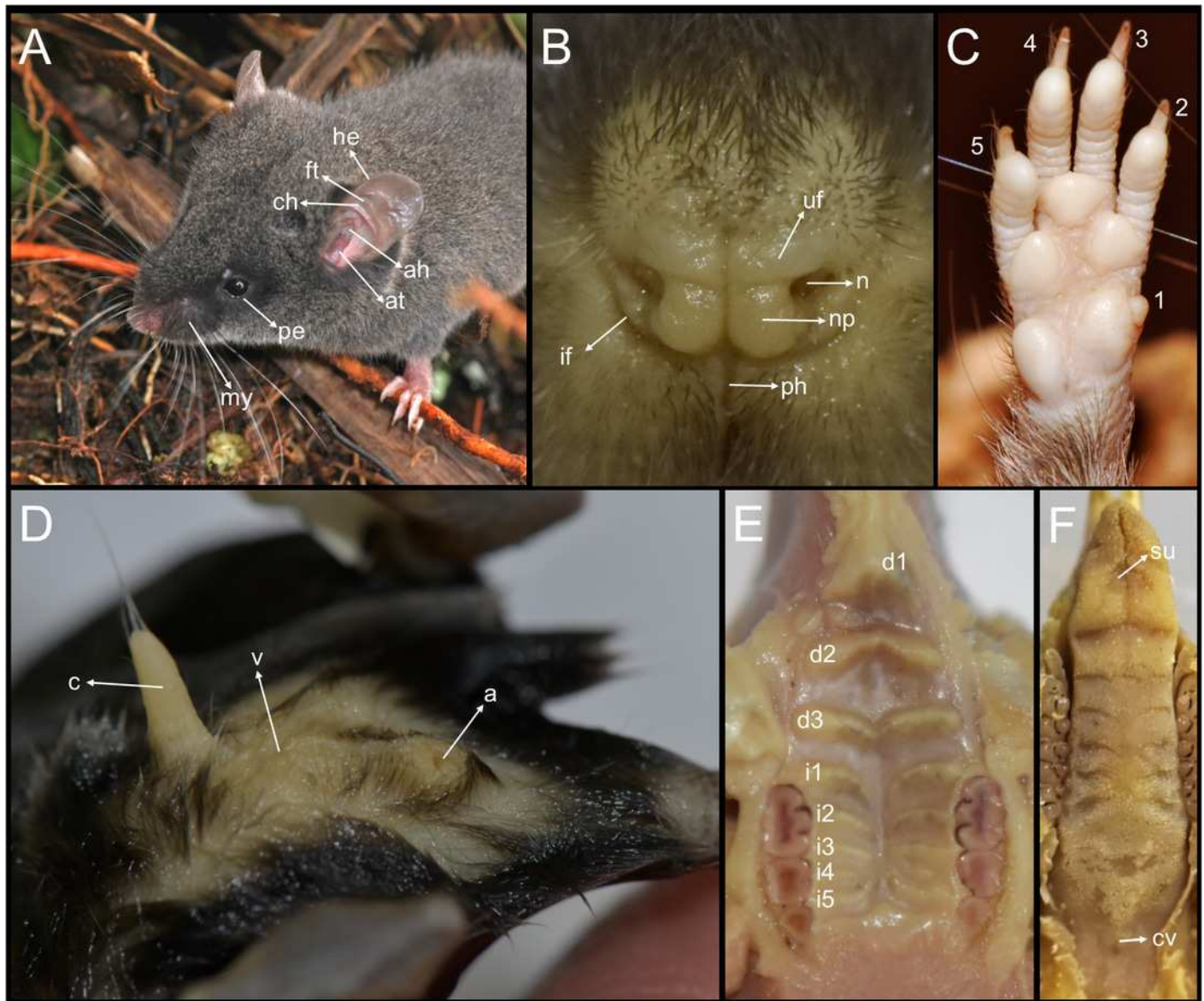
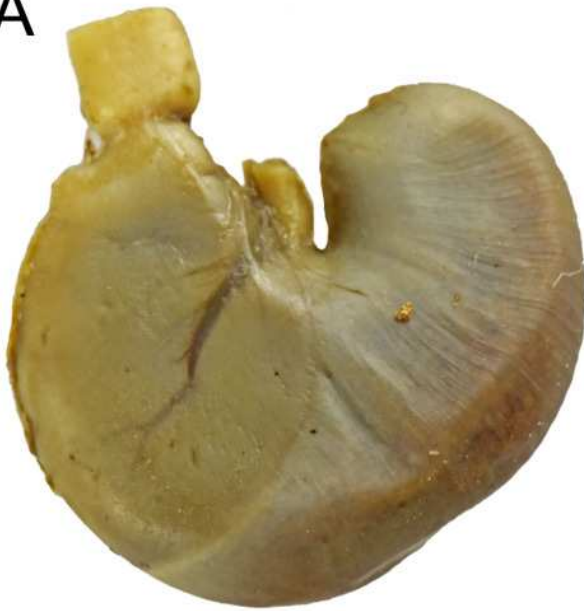


Figure 19

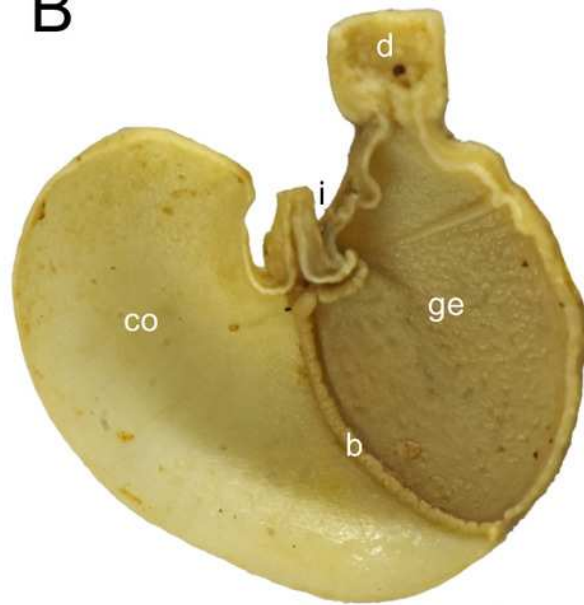
Gross morphology of the stomach in two species of *Chilomys*.

Gross morphology of the stomach in two species of *Chilomys*: (A, C) ventral external and (, D) internal views in *C. georgeledecii* sp. nov. (A, B; MECN 6337, paratype); and in *C. percequilloi* sp. nov. (MECN 6338, paratype). Abbreviations: b = bordering fold; co = cornified epithelium; d = duodenum; ge = glandular epithelium; i = incisura angularis.

A



B



C



D

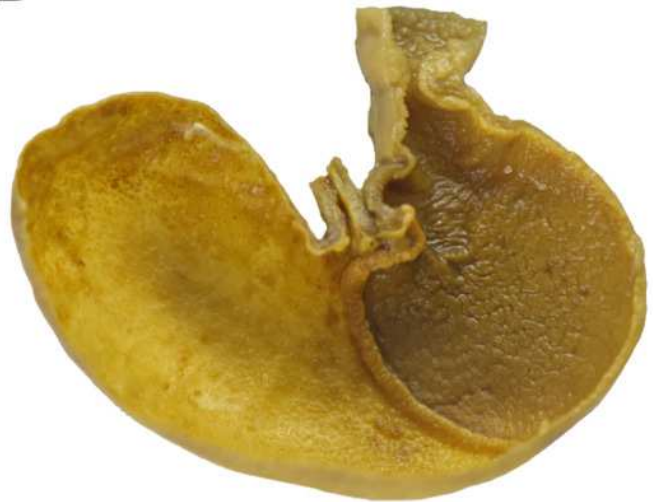


Figure 20

External views of the partial digestive system in several species of *Chilomys*.

External views of the partial digestive system in several species of *Chilomys*: (A) *C. georgeledecii* sp. nov. (MECN 6337, paratype); (B) *C. neisi* sp. nov. (MECN 6187, holotype); (C) *C. percequilloi* sp. nov. (MECN 6338, paratype); and (D) *C. weksleri* (MECN 6365, holotype).

